

**Zeitschrift:** IABSE reports of the working commissions = Rapports des commissions de travail AIPC = IVBH Berichte der Arbeitskommissionen

**Band:** 11 (1971)

**Rubrik:** Session III: Hybrid girders, fatigue problems, effects of concentrated loads, box girders, special problems

### **Nutzungsbedingungen**

Die ETH-Bibliothek ist die Anbieterin der digitalisierten Zeitschriften auf E-Periodica. Sie besitzt keine Urheberrechte an den Zeitschriften und ist nicht verantwortlich für deren Inhalte. Die Rechte liegen in der Regel bei den Herausgebern beziehungsweise den externen Rechteinhabern. Das Veröffentlichen von Bildern in Print- und Online-Publikationen sowie auf Social Media-Kanälen oder Webseiten ist nur mit vorheriger Genehmigung der Rechteinhaber erlaubt. [Mehr erfahren](#)

### **Conditions d'utilisation**

L'ETH Library est le fournisseur des revues numérisées. Elle ne détient aucun droit d'auteur sur les revues et n'est pas responsable de leur contenu. En règle générale, les droits sont détenus par les éditeurs ou les détenteurs de droits externes. La reproduction d'images dans des publications imprimées ou en ligne ainsi que sur des canaux de médias sociaux ou des sites web n'est autorisée qu'avec l'accord préalable des détenteurs des droits. [En savoir plus](#)

### **Terms of use**

The ETH Library is the provider of the digitised journals. It does not own any copyrights to the journals and is not responsible for their content. The rights usually lie with the publishers or the external rights holders. Publishing images in print and online publications, as well as on social media channels or websites, is only permitted with the prior consent of the rights holders. [Find out more](#)

**Download PDF:** 20.08.2025

**ETH-Bibliothek Zürich, E-Periodica, <https://www.e-periodica.ch>**

### III

## RAPPORTS INTRODUCTIFS / EINFÜHRUNGSBERICHTE / INTRODUCTORY REPORTS

### Stresses in Thin Cylindrical Webs of Curved Plate Girders

Contraintes dans les âmes minces cylindriques de poutres courbes  
à âme pleine

Spannungen in dünnen, zylindrischen Stegen von gekrümmten  
Vollwandträgern

**RYSZARD DABROWSKI**  
Institute of Civil Engineering  
Technical University  
Gdańsk, Poland

**JERZY WACHOWIAK**  
Polytechnic Institute  
Koszalin, Poland

#### 1. Introduction

The title subject falls beyond the scope of the present Colloquium on limit design of plane plate girders. Stresses and displacements in thin cylindrical webs of curved plate girders under design loads are analysed herein. However, in both analyses one approaches the problem as a stress problem - without bifurcation of equilibrium - on the basis of a geometrically nonlinear theory of elastic plates and shells, respectively. Whereas investigation of postcritical behaviour of plane webs is rather well advanced, the present paper ought to be considered as a first step toward a more comprehensive investigation of the title problem.

The analysis of stresses and displacements in thin cylindrical webs of curved plate girders is of practical interest to designers of horizontally curved bridge girders in multi-girder or box-type bridge structures. Curved girders are subjected to stresses and displacements under given dead and live loads. These stresses and displacements can be calculated e.g. according to the theory of torsion and bending of thin-walled girders with nondeformable or deformable cross-section [1]. Free transverse displacements of a cylindrical web panel within its supporting edges - which on two opposite sides are formed by curved flanges



and by vertical stiffeners (Fig.1) - give rise to a redistribution of stresses and, consequently, to a deviation of the final stress pattern from the original one calculated on the basis of torsion bending theory.

The problem is treated as a so-called second-order-theory stress problem within elastic range of material properties. Small deflections, say, not exceeding half web thickness, are assumed. Donnell-type equations describing bending of shallow cylindrical shells are employed. Thus second-order effects due to the original membrane stresses only are accounted for. Linearized relations do not, however, constitute a serious limitation of the present solution. More refined results can be obtained by a step-by-step procedure.

11.2

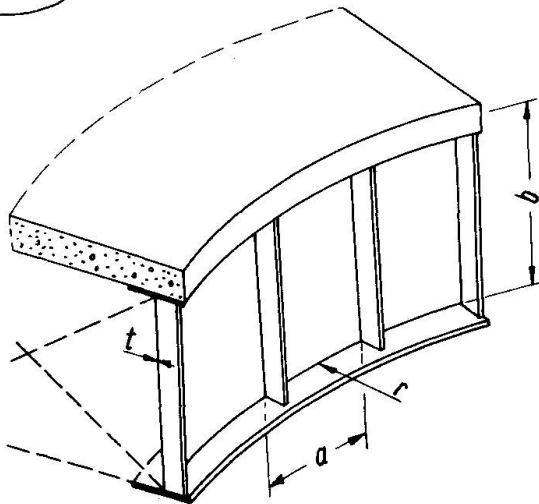


Fig. 1

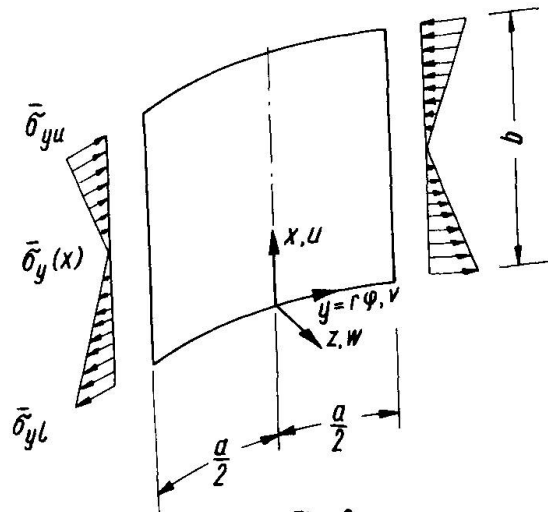


Fig. 2

## 2. Differential equations of the problem

A cylindrical panel (Fig.2) rigidly supported along curved edges at the junction with flanges and fixed along straight edges at vertical stiffeners is considered. The assumption of absolutely rigid stiffeners means a simplification of analysis and an oversimplification of the problem in many situations of practical design. It allows, however, to expose more clearly the relative importance of other parameters. Two kinds of support along curved edges are considered: (1) simple (hinged) support, and (2) fixed support with unrestricted displacement in x-direction (Fig.2).

Load acting upon cylindrical web panel is formed by original longitudinal stresses  $\bar{\sigma}_y(x) = \bar{n}_y(x)/t$  uniformly distributed over web thickness  $t$  and varying linearly over web depth  $b$  (a bar is placed over the symbol  $\sigma$  for distinction of the original stress pattern from the final one which is denoted simply by  $\sigma$  without a bar). The assumed stress pattern, constant in  $y$ -direction, corresponds realistically with the performance of a web panel at midspan sections of the girder where maximum bending and warping moments due to continuous load occur and, accordingly, shear forces and secondary torsion moments disappear. (This is, of course, not the case with panels adjacent to intermediate supports of continuous girders where large shear forces are present, and should be accounted for, and, besides, the stresses  $\bar{\sigma}_y(x)$  vary markedly in  $y$ -direction as well.)

Pertinent equations based on large deflections theory [2], [3], relating normal displacement  $w$ , stress function  $F$  with the original membrane forces  $\bar{n}_x = \bar{\sigma}_x t$ ,  $\bar{n}_y = \bar{\sigma}_y t$  and  $\bar{n}_{xy} = \bar{\tau}_{xy} t$  read as follows

$$\left. \begin{aligned} K \nabla^4 w &= (\bar{n}_y + F'') \left( \frac{1}{r} + w'' \right) + \\ &+ 2 (\bar{n}_{xy} - F'_{xy}) w'' + (\bar{n}_x + F'') w'', \\ \frac{1}{Et} \nabla^4 F &= - \frac{1}{r} w'' + (w'')^2 - w' w', \end{aligned} \right\} \quad (1)$$

in which  $K = Et^3/12(1-\nu^2)$  is the plate bending stiffness and  $r$  denotes the radius of curvature of web panel. Derivatives with respect to  $x$  and  $y$  are denoted as follows:

$$(\ )' = \frac{\partial(\ )}{\partial x}, \quad (\ )^{\cdot} = \frac{\partial(\ )}{\partial y},$$

and, furthermore,

$$\nabla^2(\ ) = (\ )'' + (\ )^{\cdot\cdot}.$$

Final membrane forces are given by the relations

$$n_x = \bar{n}_x + F', \quad n_y = \bar{n}_y + F'', \quad n_{xy} = \bar{n}_{xy} - F'_{xy}. \quad (2)$$

For a preliminary research pursued in this paper Eqs.(1) are too much involved. Linearized Donnell-type equations of small deflections theory are deduced directly from Eqs.(1) by deleting products of the unknowns  $w$  and  $F$ . Thus one obtains for the case under consideration, with  $\bar{n}_x = \bar{n}_{xy} = 0$ , the equations

$$\left. \begin{aligned} K \nabla^4 w - \frac{1}{r} F'' &= \bar{n}_y \left( \frac{1}{r} + w'' \right), \\ \frac{1}{Et} \nabla^4 F + \frac{1}{r} w'' &= 0. \end{aligned} \right\} \quad (3)$$

Second-order effect is accounted for by a single load term  $\bar{n}_y w''$  on the right-hand side of the first Eq.(3).

For convenience in dealing with boundary conditions an equivalent set of three differential equations with respect to displacement components  $u, v, w$  (Fig.2) has been used - in conjunction with Galerkin's method of solution. These equations are as follows [4]:

$$\left. \begin{aligned} u'' + \frac{1-\nu}{2} u'' + \frac{1+\nu}{2} v'' - \frac{\nu}{r} w' &= 0, \\ \frac{1+\nu}{2} u'' + v'' + \frac{1-\nu}{2} v'' - \frac{1}{r} w' &= 0, \\ -\frac{1}{r} (\nu u' + v' - \frac{1}{r} w) + \frac{t^2}{12} \nabla^4 w - \bar{n}_y \frac{1-\nu^2}{Et} \left( \frac{1}{r} + w'' \right) &= 0. \end{aligned} \right\} \quad (4)$$

Accordingly, membrane forces  $n_x, n_y$  and  $n_{xy}$  and bending moments  $m_x, m_y$  and  $m_{xy}$  are given by the relations [4]

$$\left. \begin{aligned} n_x &= \frac{Et}{1-\nu^2} \left[ u' + \nu \left( v' - \frac{w}{r} \right) \right], \\ n_y &= \bar{n}_y + \frac{Et}{1-\nu^2} \left( v' - \frac{w}{r} + \nu u' \right), \\ n_{xy} &= \frac{Et}{2(1+\nu)} (u' + v') \end{aligned} \right\} \quad (5)$$

and

$$\left. \begin{aligned} m_x &= -K(w'' + \nu n''), \\ m_y &= -K(n'' + \nu w''), \\ m_{xy} &= -(1-\nu)Kw'. \end{aligned} \right\} \quad (6)$$

The most significant stress component,  $\sigma_y$ , on the inward and outward (with relation to the centre of curvature) web surfaces is equal to

$$(\sigma_y)_{z=\pm t/2} = \frac{n_y}{t} \pm \frac{6m_y}{t^2}, \quad (7)$$

in which  $n_y$  is given by the second Eq. (5).

### 3. Galerkin's method of solution

The unknown displacement components  $u, v, w$  of Eq. (4) are assumed in form of double series with unknown coefficients  $u_{mn}, v_{mn}, w_{mn}$  as follows:

$$\left. \begin{aligned} u(x, y) &= \sum_m \sum_n u_{mn} u_m(y) u_n(x), \\ v(x, y) &= \sum_m \sum_n v_{mn} v_m(y) v_n(x), \\ w(x, y) &= \sum_m \sum_n w_{mn} w_m(y) w_n(x). \end{aligned} \right\} \quad (8)$$

( $m = 1, 2, \dots, n = 1, 2, \dots$ )

Shape functions  $u_m(y), u_n(x), v_m(y), v_n(x)$  are the sine and cosine functions satisfying appropriate boundary conditions at  $y = \pm a/2$  and  $x = 0, b$  (Fig. 2). Shape functions  $w_m(y)$  and  $w_n(x)$  are assumed in form of eigenfunctions of transverse vibrations of a beam with fixed or simply supported ends, respectively, which comply with corresponding boundary conditions of the web panel.

Taking  $m = 1, 2, 3, 4$  and  $n = 1, 2, 3, 4$  one has to determine 48 unknown coefficients of the series, Eqs. (8), from

a set of 48 linear equations obtained by means of Galerkin's method. The equations written down in general terms are as follows [5]:

$$\left. \begin{aligned} \iint_A R_u (\varphi_u)_{mn} dx dy &= 0, \\ \iint_A R_v (\varphi_v)_{mn} dx dy &= 0, \\ \iint_A R_w (\varphi_w)_{mn} dx dy &= 0. \end{aligned} \right\} \quad (9)$$

in which  $R_u$ ,  $R_v$  and  $R_w$  denote left-hand sides of equilibrium equations (4) expressed by the series, Eqs.(8), and  $(\varphi_u)_{mn}$ ,  $(\varphi_v)_{mn}$  and  $(\varphi_w)_{mn}$  are virtual displacements in x, y and z-direction, complying with given boundary conditions. Clearly, these displacements are selected as products of assumed shape functions:  $u_m(y) u_n(x)$ ,  $v_m(y) v_n(x)$  and  $w_m(y) w_n(x)$ , respectively.

All calculations involved in determination of stresses and displacements have been programmed for a digital computer [6]. Some numerical results are presented subsequently in Section 3.3.

### 3.1 Cylindrical panel fixed at vertical stiffeners and simply supported along curved edges

Boundary conditions at  $y = \pm a/2$  are as follows:  $u = v = w = w' = 0$ , and boundary conditions at  $x = 0, b$ :  $u' = v = w = w'' = 0$ . With newly introduced notations

$$\xi = x/b, \quad \eta = y/a$$

the above conditions are satisfied by the following shape functions:

$$\left. \begin{aligned} u_m(y) &= \cos(2m-1)\pi\eta, \\ u_n(x) &= \cos n\pi\xi, \\ v_m(y) &= \sin 2m\pi\eta, \\ v_n(x) &= \sin n\pi\xi, \\ (m = 1, 2, 3, 4; \quad n = 1, 2, 3, 4) \end{aligned} \right\} \quad (10)$$

$$\left. \begin{aligned} w_m(y) &= \cos 2m^*\pi\eta - \frac{\cos m^*\pi}{\cosh m^*\pi} \cosh 2m^*\pi\eta, \\ w_n(x) &= \sin n\pi\xi, \end{aligned} \right\} \quad (10a)$$

in which

$$m^* = 0,7528 \text{ for } m = 1,$$

$$m^* \approx m - 0,25 \text{ for } m = 2, 3, 4.$$

### 3.2 Cylindrical panel fixed at vertical stiffeners and fixed along curved edges while free to move in x-direction

Boundary conditions at  $y = \pm a/2$  stated in Section 3.1 do apply again, and boundary conditions at  $x = 0, b$  taking the form  $u' = v = w = w' = 0$  are satisfied by the shape functions, Eqs. 10, and by the following functions  $w_m(y)$  and  $w_n(x)$ :

$$\left. \begin{aligned} w_m(y) &= \cos 2m^*\pi\eta - \frac{\cos m^*\pi}{\cosh m^*\pi} \cosh 2m^*\pi\eta, \\ w_n(x) &= \sin n^*\pi\xi - \sinh n^*\pi\xi - \\ &\quad - \frac{\sin n^*\pi - \sinh n^*\pi}{\cos n^*\pi - \cosh n^*\pi} (\cos n^*\pi\xi - \cosh n^*\pi\xi), \end{aligned} \right\} \quad (11)$$

in which

$$m^* = 0,7528 \text{ for } m = 1,$$

$$m^* \approx m - 0,25 \text{ for } m = 2, 3, 4,$$

$$n^* = 1,5056 \text{ for } n = 1,$$

$$n^* \approx n + 0,5 \text{ for } n = 2, 3, 4.$$

### 3.3 Numerical results expressed in terms of nondimensional parameters of web panel geometry

In Fig.3 there are shown normal displacements  $w$  at middle section of a square web panel ( $a = b$ ) for both sets of boundary conditions stated in Sections 3.1 and 3.2 and three different stress patterns characterized by the ratio of the upper edge stress to the lower edge stress, i.e. by  $\varepsilon = \bar{\sigma}_{yu} / \bar{\sigma}_{yl}$ , equal

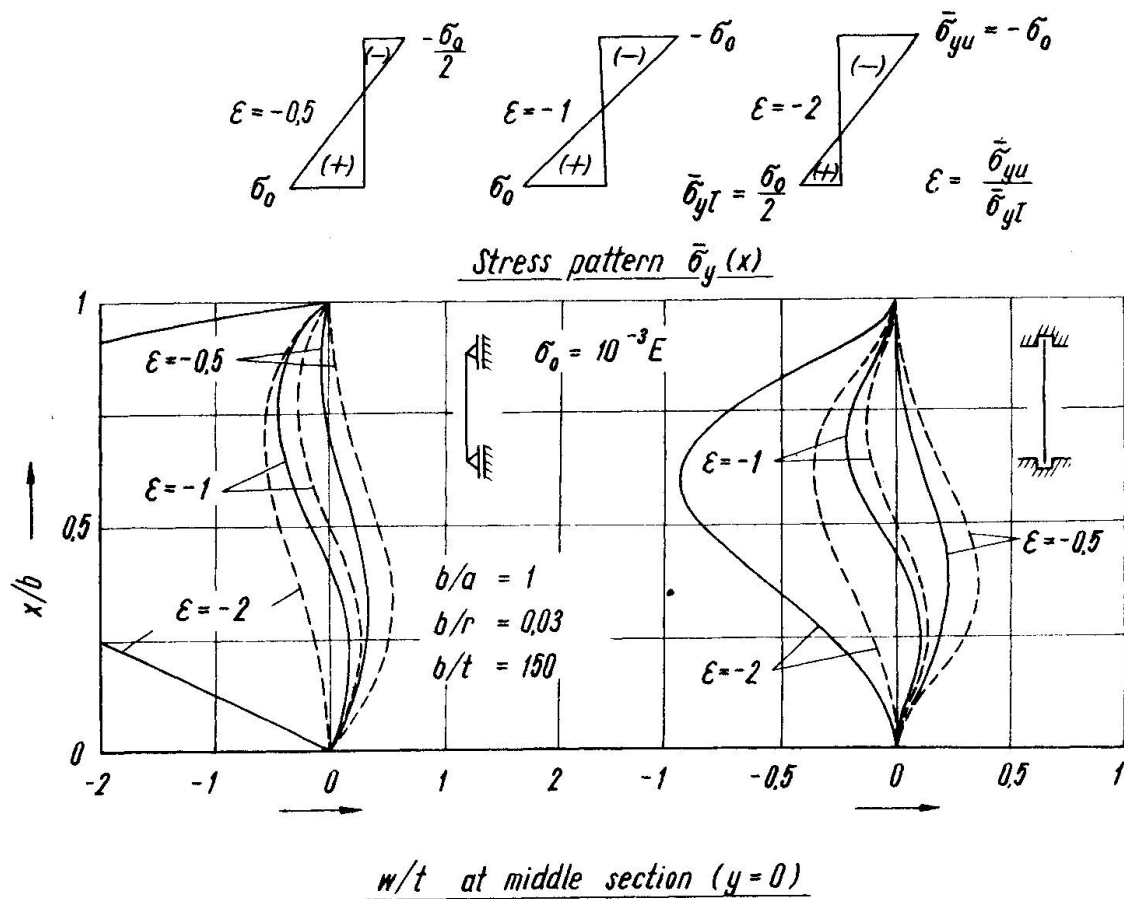


Fig. 3

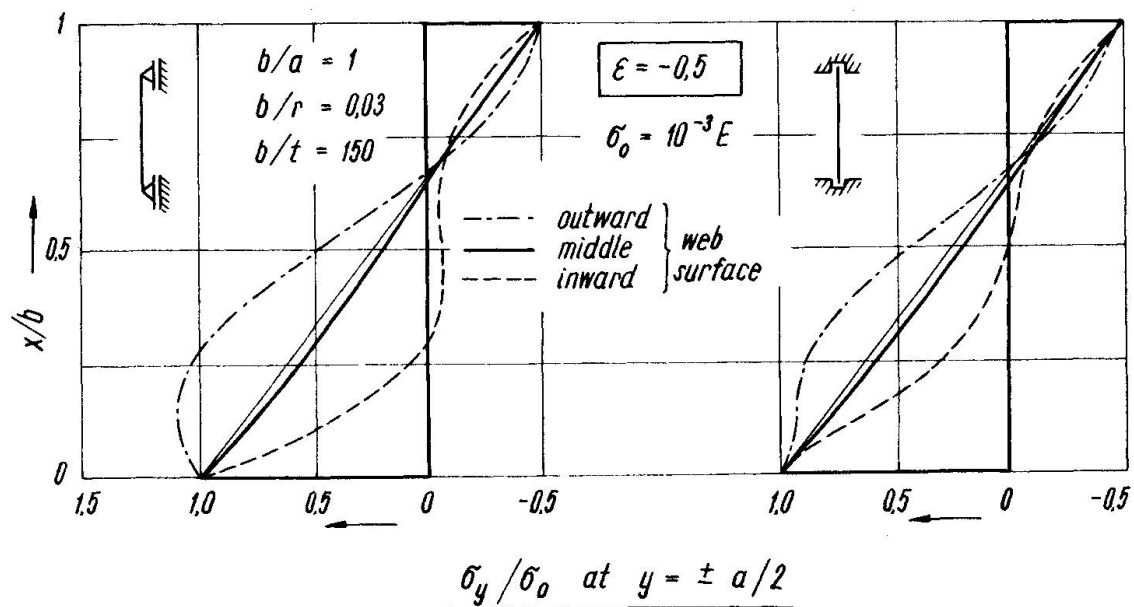


Fig. 4

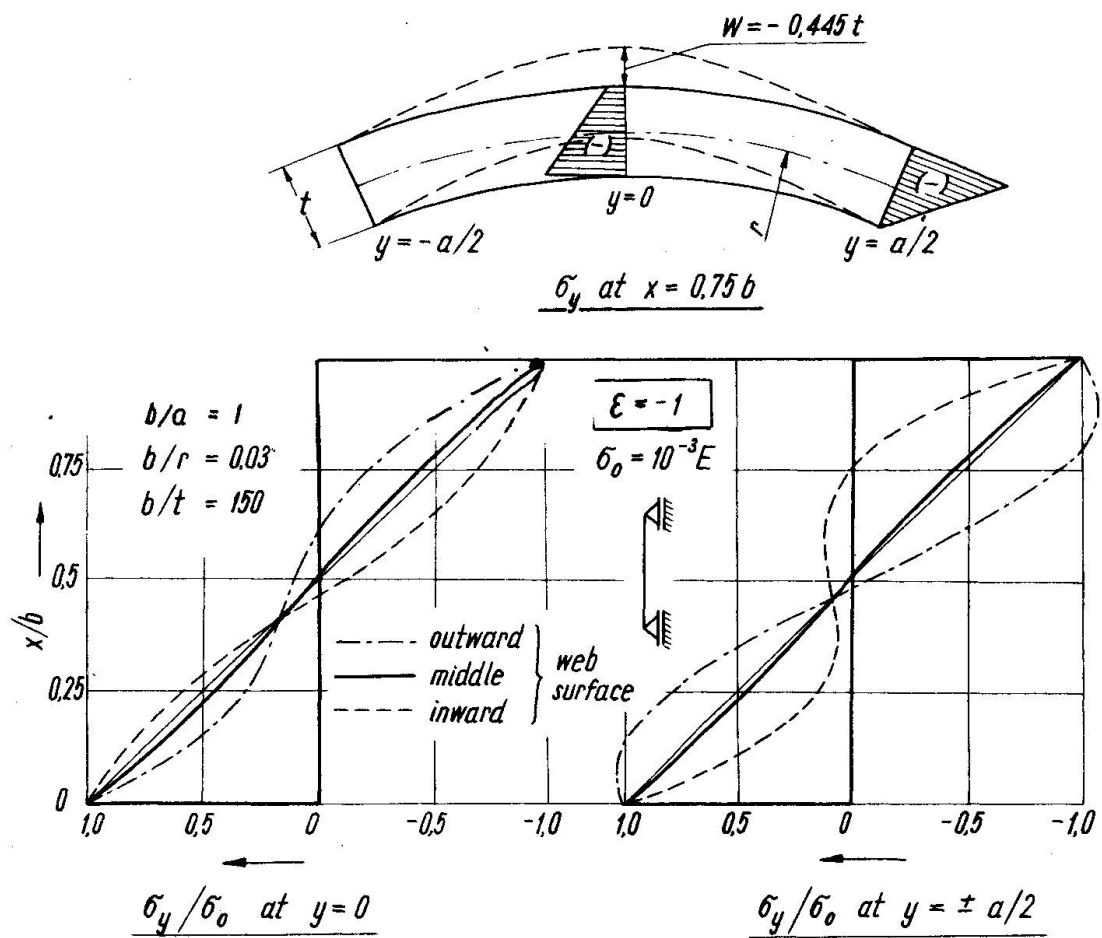


Fig. 5

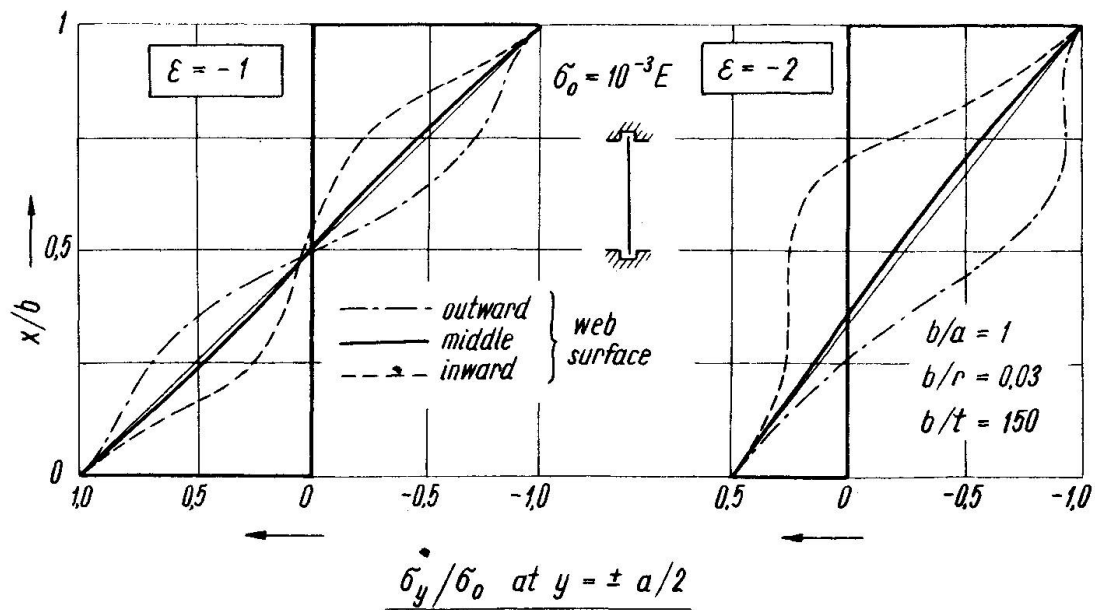


Fig. 6



to -0,5, -1,0 and -2,0. The curves of  $w/t$  (solid lines) have been calculated for indicated nondimensional parameters  $b/a$ ,  $b/r$ ,  $b/t$  and the stress level  $\sigma_0 = 10^{-3}E = 2100 \text{ Kp/cm}^2$ ,  $\sigma_0$  being the higher of the absolute values of edge stresses  $\bar{\sigma}_{yu}$  and  $\bar{\sigma}_{yl}$ . Poisson's ratio equal  $\nu = 0,3$  has been assumed.

As seen from inspection of diagrams on left-hand side of Fig.3,  $w/t$ -values for  $\epsilon = -2$  (solid line) fall beyond the range of validity of (second-order) theory of small deflections. Of course, they are somewhat exaggerated because for most of the panel area the final membrane forces  $|n_y(x)|$  are smaller than membrane forces  $|\bar{n}_y(x)|$  assumed in the third Eq.(4) - see Figs. 4 to 6 for comparison. Values obtained by first-order theory of cylindrical shells (dashed lines in Fig.3) do not convey a true picture of deformation of cylindrical web panels with relatively large radii of curvature. From comparison of diagrams in Fig.3, a favorable effect of fixity of web panel at the junction with curved flanges on limiting deflections is evident.

The stresses are of primary interest to designers. Longitudinal stresses  $\sigma_y$  in the middle web surface and on the outward and inward web surfaces are shown in Figs. 4 to 6. The curves of Fig.4 pertain to stress pattern with  $\epsilon = -0,5$ . Stresses at end section of the panel are plotted for both boundary conditions considered. Diagrams of Fig.5 pertain to  $\epsilon = -1$  and panels with simply supported curved edges, while those of Fig.6 refer to panels with fixed curved edges and two stress ratios:  $\epsilon = -1$  and  $\epsilon = -2$ .

Extremal values of normal deflection  $w$  with a corresponding ordinate  $x$  at which these values do occur are assembled for comparison in Tables 1 and 2, for two sets of boundary conditions considered. Several values of parameters  $\epsilon$ ,  $r/b$ ,  $a/b$  and  $t/b$ , and two stress levels:  $\sigma_0 = 10^{-3}E = 2100 \text{ Kp/cm}^2$  and  $\sigma_0 = (2/3)10^{-3}E = 1400 \text{ Kp/cm}^2$  are taken into account.

Tables 1 and 2 also comprise extremal values of stress increase on either surface of web panel, in the tension and the compression zone of the panel. The stress increase above the initial value  $\bar{\sigma}_y(x) = \bar{n}_y(x)/t$  at a distinct point with ordinate  $x$  is equal to

$$\Delta\sigma_y = \left( \frac{n_y}{t} \pm \frac{6m_y}{t^2} \right) - \frac{\bar{n}_y}{t} \quad (12)$$

Table 1. Extremal values of normal displacement  $w$  and of stress increase  $\Delta\sigma_y$  in cylindrical web panels simply supported along curved edges

Nondimensional parameters			Stress level $\sigma_0$ ( $10^{-3}E$ )	Extremal normal displacement at middle section				Extremal stress increase				
r/b	a/b	t/b		in tension zone		in compression zone		at middle section		at end section		
				w/t	at x/b	w/t	at x/b	in tension zone	in compression zone	in tension zone	in compression zone	
Stress pattern $\varepsilon = -0,5$												
33,3	0,5	1/100	2/3	0,016	0,25	-0,004	0,85	0,083	-0,024	0,189	-0,054	
			1	0,022	0,25	-0,006	0,85	0,077	-0,023	0,184	-0,054	
	1,0	1/150	2/3	0,047	0,25	-0,013	0,85	0,102	-0,034	0,259*	-0,080	
			1	0,063	0,25	-0,019	0,85	0,090	-0,034	0,244*	-0,080	
	100	0,5	1/100	1	0,130	0,30	-0,006	0,90	0,101	-0,026	0,328*	-0,049
				1/150	1	0,318	0,30	-0,018	0,90	0,091	-0,021	0,403*
Stress pattern $\varepsilon = -1,0$												
33,3	0,5	1/100	2/3	0,013	0,20	-0,015	0,80	0,071	-0,085	0,162	-0,176	
			1	0,019	0,20	-0,022	0,75	0,068	-0,089	0,159	-0,180	
	1,0	1/150	2/3	0,040	0,20	-0,055	0,80	0,094	-0,141	0,228	-0,276	
			1	0,056	0,20	-0,092	0,80	0,087	-0,160	0,218	-0,293	
	100	0,5	1/100	1	0,069	0,20	-0,104	0,75	0,073	-0,106	0,223	-0,258
				1/150	1	0,186	0,20	-0,445	0,75	0,082	-0,193	0,305
Stress pattern $\varepsilon = -2,0$												
33,3	1,0	1/100	1	-	-	-0,305	0,65	0,143	-0,290	0,192	-0,492*	
		1/150	1	-	-	-4,700	0,65	-	-2,518	-	-1,505*	

and is related to stress level  $\sigma_0$ .

With regard to extremal values of normal stresses  $\sigma_y$  on web surfaces the following observations should be made. As the extremal value of  $\Delta\sigma_y$  in cylindrical panels simply supported along curved edges occurs at some distance from the curved edge, the sum  $|\sigma_y| = |\sigma_y + \Delta\sigma_y|$  at that point falls in most cases below  $\sigma_0$ . Exceptional cases are indicated by an asterik in Table 1. In those cases extremal values of the sum  $|\sigma_y + \Delta\sigma_y|$  are higher than  $\sigma_0$ .

In cylindrical panels fixed along curved edges bending moments  $m_y = \nu m_x$  do occur along those edges (with the exception of corner points where  $m_x = m_y = 0$ ) and, accordingly, the sum  $|\sigma_y + \Delta\sigma_y|$  at the curved edges is higher than  $\sigma_0$ . This being taken into account, the extremal values of  $\Delta\sigma_y$  at middle section given in Table 2 refer to field or edge points of that section, wherever the absolutely largest value does occur.

Normal stresses  $\sigma_x \equiv \Delta\sigma_x$  due to bending moments  $m_x$  deserve attention. For example,  $\sigma_x$  at upper edge of middle section of a web panel with  $\epsilon = -1$ ,  $r/b = 33,3$ ,  $a/b = 1$ ,  $t/b = 1/150$  according to Table 2 is equal to  $\sigma_x = \Delta\sigma_y/\nu = -0,129 \sigma_0/\nu = -0,43 \sigma_0$ . For  $\epsilon = -2$  it is even higher compare last line of Table 2, but still below the approximate upper limit  $\sqrt{3/(1-\nu^2)} \sigma_0 = 1,81 \sigma_0$  derived from a solution to a case of rotational symmetry. (Normal stresses  $\sigma_x$  due to bending moments  $m_x$  at the joints of web panels and flanges are of secondary importance as far as ultimate strength of the girder is concerned. However, they are significant in design of welded joints for fatigue strength.)

Shear stresses  $\tau_{xy} = n_{xy}/t$  resulting from transverse deflection of the cylindrical panel are, in the considered range of curvatures, very small and amount to a few percent of  $\sigma_0$ .

#### 4. Results and conclusions

Calculations based on second-order small deflections theory for two stress levels, situated in the range of working and yield stresses of structural steel, do not provide full insight into behaviour of thin cylindrical webs in curved plate girders with increasing load. Displacements and stresses in the considered range increase virtually in proportion to load (i.e. to stress level  $\sigma_0$ ) and to girder curvature (i.e. to  $1/r$ ). More

Table 2. Extremal values of normal displacement  $w$  and of stress increase  $\Delta\sigma_y$  in cylindrical web panels fixed along curved edges with free displacement in x-direction

Nondimensional parameters			Stress level $\sigma_0$ $10^{-3}E$	Extremal normal displacement at middle section				Extremal stress increase					
r/b	a/b	t/b		in tension zone		in compression zone		at middle section		in compression zone		at end section	
				w/t	at x/b	w/t	at x/b	in tension zone	at x/b	$\Delta\sigma_y/\sigma_0$	at x/b	$\Delta\sigma_y/\sigma_0$	at x/b
Stress pattern $\epsilon = -0,5$													
33,3	0,5	1/150	1	0,051	0,30	-0,011	0,80	0,073	0,25	-0,022	0,80	0,205	-0,053
	1	1/150	1	0,223	0,35	-0,001	0,90	0,112	0	-0,022	0,70	0,294	-0,041
100	0,5	1/150	1	0,017	0,30	-0,004	0,80	0,026	0,25	-0,008	0,80	0,070	-0,018
	1	1/150	1	0,079	0,35	-		0,039	0	-0,007	0,70	0,108	-0,015
Stress pattern $\epsilon = -1,0$													
33,3	0,5	1/100	1	0,014	0,25	-0,018	0,75	0,051	0,25	-0,068	0,75	0,121	-0,138
		1/150	1	0,041	0,25	-0,071	0,75	0,063	0,25	-0,125	0,75	0,167	-0,225
	1,0	1/100	1	0,036	0,25	-0,048	0,70	0,065	0	-0,076	1,0	0,137	-0,153
		1/150	1	0,101	0,25	-0,197	0,70	0,088	0	-0,129	1,0	0,186	-0,227
100	0,5	1/100	1	0,004	0,25	-0,006	0,75	0,018	0,25	-0,024	0,75	0,041	-0,047
		1/150	1	0,014	0,25	-0,024	0,75	0,023	0,25	-0,044	0,75	0,057	-0,077
	1,0	1/100	1	0,012	0,25	-0,017	0,70	0,022	0	-0,026	1,0	0,047	-0,053
		1/150	1	0,034	0,25	-0,070	0,70	0,029	0	-0,045	1,0	0,071	-0,076
Stress pattern $\epsilon = -2,0$													
33,3	1,0	1/100	1	-		-0,154	0,60	0,064	0,30	-0,145	1,0	0,093	-0,285
		1/150	1	-		-0,934	0,60	0,221	0,30	-0,457	0,65	0,242	-0,422

relevant are the following observations: with increasing distance between vertical stiffeners deflections grow very markedly; stresses do increase as well, but to a lesser degree. A reduction of web thickness results in a very pronounced increase of deflections; remarkably enough, bending stresses become higher as well.

Flexibility of vertical stiffeners in real structures would cause a further increase of deflections and bending stresses at middle sections of web panels. Only the results obtained by ordinary (first-order) theory of cylindrical shells are available for comparison. It can be inferred from them that in moderately stiffened cylindrical panels - as is the case with plane webs designed for stability and not for ultimate strength - this increase can be as high as by one third or more

In general, displacements and additional stresses due to bending under design conditions remain within acceptable limits in the parameter range considered. As evident from Figs. 4 to 6, the mean membrane stresses  $\sigma_y$  drop only slightly - as the result of transverse web deflection - from the originally assumed linear pattern. Consequently, the reduction of web-area contribution to overall section modulus of the curved girder amounts only to a few percent and is insignificant.

#### 5. Scope of further research

A more intrinsic analysis by large deflections theory is needed to clarify the performance of thin cylindrical webs under loads well in excess of working loads - in particular, when extremely thin webs are investigated. Presumably, for higher loads, still within elastic range, deformed configuration characterized by one half-wave in longitudinal direction changes into another one with more half-waves.

Web performance under an initial stress pattern which includes longitudinal stresses  $\bar{\sigma}_y$  as well as shear stresses  $\bar{\tau}_{xy}$  remains to be investigated.

Experimental work is necessary, i.e. to check the influence of plastic zones on ultimate strength of thin cylindrical webs.

Acknowledgement. The results presented in this paper have been obtained by J. Wachowiak in 1966 in the course of prepa-

ration of his dissertation [6], under the guidance of the senior author, at the Department of Civil Engineering, Technical University, Gdańsk.

### References

- [1] Dąbrowski, R.: Gekrümmte dünnwandige Träger. Springer-Verlag, Berlin-New York, 1968.
- [2] Marguerre, K.: Theorie der gekrümmten Platte grosser Formänderung. Proceedings 5th Intern. Congress of Appl. Mech., Cambridge, Mass., 1938.
- [3] Volmir, A.S.: Gibkiye plastinki i obolochki. Gos. izdat. tekhn.-tjeoret. lit., Moscow, 1956.
- [4] Flügge, W.: Stresses in Shells. Springer-Verlag, Berlin-Heidelberg, 1960.
- [5] Kornishin, M.S.: Nielinieynye zadachi tieorii plastin i pologikh obolochek i mietody ikh resheniya. Izdat. Nauka, Moscow, 1964.
- [6] Wachowiak, J.: Obliczenie środniaka zakrzywionej belki cienkościennej na podstawie teorii powłok. Diss., Politechnika Gdańska, Gdańsk, 1967.

### SUMMARY

Stresses and displacements in thin cylindrical webs of curved plate girders are analysed on the basis of second-order theory of small deflections by means of Galerkin's method. A cylindrical web panel (Fig. 2) rigidly supported along curved edges and fixed along straight edges (at vertical stiffeners) is considered. Stresses on middle web surface and on outward and inward web surfaces as well, at end and middle section of the web panel, are shown in Fig. 4 to 6. Numerical results are assembled in Tables 1 and 2.

### RESUME

Les auteurs déterminent les contraintes et les déflexions de l'âme mince cylindrique des poutres courbes, en utilisant la théorie du second ordre pour les petites déformations à l'aide de la méthode de Galerkin. On considère un panneau d'âme cylindrique appuyé le long des membrures et encastré au droit des raidisseurs verticaux. Les figures 4 à 6 représentent les contraintes de la surface moyenne ainsi que des surfaces intérieure et extérieure, aux extrémités et au milieu du panneau d'âme. Les tableaux 1 et 2 contiennent des résultats numériques.

### ZUSAMMENFASSUNG

Spannungen und Verformungen in dünnwandigen, kreiszyklindrischen Stegen von gekrümmten Vollwandträgern werden aufgrund der Theorie II. Ordnung für kleine Verschiebungen, mit Hilfe des Galerkin'schen Verfahrens untersucht. Es wird eine Teilschale (Fig. 2), die an gekrümmten Rändern starr gestützt und an geraden Rändern (an den Vertikalsteifen) eingespannt ist, betrachtet. Spannungen in der Mittel- fläche sowie an der äusseren und inneren Schalenoberfläche, im Endquerschnitt bzw. Mittelquerschnitt der Teilschale, werden in Abb. 4 bis 6 gezeigt. Zahlenresul- tate sind in den Tafeln 1 und 2 zusammengestellt.



### III

#### **Strength of Thin Plate Girders with Circular or Rectangular Web Holes without Web Stiffeners**

Résistance des poutres à âme mince non-raïdiées, comportant des ouvertures rondes ou rectangulaires

Festigkeit dünnwandiger, unverteifter Blechträger mit runden oder rechteckigen Stegaussparungen

**TORSTEN HÖGLUND**

Techn. lic.

Department of Building Statics and  
Structural Engineering of The Royal  
Institute of Technology  
Stockholm, Sweden

#### 1. INTRODUCTION

The thin plate I-girder has become a frequently used element in roof constructions. This has been possible by the use of rational methods of fabrication and design. One essential point is to avoid web stiffeners, which have to be manually fitted and welded and thus cause considerable costs.

In modern buildings there are often a lot of service ducts and pipings which due to limited construction height intersect the steel structure. The necessary holes in the girder webs have previously been reinforced, mainly due to the lack of knowledge of the buckling conditions of perforated webs. In order to cut costs web stiffeners should be avoided even at such weakenings as holes in the web.

The web of rolled beams are thick and it is usually sufficient to check the stress concentrations around the holes. For thin plate girders web buckling at the holes has to be considered. Only if the postbuckling strength is made full use of web stiffeners around large holes can be avoided in plate girders with thin web.

Very few investigations about buckling of thin plate girder webs with holes has been published [1] and the author has not found any theoretical investigations of the postbuckling strength in the literature. This paper deals with experimental and theoretical study of the strength of statically loaded plate I-girders with circular or rectangular web holes. Girders with very thin web are treated. A more extensive report has been published in Swedish [3]. The distance between holes and web stiffeners is supported to be so large that the web alone must prevent the flanges from vertical buckling.





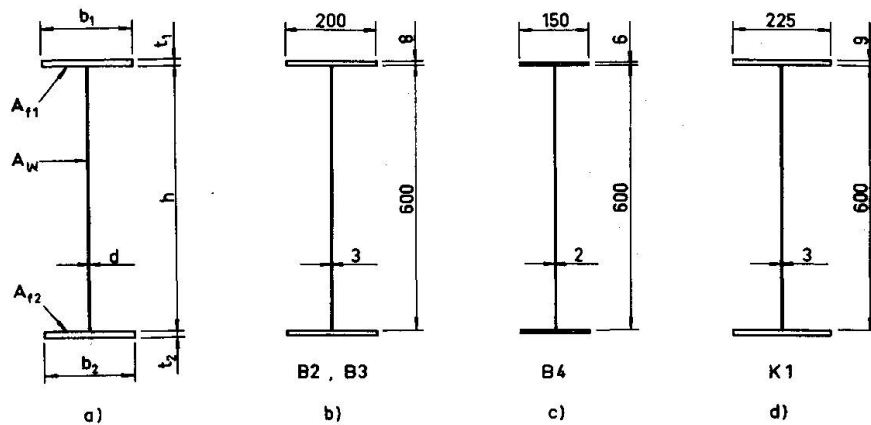


Fig. 2 a) Notations for cross section  
b), c) och d) Girder cross sections for the  
test girders.

The test girders were fabricated from flamecut flange- and webplates in an automatic welding machine. The holes were sawed and the edges around the holes were grinded. Details of the test girders are given in table 1.

The surface strains at points around the holes in the web and in the flanges were measured with electrical strain gauges. The web deflections near the holes and the centerline deflection were measured with dial gauges.

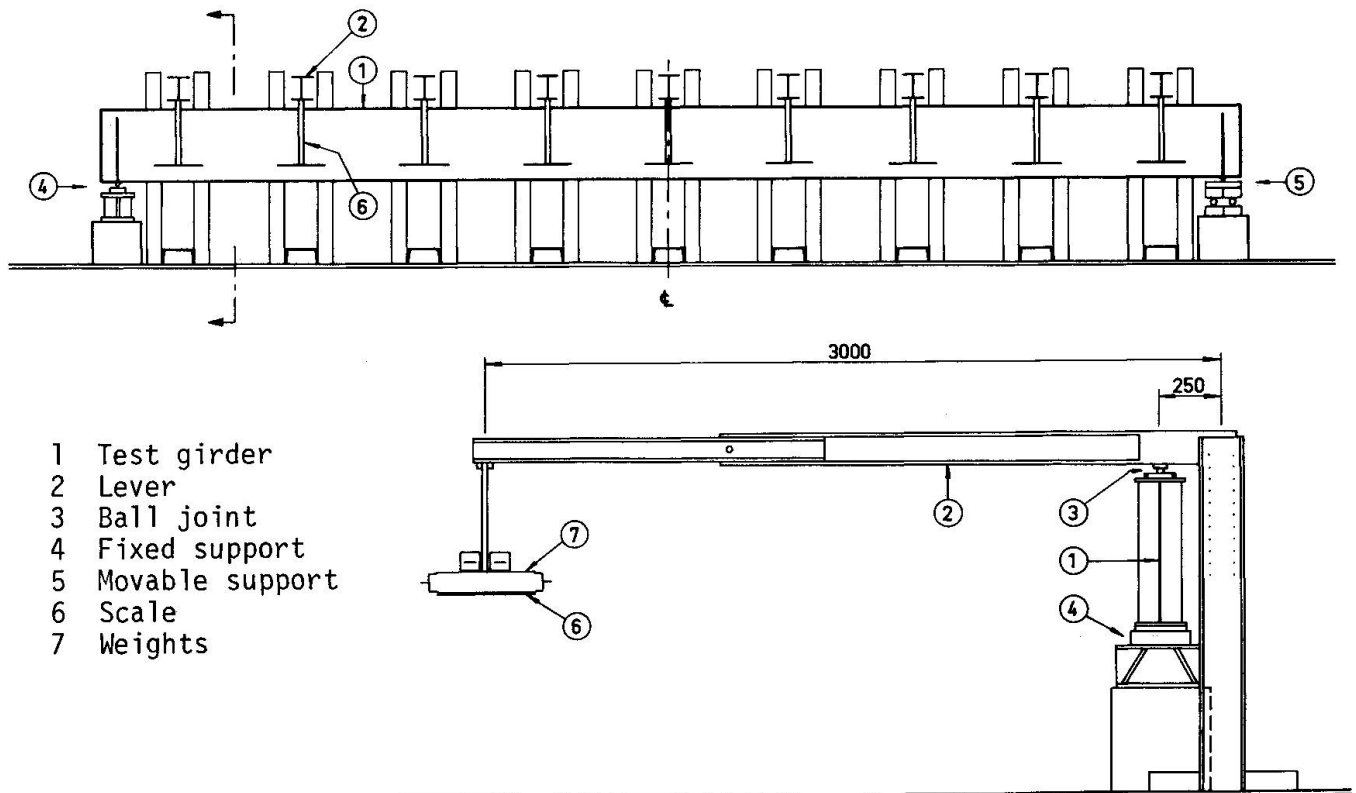


Fig. 3 Test setup.

### 3. TEST RESULT AND THEORY

Fig. 4, 5, 6 and 7 show the load deflection relationships of the test girders. The shear buckling load,  $P_{TCR}$ , for the web without holes calculated under the assumption that the web is simply supported, very long and subjected to constant shear, the buckling load in bending  $P_{\sigma cr}$  for the mid span of the girders, the load  $P_{\sigma su}$  which gives the bending moment  $\sigma_y \cdot 2I/h$  at the center of the girders and the load  $P_{\sigma red}$  which gives the reduced bending moment  $M_{red}$  according to Basler and Thürlimann [2] are given in the figures.

$$M_{red} = \frac{2I}{h} \sigma_y (1 - 0,0005 \frac{A_w}{A_f} (\frac{h}{d} - 5,7 \sqrt{\frac{E}{\sigma_y}}))$$

In fig. 4, 5, 6 and 7 are also given the ultimate loads for the girder sections with the holes ( $P_{br}^{HI}$  for hole H1 and so on). Finally the web deflection configurations at ultimate load and the stiffener arrangements round the holes after a testcycle to ultimate load are indicated in the figures.

Table 2 gives a summary of test results.

In the following some typical results of measured strain distributions and web deflection curves are given.

Table 2 Summary of test results. (1Mp = 2205 lb)

Test girder	Hole	P Mp	T Mp	$\tau$ kp/cm <sup>2</sup>	M Mpm	$\sigma$ kp/cm <sup>2</sup>	$\frac{\tau}{\tau_y}$	$\frac{\sigma}{\sigma_y}$
B2	H1	2,21	7,73	449	8,84	734	0,223	0,267
	H3	2,27	7,94	461	9,08	753	0,229	0,274
	H4	3,04	4,56	264	27,36	2270	0,131	0,825
	H2	3,25	4,87	283	29,25	2430	0,141	0,883
B3	H7	1,52	5,32	307	6,08	507	0,152	0,184
	H5	1,68	5,88	340	6,72	560	0,169	0,203
	H6	3,02	1,51	87	30,20	2517	0,043	0,915
B4	H8	1,07	3,74	312	4,28	636	0,193	0,209
	H9	1,40	0,70	58	14,00	2080	0,036	0,685
	H9A	2,00	0	0	16,00	2380	0	0,783
K1	H11	4,53	13,60	792	3,40	223	0,328	0,076
	H12	4,77	14,30	834	3,58	234	0,345	0,079
	H13	4,71	9,42	543	16,49	1080	0,229	0,366

#### 3.1 Circular holes.

##### 3.1.1 Shear force.

Fig. 8a shows the distribution of the tangential middle surface strains in the web around the hole H1 which was situated in a girder section essentially subjected to shear. Two stages are shown; one at a load lower than the buckling load and one near the ultimate load. When the load is small the

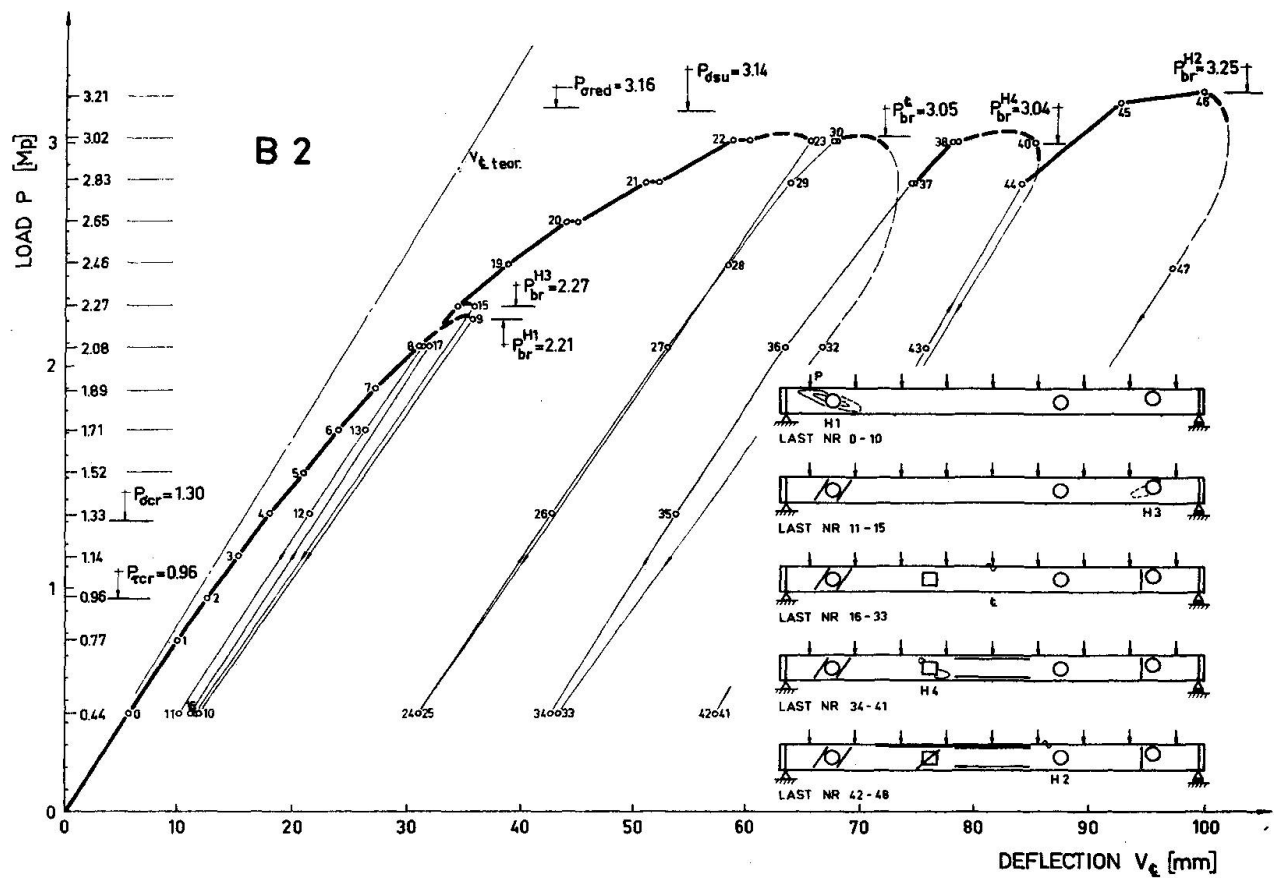


Fig. 4 Load-deflection curve of girder B2.

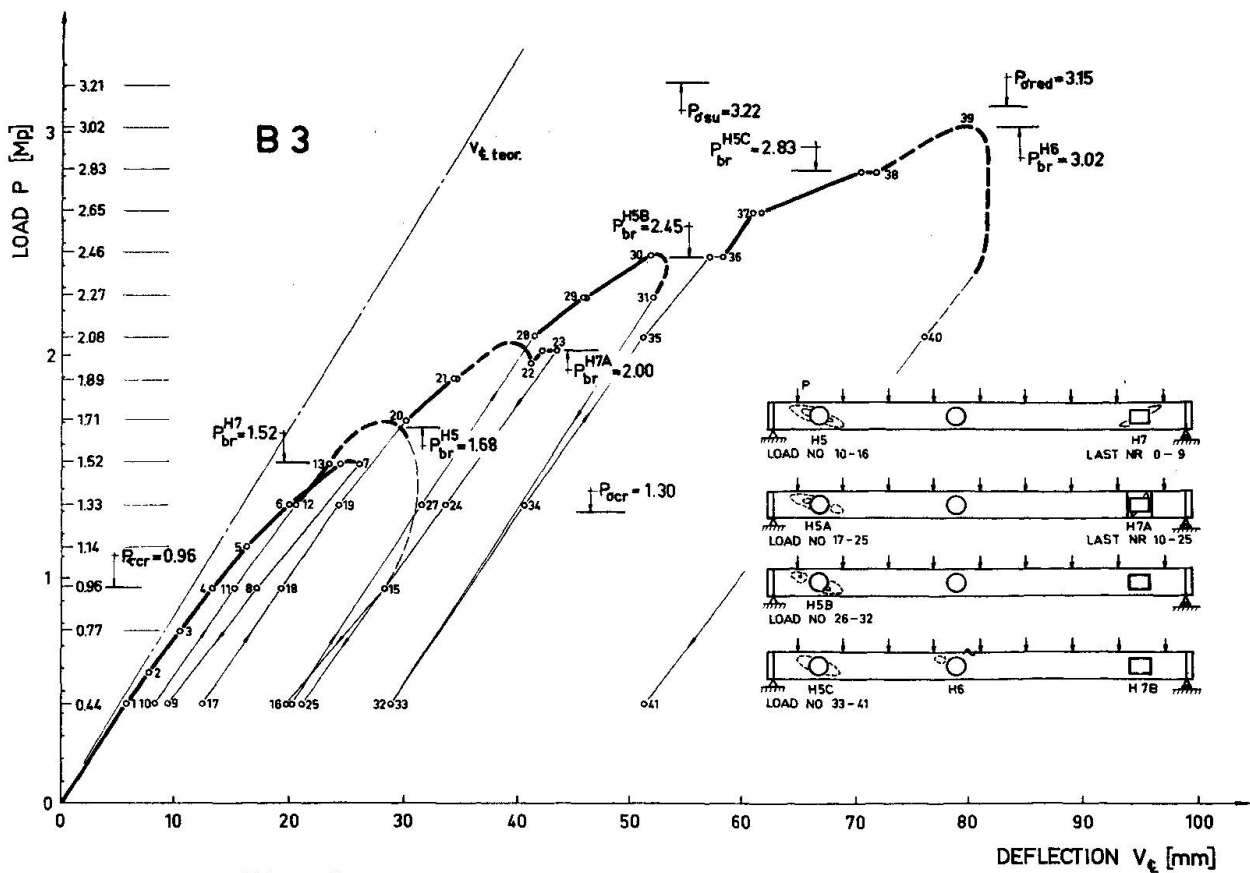


Fig. 5 Load-deflection curve of girder B3.

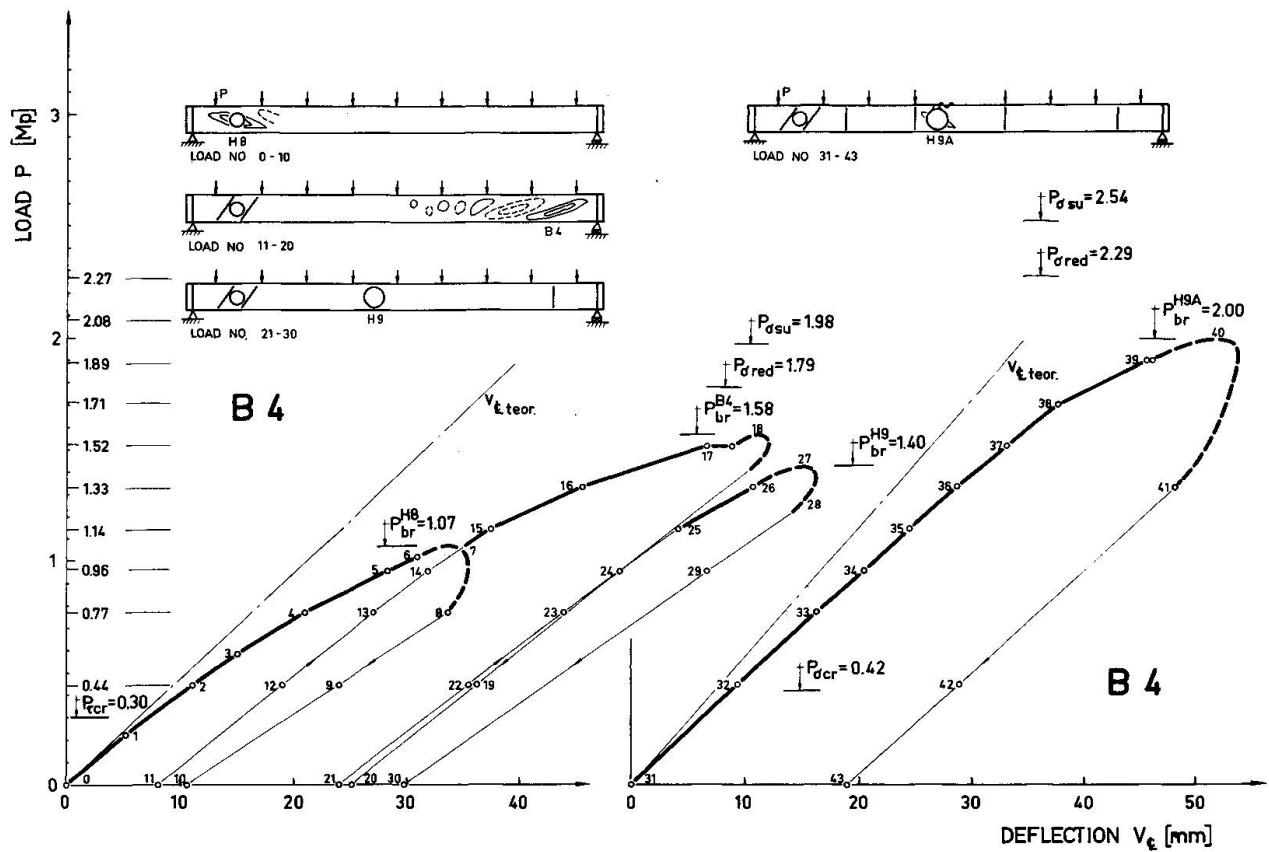


Fig. 6 Load-deflection curve of girder B4.

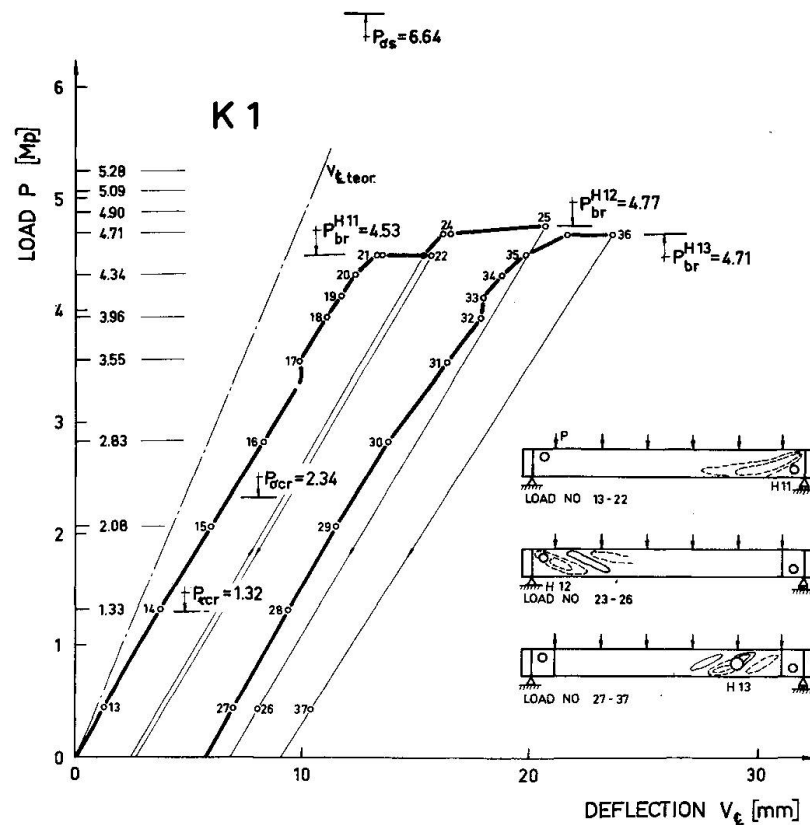


Fig. 7 Load-deflection curve of girder K1.

maximum tangential compressive and tensile strain is about of the same size. When the load is increased the compressive strain remains at a certain level while the tensile strain increases rapidly because of redistribution of stresses after web buckling and lokal yielding.

A model of a shear loaded girder section with a circular hole is shown in fig. 9. The web is supposed to consist of tension fields with the stress equal to the yield stress  $\sigma_y$  and compression fields with a stress estimated as the elastic buckling stress for a web strip with the buckling length  $\ell$ , see fig. 9. The inclinations of the tension and compression fields are postulated to be those which furnish the greatest total vertical shear component of the fields.

The diagram in fig. 10 shows curves for the calculated ultimate load as a function of the web slenderness ratio and the size of the hole. The results of the tests of girders with circular web holes in sections essentially loaded in shear are compared with calculated ultimate loads in fig. 10 and in table 3.

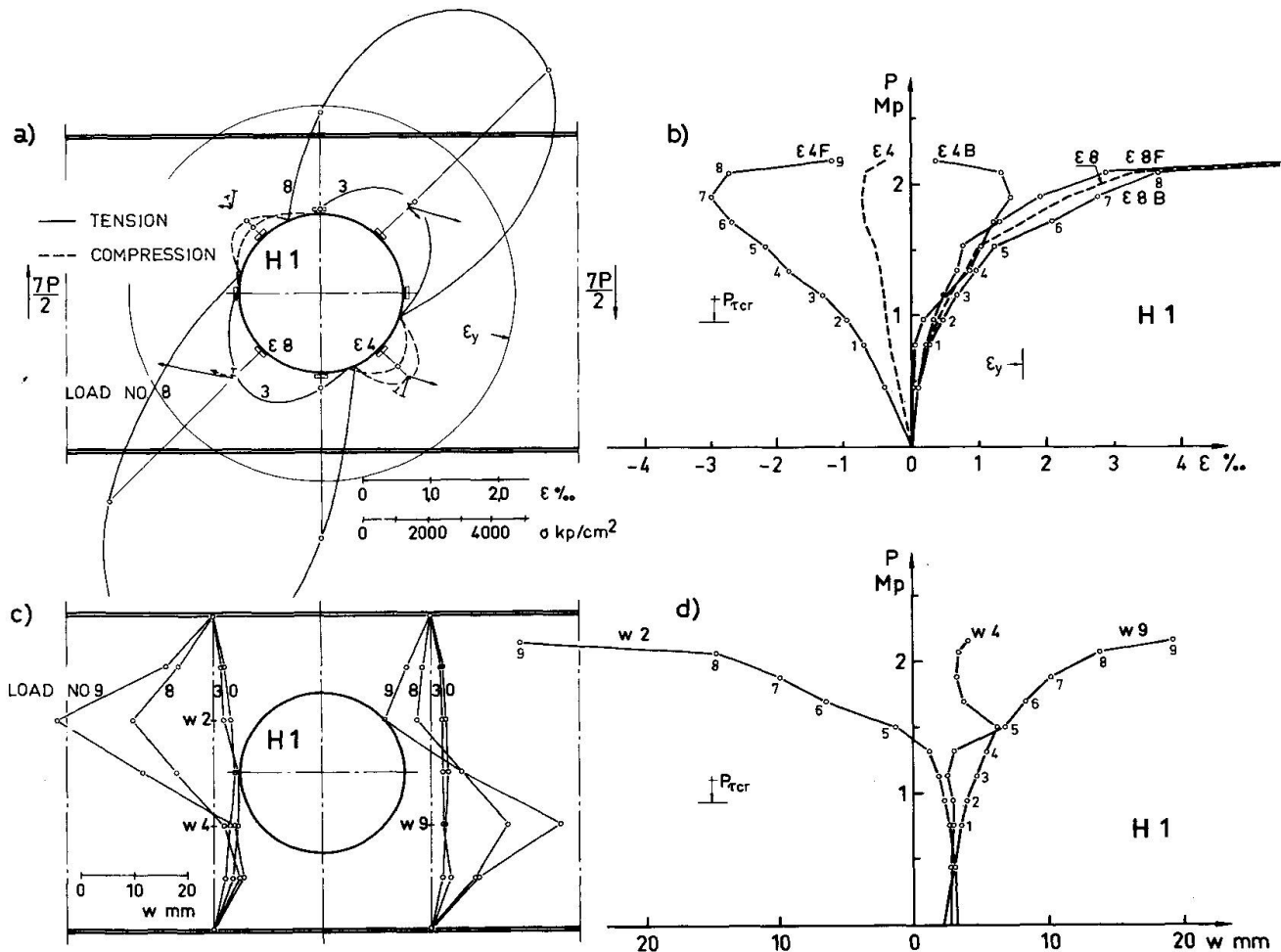


Fig 8 Web strains and web deflections at hole H1.

- Tangential mean strains and principal mean stresses in the web evaluated from measurements with strain rosettes.
- Tangential strain in the points  $\epsilon 4$  and  $\epsilon 8$  see fig. a).  $\epsilon 4f$  and  $\epsilon 8f$  are the strains in the front surface,  $\epsilon 4B$  and  $\epsilon 8B$  are the strains in the back surface of the web. The dashed lines marked  $\epsilon 4$  and  $\epsilon 8$  are the mean stresses in point  $\epsilon 4$  and  $\epsilon 8$ .
- Web deflections in ten points near the hole.
- Load-web deflection curves for points  $w 2$ ,  $w 4$  and  $w 9$ , see fig. c)



Table 3 Summary of test loads and theoretical ultimate loads for girders with circular web holes loaded with shear forces.

Hole	Girder	$\frac{D}{h}$	$\frac{h}{d}$	$\tau_y$ a) kp/cm <sup>2</sup>	$\tau_{cr}$ b) kp/cm <sup>2</sup>	$\alpha$ c)	$\frac{T_{th}}{T_y}$ d)	$\frac{T_u}{T_y}$ e)	$\frac{T_u}{T_{th}}$
H1	B2	0,51	202	2015	249	2,85	0,237	0,223	0,94
H3	B2	0,51	202	2015	249	2,85	0,237	0,228	0,96
H5	B3	0,67	202	2015	249	2,85	0,154	0,169	1,10
H8	B4	0,50	300	1617	113	3,78	0,187	0,193	1,03
H11	K1	0,25	210	2416	230	3,24	0,322	0,328	1,02
H12	K1	0,25	210	2416	230	3,24	0,322	0,345	1,07

a)  $\tau_y = \sigma_y / \sqrt{3}$  for the web plate

d)  $T_{th}$  = predicated ultimate load.

b)  $\tau_{cr} = 5,34 \frac{\pi^2 E}{12(1 - \nu^2)} \left(\frac{h}{d}\right)^2$

e)  $T_u$  = ultimate test load.

c)  $\alpha = \sqrt{\frac{\tau_y}{\tau_{cr}}}$

### 3.12 Bending moment

The distribution of the tangential middle surface strains in the web round the hole H6, situated in a section essentially subjected to bending moment is shown in fig 11a.

A possible mode of action is given in fig. 12. At a distance from the hole the stresses are not influenced of the hole and the stress distribution will be as shown to the right. As the web is thin the stress distribution on the compression side is not triangular. The tension force  $D_1$  and the compression force  $T_1$  corresponding to the parts of the stresses which cannot be transferred through the hole will be transferres downward and upward respectively to the remaining parts of the girder below and above the hole. The conditions of equilibrium leads to compressive stresses along the line B-A' and tensile stresses along A-B', which explains the tangential stress distributions in fig. 11a.

If the web is thin the compressive stress at C may produce buckling of the web, which reduces the compressive stress along B-A' and increases the stress at E.

On the compression side the stresses at E' leads to buckling of the web and an increase of the stresses in the compression flange. Furthermore the web buckling at E' causes an upward deflection of the compression flange above the hole. Downward buckling of the compression flange can take place at a distance from the hole at point A' in fig. 12 but hardly just above the hole.

The reduction of the bending strength of a girder with a centrically placed web hole is usually small because the flanges carry most of the bending moment. For this to be true the size of the hole must be restricted to avoid



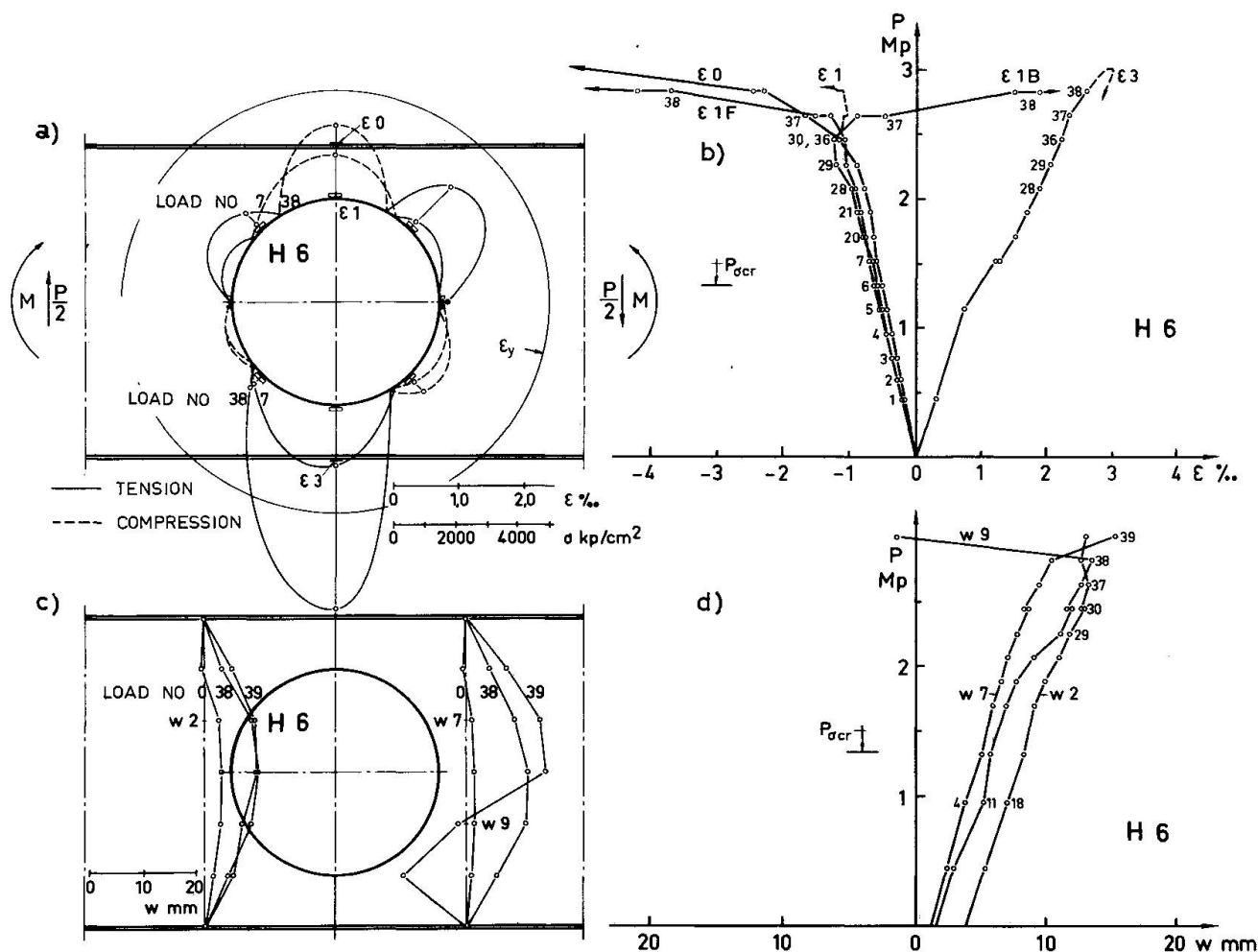


Fig. 11 Web strains and web deflections near hole H6, Notations compare fig 8.

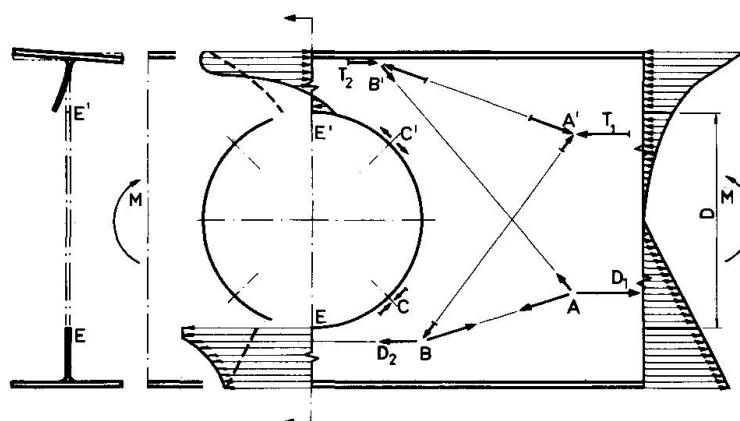
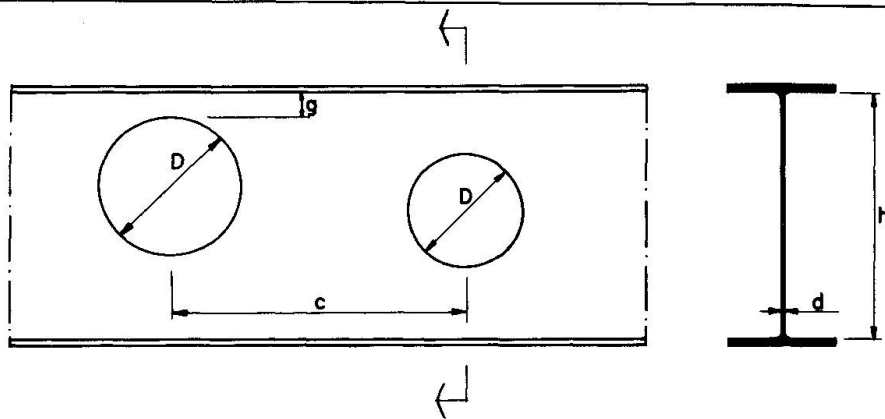


Fig. 12 Stress model for a girder with a circular web hole. Bending moment.

torsional buckling, upward or downward vertical buckling and lateral buckling of the compression flange over the hole. Such restrictions are given in fig. 13.



Allowable moment in the section through a hole:

$$M_D = M_{all} \left( 1 - \frac{d(h - 2g)^3}{12 \cdot I_x} \right)$$

$M_{all}$  = allowable moment without hole

$I_x$  = moment of inertia for the cross-section without hole.

Allowable shear force in the section through a hole:

$$T_D = \left(1 - \frac{D}{h}\right) T_{all} \quad \text{when } M \leq 0,6 M_D$$

$$T_D = \left(1 - \frac{D}{h}\right) \left(1 - \frac{M}{M_D}\right) \cdot 2,5 \cdot T_{all} \quad \text{when } M > 0,6 M_D$$

where

$$T_{all} = \left(\frac{0,26}{\alpha^2} + 0,10\right) h \cdot d \cdot \sigma_y \quad \text{when } 1 < \alpha < 2,72$$

$$T_{all} = \frac{1}{\alpha^2} h \cdot d \cdot \sigma_y \quad \text{when } 2,72 < \alpha$$

$$\alpha = 0,35 \frac{h}{d} \sqrt{\frac{\sigma_y}{E}}$$

$$g > 12d$$

$$D < 0,75h$$

$$c > D_{max}$$

Fig. 13 Design rules for thin walled plate girders with circular web holes. [4]

### 3.13 Shear force and bending moment.

The strength of a plate girder with a hole in a girder section subjected to shearing force and bending moment can be given with an interaction method. Fig. 14 shows possible interaction curves compared with test results.

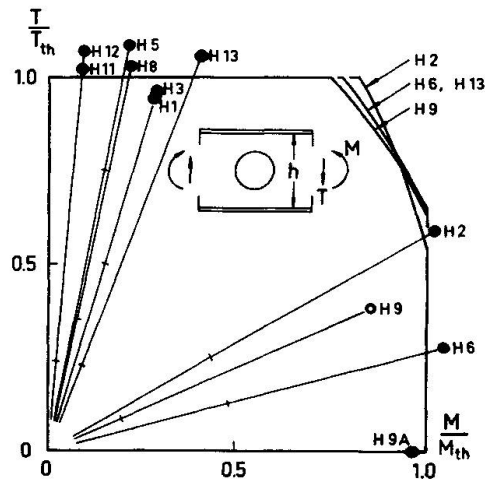


Fig. 14 Comparison between theory and test results for girders with circular holes.

### 3.2 Rectangular holes.

Stresses and web deflections are concentrated to the corners. A girder with a rectangular web hole may be described as a vierendeel truss with reduced bending capacity of the horizontal and vertical members at the compression corners, see fig. 15.

The risk of vertical buckling or lateral buckling of the compression flange is greater for girders with rectangular holes than for girders with circular holes for the same size of the holes. The size of the hole must therefore be restricted, see [3].

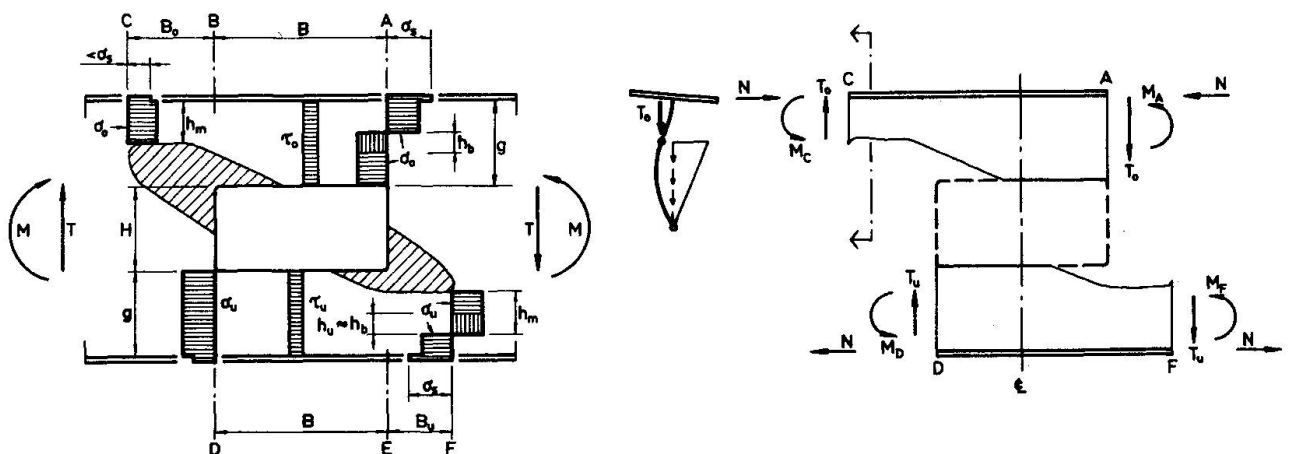


Fig. 15 Model for a girder with a rectangular web hole. Combined bending and shear.

#### 4. ACKNOWLEDGEMENT

This report is based on research work at the Department of Building Statics and Structural Engineering of the Royal Institute of Technology, Stockholm, Sweden. Head of the department is Professor Henrik Nylander whom the author wishes to thank for valuable support. The author also wishes to thank the Swedish Council for Building Research and Gränges Hedlund AB, Stockholm for sponsoring the investigation.

#### 5. REFERENCES

- [1] Rockey, K.C., Andersson, R.G. & Cheung, Y.K. The behaviour of square shear webs having a circular hole. P. 148-172 in Thin walled steel structures, ed. by Rockey and Hill, Crosby Lookwood, 1969.
- [2] Basler, K & Thürlimann, B. Strength of plate girders in bending. Journal Structural Division, ASCE, Aug. 1961.
- [3] Höglund, T. Bärförmåga hos tunnväggig I-balk med cirkulärt eller rektangulärt hål i livet (Strength of thin plate I-girders with circular or rectangular web holes). Bulletin nr 87 of the Division of Building Statics and Structural Engineering, The Royal Institute of Technology, Stockholm 1970. (In Swedish)
- [4] Provisoriska normer för svetsade stålbalkar, Typ HSI (Specifications for the design of welded steel girders, type HSI) Gränges Hedlund AB, Stockholm 1966. (In Swedish)

#### SUMMARY

This paper deals with an experimental and theoretical study of the strength of statically loaded plate I-girders with circular or rectangular web holes without web stiffeners. Girders with very thin web are treated. The web depth to thickness ratio ranges from 200 to 300. The load-carrying capacity is then delimited by web failure in the postbuckling range.

#### RESUME

L'auteur présente une étude expérimentale et théorique de la résistance statique des poutres en I non raidies, comportant des ouvertures rondes ou rectangulaires dans les âmes. Il s'agit de poutres à âme très mince, le rapport de la hauteur à l'épaisseur variant entre 200 et 300. La résistance ultime est ainsi limitée par la ruine de l'âme dans le domaine de voilement post-critique.

#### ZUSAMMENFASSUNG

Dieser Bericht behandelt eine experimentelle und theoretische Untersuchung über die Beanspruchung statisch belasteter Vollwandträger mit runden oder rechteckigen Stegaussparungen, aber ohne Stegaussteifungen. Es werden Träger mit sehr dünnen Stegen untersucht. Das Verhältnis der Stegdicke zur Höhe variiert zwischen 200 und 300. Damit ist die Traglast durch das Versagen des Steges im überkritischen Beulbereich beschränkt.

Leere Seite  
Blank page  
Page vide

### III

#### Essais sur le comportement post-critique de poutres en caisson raidies

Versuche über das überkritische Verhalten längsversteifter Kastenträger

Tests about Post-Critical Behaviour of Stiffened Box Girders

PIERRE DUBAS

Institut de Statique Appliquée  
et de Construction Métallique  
Ecole Polytechnique Fédérale  
Zurich, Suisse

#### INTRODUCTION

Les recherches expérimentales entreprises entre autres par MASSONNET [1-2], COOPER [3-4] et ROCKEY [5-6] ont prouvé que, pour les raidisseurs longitudinaux d'âmes fléchies, les rigidités relatives  $\gamma$  auxquelles conduit la théorie linéaire du voilement doivent être considérablement augmentées pour que les raidisseurs conservent toute leur efficacité dans le domaine post-critique. Une majoration des valeurs  $\gamma$  théoriques est évidemment nécessaire aussi pour les semelles comprimées de poutres-caissons raidies longitudinalement, poutres dont l'emploi est fréquent dans la construction des ponts, des engins de manutention lourds, des vannes, etc.

Le comportement post-critique de la semelle comprimée d'une poutre-caisson fixe pratiquement la valeur du moment limite: les âmes sont en effet très minces et n'apportent qu'une faible contribution à la résistance, même lorsqu'elles sont convenablement raidies. Lorsque les raidisseurs longitudinaux de semelle ne sont pas assez rigides, la sécurité à la ruine d'une poutre-caisson diminue donc dangereusement.

Pour dégrossir le problème, on a procédé à des essais préliminaires sur des poutres dont la semelle comprimée est raidie de différentes façons. On détermine ainsi expérimentalement l'ordre de grandeur de la majoration de rigidité nécessaire pour assurer un comportement optimum dans le domaine post-critique, jusqu'à la ruine.

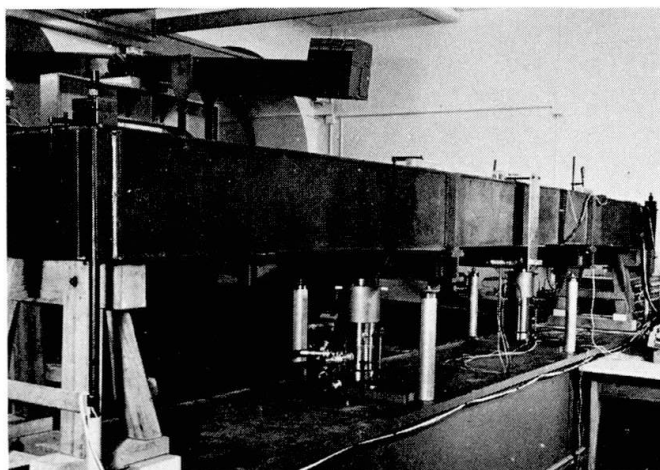
#### CONSTITUTION DES POUTRES D'ESSAI ET MODE DE CHARGE

Les dimensions des poutres auscultées sont relativement modestes, notamment en ce qui concerne la hauteur d'âme. Ces modèles ne permettent donc pas d'étudier l'influence réciproque des âmes sur les

semelles. Comme la constitution des semelles tendues ne modifie pratiquement pas le comportement de la membrure comprimée, ces semelles sont concentrées au bord des âmes, ce qui facilite la fabrication ainsi que la pose de l'appareillage.

La figure 1 (page 369) donne les dimensions principales des deux poutres du type A, comportant une semelle comprimée de 3 mm, raidie par trois nervures espacées de 200 mm. Pour les deux poutres du type B la disposition est analogue mais la membrure comprimée, forte de 4 mm, comprend seulement trois panneaux de 200 mm; la section est ainsi la même que pour le type A. Les poutres A2 et B2 ont des raidisseurs longitudinaux en plats de 36-3, disposés d'un seul côté, et des raidisseurs transversaux de 45-3. Pour les poutres A1 et B1, par contre, les raidisseurs sont beaucoup plus rigides.

Les efforts sont appliqués symétriquement, avec un bras de levier de 1,70 m (fig. 1); la partie centrale de la poutre, seule auscultée, est ainsi soumise à une flexion pure. La figure 2 donne une idée d'ensemble de l'essai sur la poutre A2.

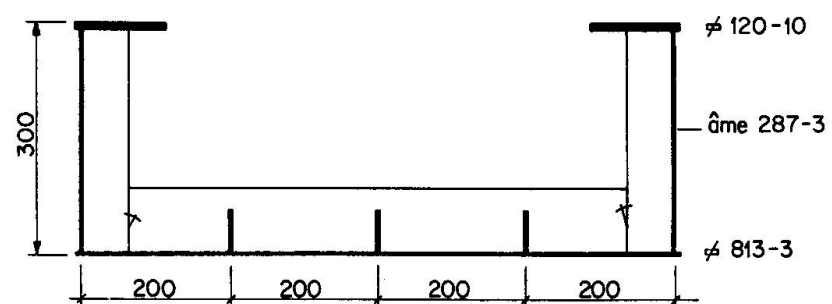
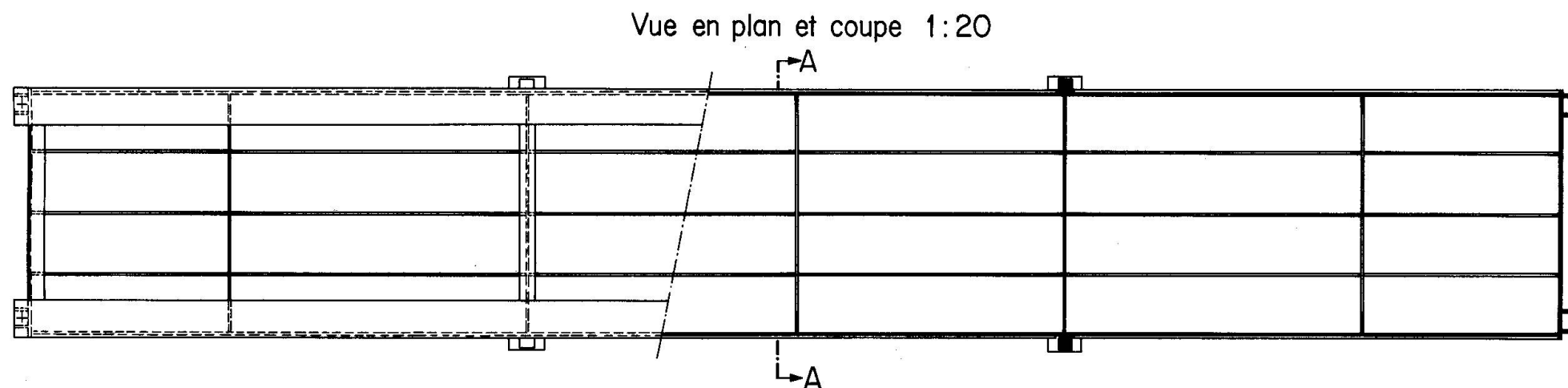
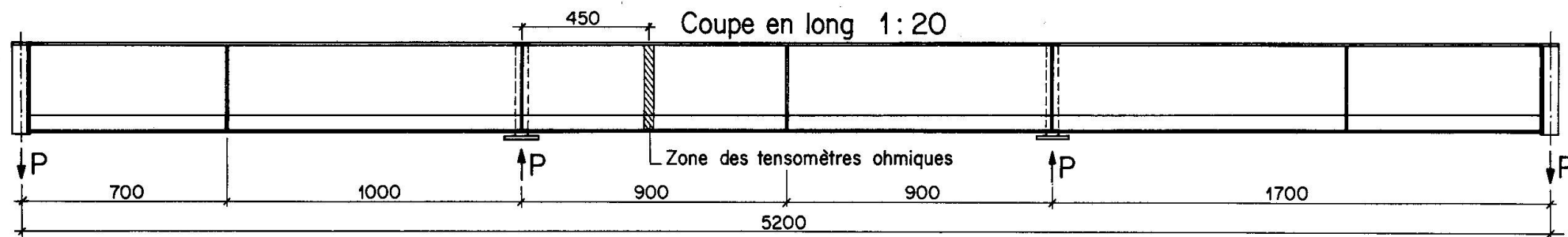


#### CRITÈRE DE DIMENSIONNEMENT DU RAIDISSAGE DES POUTRES D'ESSAI

##### a) Rigidités $\gamma$ d'après la théorie linéaire du voilement

Les rigidités nécessaires dans le domaine post-critique sont à exprimer en multiple des valeurs  $\gamma$  classiques; il convient dès lors de calculer d'abord ces rigidités  $\gamma$  théoriques pour les raidissages réalisés. On a utilisé à cet effet la méthode numérique présentée sous [7]. Avec les abréviations bien connues

$$\gamma = \frac{EJ_{\text{raid.}}}{b D} \quad , \quad (b = \text{largeur du panneau})$$



Coupe A-A  
1:10

Poutres d'essais type A

fig. 1



$$\delta = \frac{F_{\text{raid.}}}{b \cdot t}, \quad (t = \text{épaisseur de la tôle})$$

on peut exprimer les résultats des calculs sous la forme suivante:

- Poutres A: panneaux longueur  $a = 900$  mm, largeur  $b = 800$  mm, avec trois raidisseurs longitudinaux équidistants

$$k < 64 : \gamma = -1,31 + 0,317 k + 0,00013 k^2 + 1,266 \cdot k \cdot \delta$$

$$k = k_{\text{max}} = 64 : \gamma^* = 19,5 + 81 \delta \quad (\text{rigidité optimum})$$

- Poutres B: panneaux longueur  $a = 900$  mm, largeur  $b = 600$  mm, avec deux raidisseurs longitudinaux équidistants

$$k < 36 : \gamma = -3,49 + 0,742 k + 0,00075 k^2 + 2,25 \cdot k \cdot \delta$$

$$k = k_{\text{max}} = 36 : \gamma^* = 24,2 + 81 \delta \quad (\text{rigidité optimum})$$

Pour des raidisseurs possédant la rigidité optimum  $\gamma^*$  le voilement de la membrure comprimée devrait se produire indifféremment, soit en une onde transversale (panneau entier raidi), soit en quatre (A) ou trois (B) ondes juxtaposées dont les axes des raidisseurs forment les lignes nodales.

#### b) Raidisseurs transversaux

Ces raidisseurs sont choisis plus rigides que les longitudinaux, ceci avant tout pour des raisons pratiques d'exécution (croisement des raidisseurs), comme cela est aussi le cas en réalité. Le rapport des rigidités atteint environ 2.

#### c) Hypothèses concernant le comportement à la ruine

Une analyse théorique du comportement effectif d'un panneau raidi dans le domaine post-critique présente des difficultés sérieuses (voir par exemple la réf. [8]). On se limitera ici à formuler des hypothèses plausibles.

Pour des panneaux comprimés uniformément, non raidis longitudinalement, on dispose des résultats de nombreux essais, en particulier de ceux de WINTER [9]. Avec la notion de largeur utile introduite par VON KÁRMÁN [10], on obtient selon réf. [11] une bonne concordance avec les valeurs expérimentales moyennes en posant

$$b_r / b = \sqrt{\sigma_{cr} / \sigma_{\text{max}}}$$

Dans cette expression  $\sigma_{cr}$  désigne la contrainte critique selon la théorie linéaire et  $\sigma_{\text{max}}$ , la contrainte au bord, atteignant

à la ruine la limite élastique  $\sigma_F$  de la tôle.

Pour un panneau raidi, on admettra que le comportement optimum dans le domaine post-critique est atteint lorsque chaque sous-panneau, compris entre deux raidisseurs longitudinaux, travaille comme une tôle comprimée appuyée uniquement sur ses bords et possède ainsi la largeur utile  $b_r$  exprimée par la formule précitée (fig. 3). Ceci n'est qu'une première approximation puisque les conditions au contour, en particulier pour l'état de membrane qui se développe dans le domaine post-critique, ne sont pas identiques.

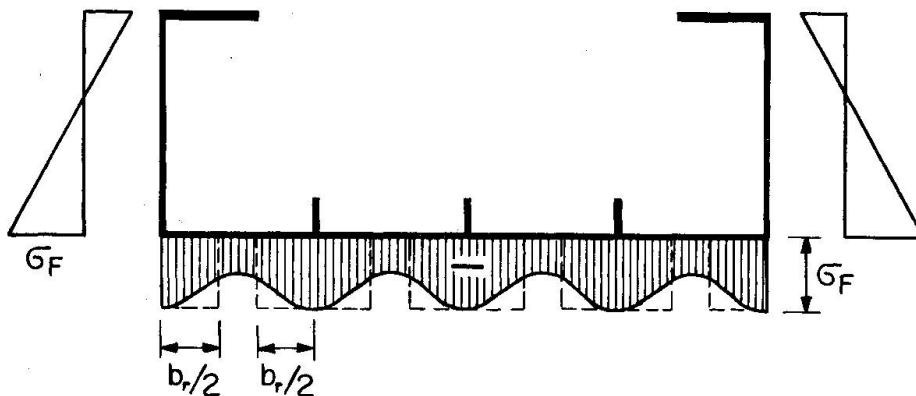


fig. 3

A la ruine, la contrainte au bord de l'âme en contact avec la membrure comprimée atteint également  $\sigma_F$ . La répartition des contraintes sur la hauteur de l'âme est par contre inconnue. Comme cet élément, surtout si l'on tient compte du déplacement de l'axe neutre dû à la réduction de la surface comprimée effective, est également en danger de voilement, il serait imprudent de supposer une plastification totale. Nous admettrons provisoirement une répartition triangulaire, conforme aux règles de la Résistance des Matériaux. Pour une largeur  $b_r$  connue, le moment maximum à la ruine  $M_{th,max}$  est ainsi aisément calculable à partir des caractéristiques géométriques de la section et de la limite élastique du matériau.

La rigidité optimale des raidisseurs dans le domaine post-critique sera alors définie comme la rigidité permettant juste d'atteindre, dans l'essai à la ruine, la valeur calculée  $M_{th,max}$ . Cette valeur  $\gamma^*_{post-cr.}$  est à comparer à celle de la théorie linéaire, ce qui fixe la grandeur du coefficient de majoration de MASSONNET

$$m = \gamma^*_{post-cr.} / \gamma^*_{linéaire}$$

Pour des nervures dont la rigidité est inférieure à  $\gamma^*_{post-cr.}$ , le calcul se fera de façon analogue: la rigidité "effective" sera admise égale à  $\gamma/m$  et la valeur du  $\gamma_{linéaire}$  ( $< \gamma^*_{linéaire}$ ) ainsi obtenue fixera, à partir des relations du paragraphe a), le coefficient de voilement  $k$  et la contrainte théorique  $\sigma_{cr}$ . Avec la largeur utile correspondante  $b_r = b \sqrt{\sigma_{cr} / \sigma_F}$ , naturellement inférieure à celle trouvée pour le raidissage optimum, on calculera comme ci-dessus un moment de ruine  $M_{th}$ . Si les valeurs  $m$ , déterminées à partir des essais sur diverses poutres, concordent dans le cadre de la dispersion inévitable, les hypothèses introduites seront confirmées.

### DISPOSITIF EXPÉRIMENTAL

Les mesures portent sur les flèches d'un des panneaux centraux de 900 mm de longueur (voir fig. 1) ainsi que sur les allongements spécifiques dans une section médiane. On a utilisé à cet effet l'appareillage suivant:

#### Capteur inductif

Les déformations verticales du panneau de semelle comprimée, relatives aux bords des âmes, sont mesurées dans sept sections transversales à l'aide d'un capteur inductif relié à un coordinatographe électronique dessinant directement, à l'échelle désirée, les courbes de déformations. L'étude de ces flèches permet de suivre le processus de voilement.

#### Tensomètres ohmiques

Ces tensomètres, collés dans la section de mesure médiane (voir fig. 1), servent à déterminer la répartition des allongements le long du contour de la section. Pour éliminer l'influence des contraintes locales de flexion, tous les extensomètres sont groupés par paires de chaque côté des tôles. Les quatre tiges d'extrémité, reprenant les réactions, sont également pourvues d'extensomètres, ce qui donne un contrôle de l'effort appliqué.

### RÉSULTATS EXPÉRIMENTAUX

#### Données caractéristiques

Poutre	Largeur b	Longueur a	Epaisseur t (mesuré) mm	Raidisseur longitudinal			
	mm	mm		Section	Inertie cm <sup>4</sup>	$\gamma$	$\delta$
A1	800	900	3,2	60 x 2,9	21	87	0,068
A2	800	900	3,3	37 x 3,3	5,5	21	0,046
B1	600	900	4,0	renf.	58	165	0,123
B2	600	900	4,0	37 x 3,1	5,2	15	0,048

#### Résultats expérimentaux

Poutre	Limite élastique t/cm <sup>2</sup>	A la ruine		Nombre de cloques		Déformée initiale mm
		Charge t	Moment tcm	sur b	sur a	
A1	2,95	12,4	2110	4	5	5
A2	3,0	8,0	1360	1	1	5
B1	2,9	14,5	2470	3	5	3
B2	2,9	8,8	1500	1	1	4

### Comparaison des valeurs calculées aux valeurs expérimentales

P.	Moment expér. $t_{cm}$	Calculs pour $m = 5$					Théorie linéaire sans réduct.				
		$\gamma/m$	$k$	$\sigma_{cr}$	$b_r/b$	$M_{th}$	$\gamma$	$k$	$\sigma_{cr}$	$M_{cr}$	$M_{adm}$ $n=1,35$
A1	2110	17,4	46	1,40	0,69	2060	87	64	1,95	1820	1350
A2	1360	4,2	14,5	0,47	0,39	1390	21	58	1,87	1760	1310
B1	2470	33	35	2,48*	0,92	2650	165	36	2,50*	2450	1810
B2	1500	3	7,6	0,64	0,47	1440	15	21,5	1,82	1590	1180

Dans le calcul des moments de ruine  $M_{th}$  on a tenu compte des bandes extérieures (largeur  $2 \times 6,5$  mm) qui travaillent de toute façon à la limite élastique. Pour les nervures longitudinales, on a admis en première approximation la même efficacité que pour la tôle. Pour des contraintes critiques  $\sigma_{cr}^*$  dépassant la limite de proportionnalité  $\sigma_p$ , admise à  $2 \text{ t/cm}^2$ , on a réduit les valeurs selon les indications des règles DIN 4114, Ri 7.42 (module d'Engesser-Kármán).

L'examen des tableaux précédents montre que les poutres à raidisseurs plus rigides (A1 et B1) se comportent nettement mieux que les autres. Il n'existe de plus aucune relation directe entre les valeurs expérimentales à la ruine et celles données par la théorie linéaire du voilement, sans réduction des rigidités  $\gamma$ ; ceci ressort particulièrement bien de la comparaison des poutres A1 et A2. La théorie linéaire conduit ici à des moments critiques pratiquement égaux pour les deux poutres, ce qui est normal puisque même la rigidité  $\gamma$  de la poutre A2 atteint pratiquement la valeur optimale  $\gamma^*$ . Un renforcement des raidisseurs (poutre A1) ne devrait dès lors pas amener d'augmentation substantielle de la résistance; en réalité, le rapport des moments de ruine vaut 1,55. Comme une partie non négligeable de la flexion est reprise par les âmes, ceci surtout pour la poutre A2 qui est fortement dissymétrique à l'état de ruine, il est plus juste de comparer les efforts de compression dans la membrure comprimée ou, ce qui revient au même, les largeurs utiles expérimentales; ce rapport dépasse 1,8.

Pour expliquer le comportement totalement différent des poutres A1 et A2, le plus simple est de comparer l'allure des déformations et des allongements. Dans le sens transversal la poutre A2 a voilé en une seule onde (fig. 4), la poutre A1 par contre en quatre ondes, avec lignes nodales au droit des raidisseurs (fig. 5), bien que la déformation initiale comprenne une seule onde. La figure 6 montre l'allure des déformations le long du raidisseur central, avec de grandes déflections pour la poutre A2 et des valeurs pratiquement négligeables pour A1. En fonction des charges appliquées, les déformations au droit des raidisseurs et en travée diffèrent également: pour A2 (fig. 7a) toutes les déformations ont la même allure et atteignent rapidement des valeurs considérables, tandis que pour A1 (fig. 7b) les raidisseurs restent pratiquement rectilignes, avec même au début une tendance à des déflections de sens inverse; de plus, les déformations des panneaux sont de beaucoup inférieures à celles de la poutre A2.

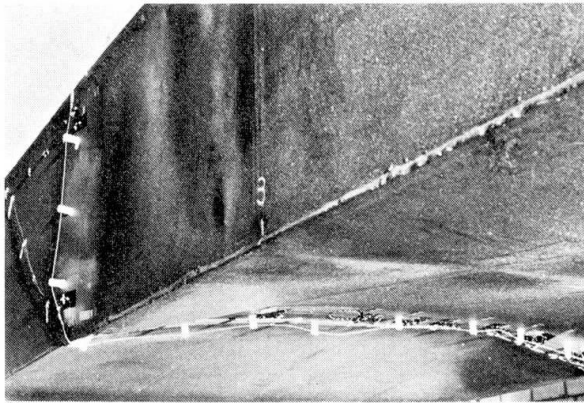


fig. 4 Poutre A2

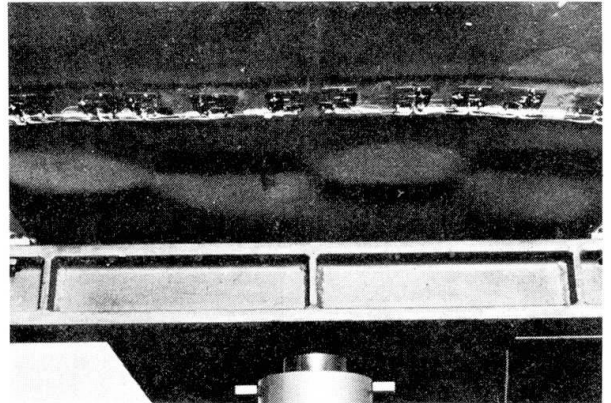


fig. 5 Poutre A1

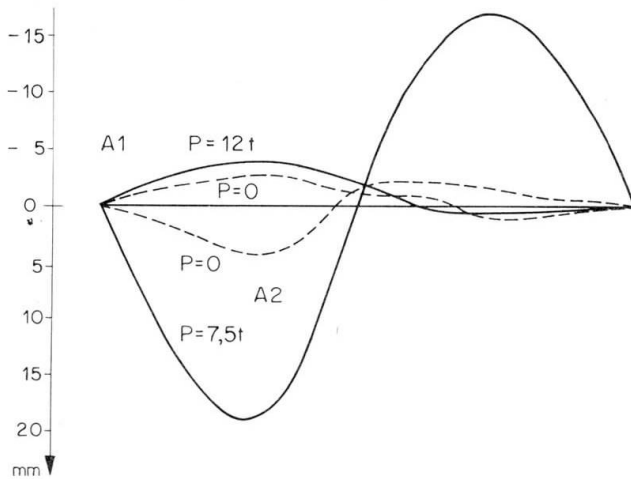
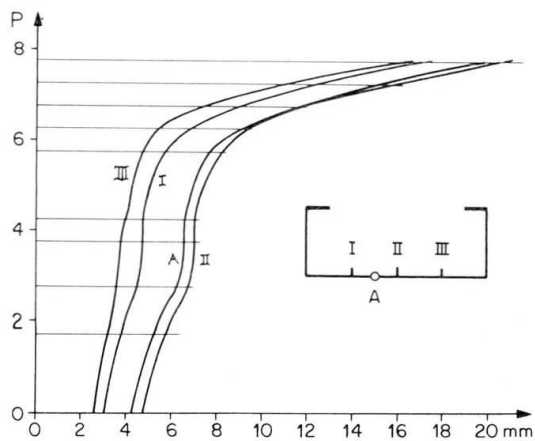
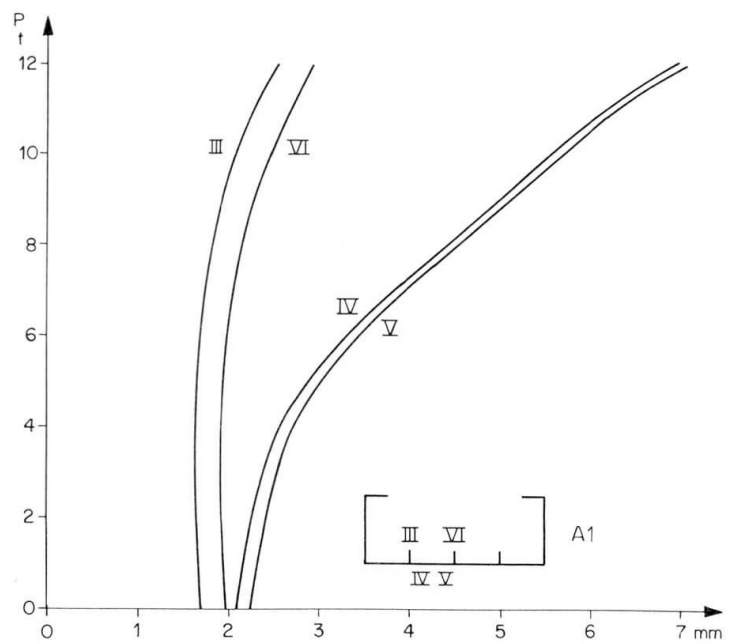


fig. 6  
Déformations le long  
du raidisseur central

fig. 7  
Progression des défor-  
mations dans la section  
médiane en fonction de P

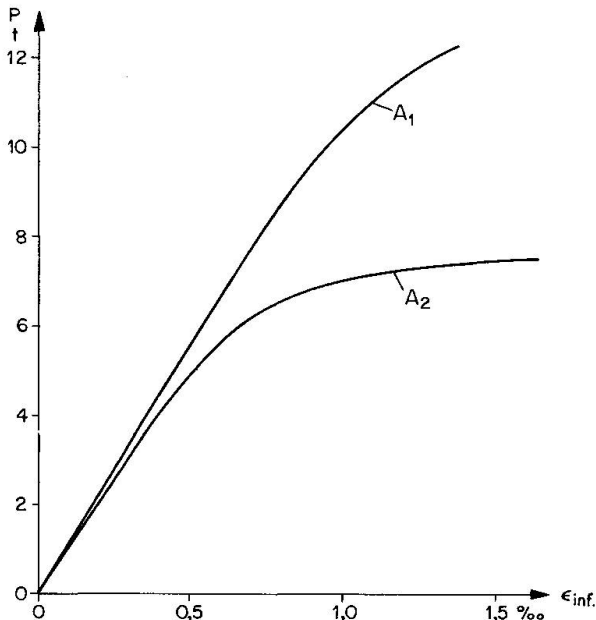


a) Poutre A2



b) Poutre A1

Pour les allongements au bord de la semelle comprimée (fig. 8a) resp. tendue (fig. 8b) en fonction de la charge, l'allure est en principe la même, mais le diagramme A2 s'incurve déjà à partir de 5 t pour arriver rapidement à la limite élastique.



Progression des allongements dans la section de P  
fig. 8a Semelle comprimée

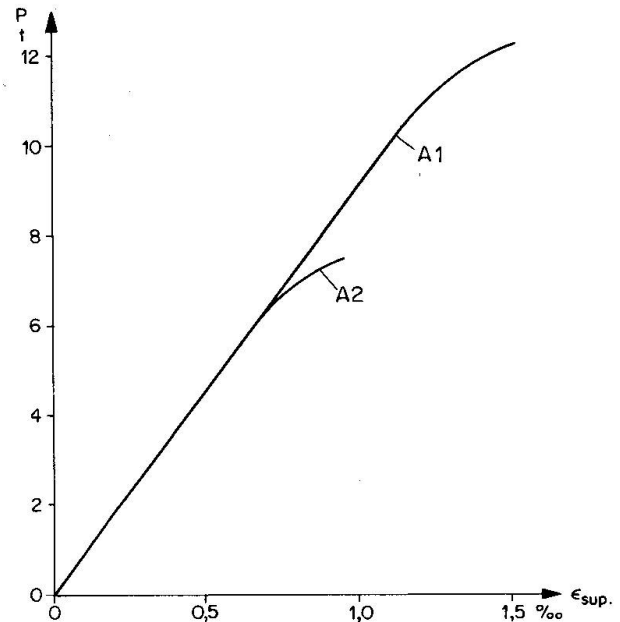
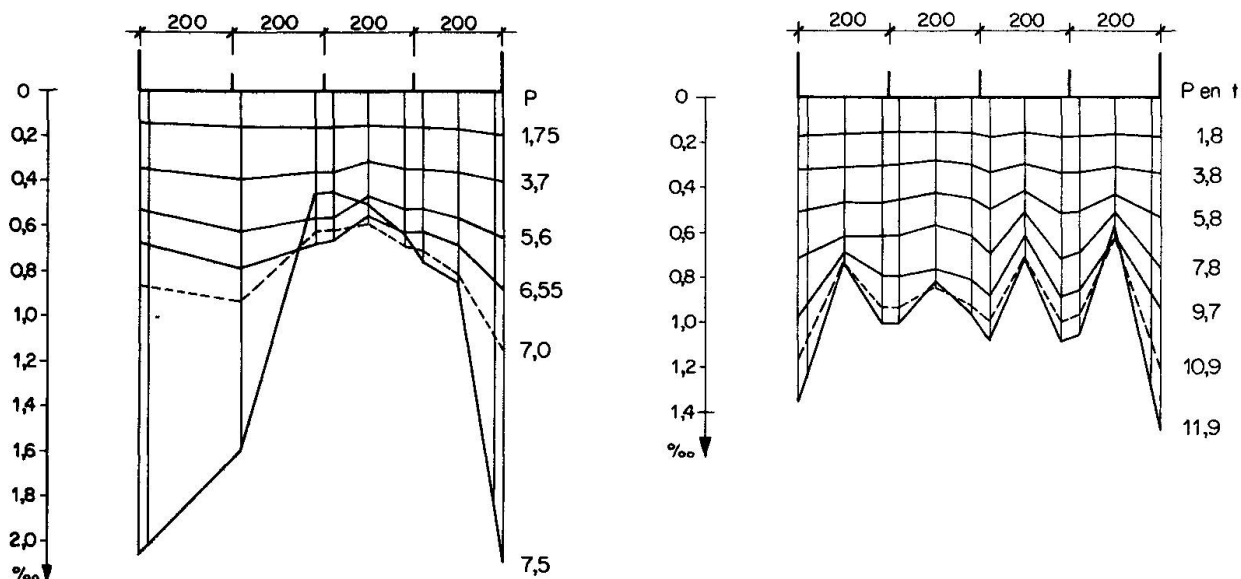


fig. 8b Semelle tendue

Les diagrammes les plus instructifs sont certainement ceux donnant la répartition des allongements dans une section transversale, avec les charges en paramètres. Pour A2 (fig. 9a) on remarquera la poche centrale qui se creuse de plus en plus, avec des allongements qui finissent même par décroître; à la ruine les efforts de compression sont concentrés le long des âmes et le panneau se comporte donc dans l'ensemble comme une plaque non raidie (voir par exemple [9]), ce qui montre bien que la rigidité des nervures est insuffisante dans le domaine post-critique. Pour la poutre A1, par contre, la répartition est beaucoup plus régulière (fig. 9b) et les poches se forment ici entre les raidisseurs; même pour une tôle parfaitement soutenue tous les 200 mm, le rapport de la largeur à l'épaisseur est en effet tel que la largeur utile à la ruine serait inférieure à 1, de l'ordre de 0,85. De plus, comme les raidisseurs n'ont pas tout-à-fait la rigidité optimum, compte tenu du facteur de majoration  $m$  d'environ 5 ( $k = 46$  au lieu de 64, voir tableau), il existe également une poche générale, d'ailleurs assez peu marquée. La figure semble aussi montrer que les déformations initiales (de l'ordre de l'épaisseur), n'influent guère sur l'allure des répartitions à la ruine et ne devraient donc pas jouer un rôle important.

Comme il est prévu de publier ailleurs un compte-rendu plus détaillé des essais, nous renonçons à analyser les résultats des poutres B, la comparaison étant semblable à celle des poutres A.





Répartition des allongements dans la section médiane du panneau comprimé (feuillet moyen), pour div. valeurs des charges appliquées  
fig. 9a Poutre A2  
fig. 9b Poutre A1

### CONCLUSIONS GÉNÉRALES

#### a) Valeur expérimentale du coefficient $m = \gamma_{\text{post-cr.}} / \gamma_{\text{linéaire}}$

La comparaison des valeurs calculées aux valeurs expérimentales des moments de flexion montre une concordance satisfaisante lorsque l'on donne au coefficient  $m$  une valeur moyenne de 5. Le nombre d'essais réalisés est évidemment insuffisant pour généraliser ce résultat. On peut toutefois remarquer que les quatre poutres étudiées couvrent un domaine assez vaste, tant pour ce qui concerne la géométrie des panneaux que pour la rigidité relative des raidisseurs. Pour calculer la résistance à la ruine d'un panneau raidi comprimé, nous proposons donc, dans l'attente de résultats plus nombreux, de diviser par 5 la rigidité effective des raidisseurs et de calculer la contrainte de voilement  $\sigma_{cr}$  à partir de cette valeur  $\gamma$  réduite. La formule précitée de von Kármán donnera alors la largeur effective du panneau et fixera ainsi la grandeur du moment limite.

Pour dimensionner les raidisseurs dans une construction nouvelle, on procédera de façon analogue, c'est-à-dire qu'on multipliera par 5 les rigidités théoriques données par la théorie linéaire; ceci vaut aussi bien pour la rigidité optimale  $\gamma^*$  correspondant à  $k_{\text{max}}$  que pour des rigidités plus faibles, conduisant à des coefficients de voilement  $k$  inférieurs à celui du voilement en ondes transversales juxtaposées.

#### b) Contrôle au voilement habituel, sans réduction des rigidités

Pour les poutres A2 et B2, à raidisseurs non renforcés, les moments expérimentaux à la ruine sont inférieurs aux moments critiques de

la théorie linéaire; pour A2 le rapport  $M_{\text{ruine}}/M_{\text{cr th}}$  est inférieur à 0,8. Même le moment admissible, pour une sécurité au voilement de 1,35 (DIN 4114, 17.4), atteint pratiquement la valeur à la ruine! Le contrôle au voilement habituel conduit dès lors dans ce cas à une sécurité effective à la ruine de l'ordre de 1, alors que l'on devrait avoir de l'ordre de 1,7. Il est donc urgent de modifier certains règlements dangereux lorsqu'on les applique à des tôles raidies comprimées.

Si, par contre, l'on tient compte du facteur  $m = 5$ , une sécurité de 1,35 par rapport à  $\sigma_{\text{cr}}$  paraît suffisante, puisque l'on dispose de la réserve post-critique donnée par le rapport  $\sqrt{\sigma_{\text{F}}/\sigma_{\text{cr}}}$ . Pour un raidissage très serré, conduisant à des valeurs  $\sigma_{\text{cr}}$  proches de  $\sigma_{\text{F}}$ , cette réserve devient cependant insuffisante; dans ce domaine, il paraît prudent d'augmenter quelque peu le facteur de sécurité.

### c) Dimensionnement des raidisseurs au flambement

Un dimensionnement des raidisseurs longitudinaux au flambement, comme cela a été proposé en 1916 déjà par Rode, n'est pas en accord avec les résultats expérimentaux. Avec une largeur utile de 20 t, comme proposé par divers auteurs, on obtient les élanements suivants:

A1	A2	B1	B2
46	78	36	84

Les rapports des contraintes critiques au flambement correspondantes, données par la droite de Tetmajer, la parabole de Johnson etc., ne correspondent pas aux valeurs expérimentales et surestiment la résistance. Pour les poutres A2 et B2, on remarque même que l'élanement est inférieur pour A2, c'est-à-dire que la résistance devrait être ici plus grande, alors que c'est le contraire qui s'est produit. Le calcul des raidisseurs au flambement, qui ne tient compte ni du nombre de raidisseurs, ni de leur disposition dans le panneau, ni du rapport  $a/b$ , ne saurait résoudre correctement le problème du dimensionnement de ces raidisseurs.



### BIBLIOGRAPHIE

1. MASSONNET, CH.: Essais de voilement sur poutres à âmes raidies, Mémoires AIPC, Vol. 14, pp. 125-186, Zurich 1954.
2. MASSONNET, CH., MAS, E., MAUS, H.: Essais de voilement sur deux poutres à membrures et raidisseurs tubulaires, Mémoires AIPC, Vol. 22, pp. 183-228, Zurich 1962.
3. D'APICE, M.A., COOPER, P.B.: Static Bending Tests on Longitudinally Stiffened Plate Girders; Fritz Engineering Lab. Report No 304.5, Lehigh University 1965.
4. COOPER, P.B.: Bending and Shear Strength of Longitudinally Stiffened Plate Girders; Fritz Engineering Lab. Report No 304.6, Lehigh University 1965.
5. ROCKEY, K.C.: Aluminium Plate Girders; Proceedings of Symposium "Aluminium in Structural Engineering", Institution of Structural Engineers 1964.
6. OWEN, D.R.J., ROCKEY, K.C., ŠKALOUD, M.: Ultimate Load Behaviour of Longitudinally Reinforced Webplates Subjected to Pure Bending; Mémoires AIPC, Vol. 18, pp. 113-148, Zurich 1970.
7. STÜSSI, F., DUBAS, CH., DUBAS, P.: Le voilement de l'âme des poutres fléchies, avec raidisseur au cinquième supérieur; Mémoires AIPC, Vol. 17, pp. 217-240, Zurich 1957; Etude complémentaire, Mémoires AIPC, Vol. 18, pp. 215-248, Zurich 1958.
8. ŠKALOUD, M.: Comportement post-critique des âmes comprimées uniformément et renforcées par des raidisseurs longitudinaux; Acier/Stahl/Steel 1964, pp. 193-198.
9. WINTER, G.: Performance of Thin Steel Compression Flanges; 3ème Congrès de l'AIPC, Liège 1948, Publication Préliminaire, pp. 137-148.
10. V. KÁRMÁN, TH., SECHLER, E.E., DONNEL, L.H.: The Strength of Thin Plates in Compression; Trans. Americ. Soc. Mech. Eng., Vol. 54, 1932.
11. STÜSSI, F.: Grundlagen des Stahlbaues, 2. Auflage, Springer 1971, S. 445.

## RESUME

Pour les semelles comprimées de poutres-caissons, les rigidités de la théorie linéaire sont nettement insuffisantes dans le domaine post-critique. Pour les conditions des quatre essais réalisés, le coefficient  $m = \gamma_{\text{post-cr.}} / \gamma_{\text{linéaire}}$  est de l'ordre de 5. Un dimensionnement des raidisseurs longitudinaux partant de leur résistance au flambement n'est par contre pas en accord avec les résultats expérimentaux.

## ZUSAMMENFASSUNG

Für gedrückte Gurtbleche von Kastenträgern genügen die sich aus der linearen Beultheorie ergebenden Steifigkeitswerte im überkritischen Bereich bei weitem nicht mehr. Unter den Bedingungen der vier durchgeführten Versuche beträgt der einzuführende Vergrößerungsfaktor  $m = \gamma_{\text{überkr.}} / \gamma_{\text{linear}}$  rund 5. Eine Bemessung der Längssteifen aufgrund ihrer Knickfestigkeit steht dagegen mit den Versuchsergebnissen nicht im Einklang.

## SUMMARY

For stiffened compression flanges of box-girders the required longitudinal stiffness based on the linear theory of plate buckling is by much insufficient in the post-critical range. Under the conditions of the four performed tests the factor  $m = \gamma_{\text{post-cr.}} / \gamma_{\text{linear}}$  reaches about 5. On the other hand, proportioning requirements of the longitudinal stiffeners based on their buckling loads do not seem to agree with the test results.

Leere Seite  
Blank page  
Page vide

## DISCUSSION PRÉPARÉE / VORBEREITETE DISKUSSION / PREPARED DISCUSSION

**Discussion of the Report by Professor P. Dubas:****"Essais sur le comportement post-critique de poutres en caisson raidies"**

The Conventional Design of Box Girders is unsafe and must be the — at least partial — Cause of the Recent Collapse of Three Large Box Girders Bridges

Discussion du rapport du Prof. P. Dubas:

"Essais sur le comportement post-critique de poutres en caisson raidies"

Diskussion über den Bericht von Prof. P. Dubas:

"Essais sur le comportement post-critique de poutres en caisson raidies"

**R. MAQUOI**

Aspirant du Fonds National  
de la Recherche Scientifique  
Belgique

**CH. MASSONNET**

Professeur  
à l'Université de Liège

1. INTRODUCTION.

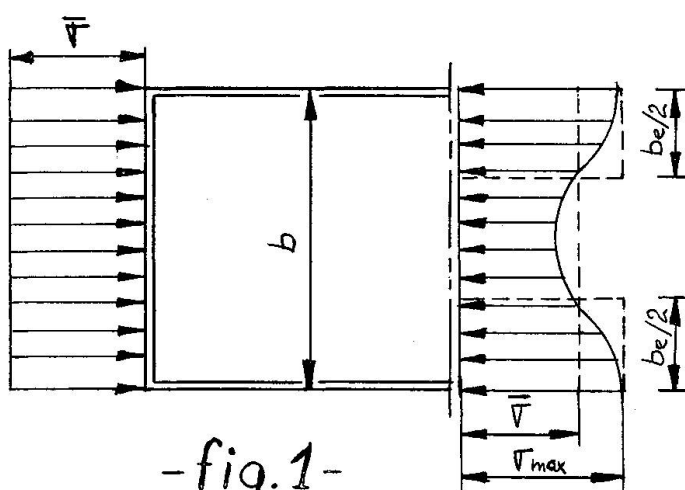
The striking result obtained by professor DUBAS in the test of a box girder described in his report, namely a mean collapse stress less than the critical stress derived from linear buckling theory (see sec.8), has crystallized some grave doubts we had since several years about the safety of the conventional design of box girders. We hold the opinion that, if the safety factor  $s$  of about 1.35 against the critical stress of linear buckling theory, adopted in several countries, was justified in the case of the web of a plate girder, because of the stabilizing effect of a postcritical diagonal tension field, the use of the same coefficient for designing the compressed flange of a box girder was totally unjustified, because the stabilizing effect of membrane stresses is, in this case, much less than in the first one.

It may be appropriate to recall here that the senior author has repeatedly insisted [1, 2] on the fact that theoretically strictly rigid stiffeners, (that means stiffeners of relative rigidity  $\gamma^*$  given by linear buckling theory) were never rigid in practice and gave girders with a low safety, barely able to reach 0.95 to 1 times the yield point in the flanges at collapse. To ensure stiffeners remaining effectively straight up to collapse, it was necessary to adopt values  $\gamma = m\gamma^*$  with  $m$  varying between 3 and 8. The effect of this increase in the rigidity of the stiffeners was to increase the strength by about 25 per cent. This experimental fact has been confirmed recently by OWEN, ROCKEY and SKALoud [3]. The senior author was therefore convinced that box girders with flanges stiffened by  $\gamma^*$  stiffeners had a particularly low effective safety against collapse.

Now, the spectacular accidents which have struck, during last year, three large steel box girder bridges, namely the bridge over the Danube in Vienna on 6 November 1969, the bridge of Milford Haven in Great Britain on 2 June 1970 and the bridge over the lower Yarra in Melbourne (Australy) on 15 October 1970, have reinforced these doubts about the validity of the linear buckling theory.

It seems demonstrated that, in the case of the Danube bridge at least, the collapse occurred for mean compression stresses barely equal to the critical stress of the linear theory. This would mean that, in this case, at least, no reserve of postcritical strength existed. One of the purposes of present report is to show theoretically that this is actually the case (see section 6).

The compressed flange of a box girder subjected to bending is not, like the web of a plate girder, strengthened by a rigid frame constituted of the flanges of the girder and the adjacent transverse stiffeners. On the contrary, the most plausible assumption regarding the boundary conditions of this flange is simple support with complete freedom of the plate edges to move and deform in the plane of the plate. The instability phenomenon of such plates is nearer to that of the compressed column than to that of a plate girder web subjected to shear. In particular, unavoidable imperfections such as buckles due to the welding sequence should exert a strong deteriorating influence. (see sec. 6). In other words, the transverse distribution of compressive stresses is far from remaining uniform up to collapse. Effectively, as is clearly shown in fig. 8 of DUBAS report, the stress diagram shows a central pocket of increasing magnitude. The stresses in the middle are lagging behind the edge stresses (Fig. 1). When these latter reach the yield point, the capacity of the box girder is practically exhausted (see sec. 4) and the box girder collapses.



buckling.

Summarizing, the aim of present report is to prove that the reduction of the mean stress due to buckling, enhanced by imperfections, may upset the gain due to non linear membrane stresses, so that finally the mean collapse stress  $\bar{\sigma}$  of the imperfect flange may become even less than the critical stress of the perfect flange according to linear buckling theory (see sec. 6). There is therefore an urgent need to push forward the theoretical and experimental investigation and, pending these researches, to increase notably the safety factors of box girders against plate

In waiting for these investigations, we have tried to draw the best information from the few papers at our disposal (sec. 2 to 4).

## 2. SOME CONSIDERATIONS ABOUT THE COLLAPSE OF THREE BOX GIRDER BRIDGES.

As told above, we imagine that the fundamental inadequacy of linear buckling theory as applied to the design of large box girders may have played a role in the recent collapse of three large box girder bridges. As we have been able to collect detailed information only in the case of the bridge at Vienna, we shall restrict ourselves to the study of this case.

The circumstances of the collapse of the Danube bridge near Vienna seem rather clear [4, 5]. According to professor SATTLER's paper [5], the three experts took following position regarding the causes of the accident:

1. The calculation of erection stresses was made for a uniformly distributed

loading. The actual distribution of the dead weight differs from this assumption and gave at one of the damaged places more unfavourable conditions, so that in reality at this place larger stresses have existed and therefore smaller-buckling and collapse safeties.

2. The temperature effect in the steel structure on the day of the bridge closing had a value that was not to be expected from the responsible personnel from the temperature observations of the preceeding days. This fact diminished the safety factor against collapse.
3. Besides, there existed constructive as well as unavoidable imperfections (which diminished the safety factor). Taking these imperfections into account is not necessary, according to the specifications, but is covered by the required safety factors. In present case, where the safety against collapse was already diminished by circumstances 1 and 2 above, the imperfections have played a non negligible role as partial cause of the accident
4. The collapse of the entire lower flange of the box girder at a place precipitated the collapse of the whole cross section. The redistribution of internal forces which ensued necessarily explain all other damages as consequences of the first one.

Professor SATTLER has been very kind to send us the detailed report he established as expert for the bridge collapse. According to this report: The safety factor adopted during erection was :

- 1.25. against yielding
- 1.25 against buckling calculated by linear theory.

The steel used was St 44, with a yield point of  $\sigma_y = 2900 \text{ Kg/cm}^2$ .

At the section where the first buckling damage must have occurred, the lower compressed flange had a breadth of 7600 mm, a thickness of 10 mm ( $b/t = 760$ ) and was stiffened by 12 flat stiffeners  $160 \times 12 \text{ mm}$ .

According to professor SATTLER's report, the relative rigidity of these stiffeners was chosen strictly to obtain a buckling coefficient  $k$  of the whole panel equal to that of a subpanel, namely  $k = 4 \times (12 + 1)^2 = 676$ .

In other words, the relative rigidity of these stiffeners was equal to  $\gamma^*$

The ideal buckling stress found in the calculations was  $\sigma_{id}^{cr} = 2,235 \text{ Kg/cm}^2$  and the reduced buckling stress taking account of plasticity,  $\sigma_{cr}$  was, according to the Austrian Specifications,  $\sigma_{cr} = 2,213 \text{ Kg/cm}^2$ .

According to professor SATTLER's calculations, due to the circumstances indicated above, the mean stress in the compressed flange must have reached at the time of collapse, the value

$$\bar{\sigma}_{max} = 2,224 \text{ Kg/cm}^2.$$

SATTLER considers that the condition  $\sigma_{max} = \sigma_{cr}$  is the explanation of the collapse.

We completely agree with this explanation, especially because we shall show in section 6 that collapse can occur even for values of the mean stress  $\bar{\sigma}$  less than  $\sigma_{cr}$ .

### 3. FOUNDATIONS OF THE NON LINEAR THEORY OF BUCKLING OF COMPRESSED PLATES.

The non linear theory of buckling of plates has been developed by von Karman and is represented by following coupled fourth order equations

$$\frac{D}{t} \nabla^2 \nabla^2 w = \frac{\partial^2 \phi}{\partial x^2} \frac{\partial^2 w}{\partial y^2} + \frac{\partial^2 \phi}{\partial y^2} \frac{\partial^2 w}{\partial x^2} - 2 \frac{\partial^2 \phi}{\partial x \partial y} \frac{\partial^2 w}{\partial x \partial y} \quad (1)$$

$$\nabla^2 \nabla^2 \phi = E \left[ \left( \frac{\partial^2 w}{\partial x \partial y} \right)^2 - \frac{\partial^2 w}{\partial x^2} \frac{\partial^2 w}{\partial y^2} \right] \quad (2)$$

where:  $w$  is the transverse displacement of the plate,

$$D = \frac{Et^3}{12(1-\nu^2)} \text{ its flexural rigidity ,}$$

$t$  the thickness

$\nu$  Poisson's ratio,

$\phi$  Airy's stress function.

The stiffened plates constituting the compressed flanges of box girders are supported at their edges in such a way that these edges can move freely in the plate's plane. If the box girder is subjected to pure bending, as in professor DUBAS experiments, there are no shear stresses along the lateral edges before buckling, and it seems reasonable to admit that these shear stresses remain very small even in the postbuckling range. Therefore, the

boundary conditions of the stiffened compressed plate ( $a \times b$ ) of fig. 2 may be taken as :

for  $x = 0$  and  $x = a$  :

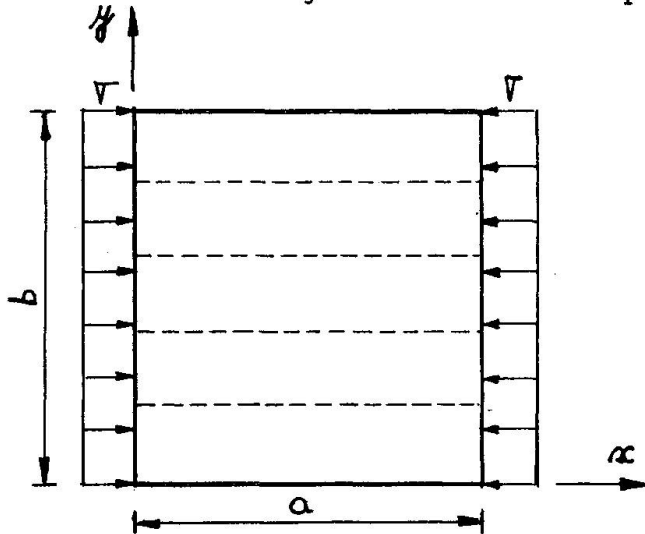
$$w = \frac{\partial^2 w}{\partial x^2} + \nu \frac{\partial^2 w}{\partial y^2} = 0 \quad (3)$$

$$\frac{\partial^2 \phi}{\partial y^2} = \sigma, \quad \frac{\partial^2 \phi}{\partial x \partial y} = 0$$

for  $y = 0$  and  $y = b$  :

$$w = \frac{\partial^2 w}{\partial y^2} + \nu \frac{\partial^2 w}{\partial x^2} = 0 \quad (4)$$

$$\frac{\partial^2 \phi}{\partial x^2} = 0, \quad \frac{\partial^2 \phi}{\partial x \partial y} = 0$$



-fig.2-

Starting from equations (1) and (2) with boundary condition (3), (4), SKALOUD and NOVOTNY, in two papers ([7], [8]), have brought a very important contribution to the solution of the problem, for the case of one median longitudinal stiffener or of two stiffeners placed at the thirds of the width. Later on, they have sketched the solution of the same problem when account is taken of the effect of initial deformation or stresses ([9], [10]). The solution is based on Rayleigh-Ritz energy method. As the authors have not taken account of the potential energy corresponding to the compression of the stiffeners, the results obtained do not depend on the relative area of the stiffeners, and are valid only for  $\delta = \frac{A}{bt} = 0$ .

On the other hand, numerical results are given only for the square plate



( $\alpha \equiv a/b = 1$ ); however, their paper contains the cubic equations which would enable to develop the calculations for other values of  $\alpha$

#### 4. COLLAPSE CRITERION ADOPTED.

SKALLOUD and NOVOTNY admit that the strength of the plate is exhausted when the maximum membrane stress  $\sigma_{xm}$  which occurs along the unloaded edges reaches the yield point  $\sigma_y$  of the steel used. In the case where the stiffeners remain rigid up to collapse, the membrane stresses  $\sigma_{xm}^r$  in the plate at the location of the stiffeners reach also  $\sigma_y$ .

The validity of above collapse criterion has been extensively discussed by SKALLOUD in other papers (see e.g. [11]). It neglects two circumstances which have opposite effects: the bending stresses in the plate and the plastic redistribution after the yield point has been reached. We admit that these effects cancel each other and therefore the validity of SKALLOUD's criterion.

#### 5. CHARTS FOR THE SQUARE PLATE.

From the diagrams obtained by SKALLOUD and NOVOTNY for a square plate with one or two equidistant stiffeners, we have constructed the charts of figures 3 and 4. Figures 3a and b apply to the plate with one stiffener, figures 4a and b to the plate with two stiffeners. We have only considered values of the stiffener's relative rigidity  $\gamma = \frac{EI}{bD}$  for which  $\gamma > \gamma^*$ .

##### First problem.

Given a square steel plate whose dimensions  $a = b$ ,  $t$ , are known, it is asked to determine the rigidity  $\gamma_p^*$  required from the stiffener(s), in order that this (these) remain rigid up to collapse, as well as the value of the collapse mean stress  $\bar{\sigma}$ .

The solution is immediate by figures 3a and 4a.  $\bar{\sigma}$  and  $\gamma^*$  depend only on the thinness  $b/t$  of the plate and their values are obtained<sup>p</sup> at the intersection of the corresponding curves with the horizontal of the ordinate  $b/t$ .

A vertical drawn from the  $\gamma_p^*$  value to the curve of factors  $m = \frac{\gamma^*}{\gamma_p}$ , gives the multiplier of value of  $\gamma^*$ , which itself is known in function of  $\alpha$  and of the relative area  $\delta$  (see note at the bottom of next page)

By the relation

$$m \gamma^* = 10,92 \frac{I_r}{bt^3},$$

the moment of inertia of the stiffener(s) required becomes

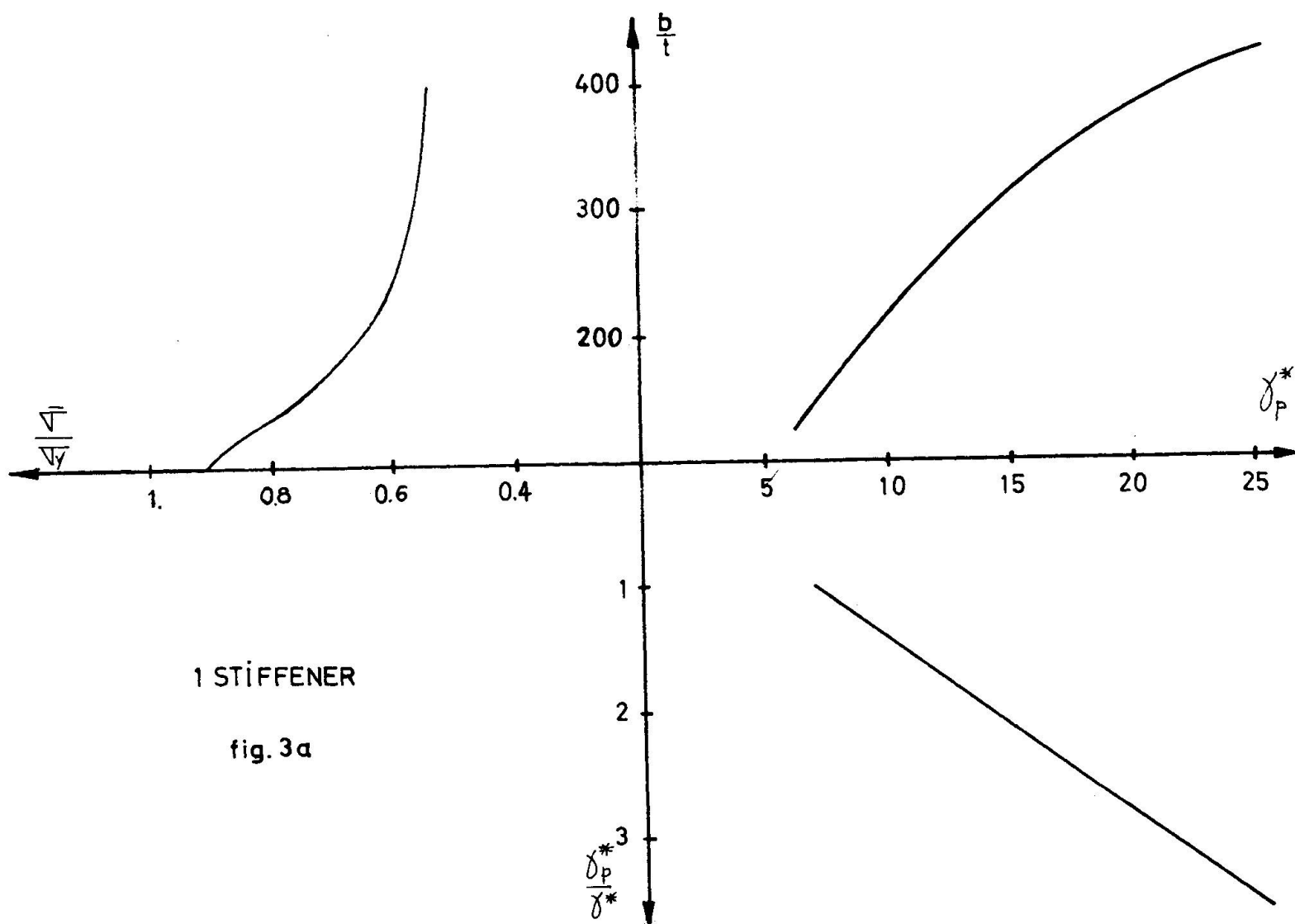
$$I_r = \frac{m \gamma^* b t^3}{10,92}$$

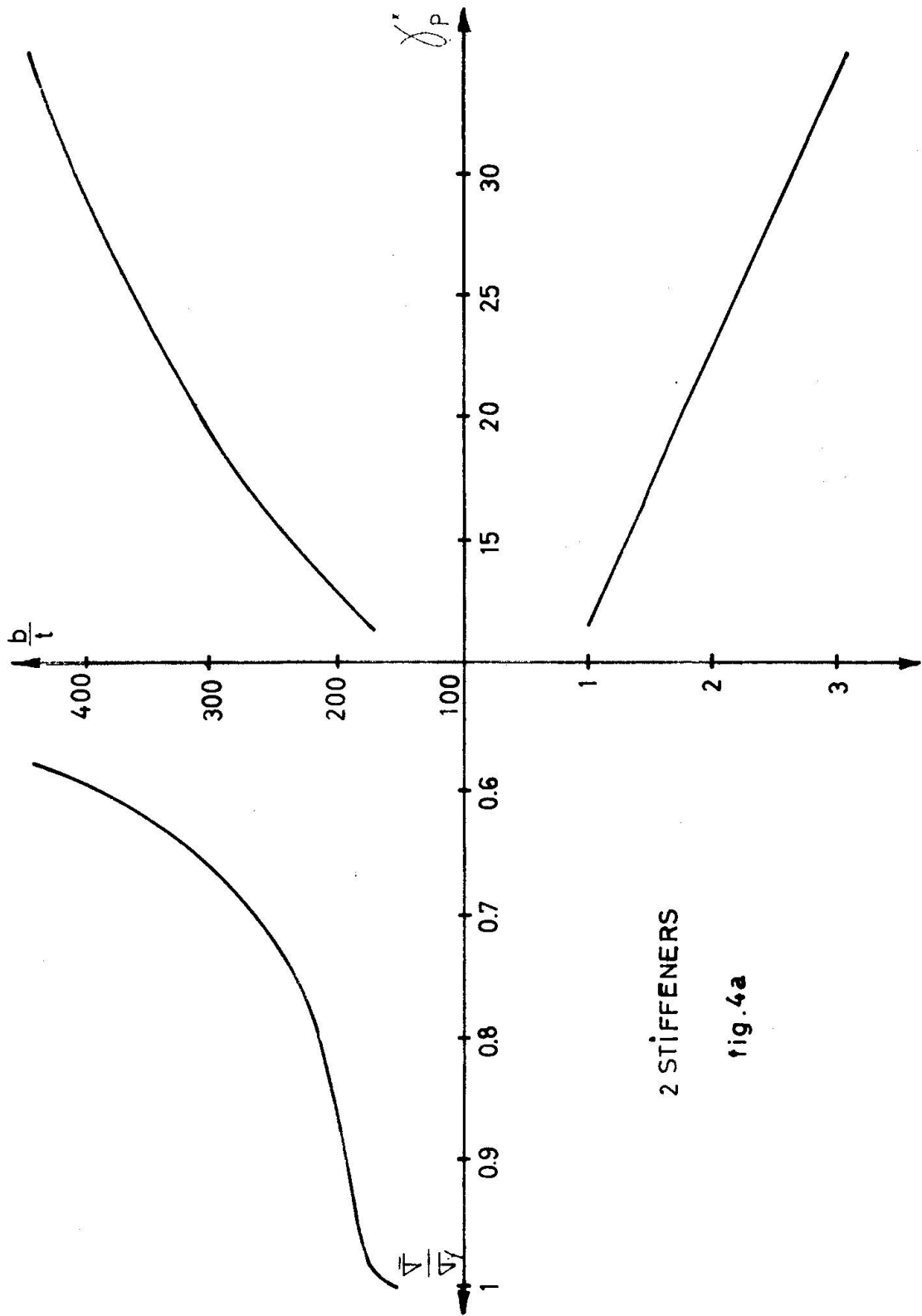
##### Example:

$a = b = 200$  cm,  $t = 0,8$  cm. One stiffener

Figure 4a gives for  $b/t = 200/0,8 = 250$

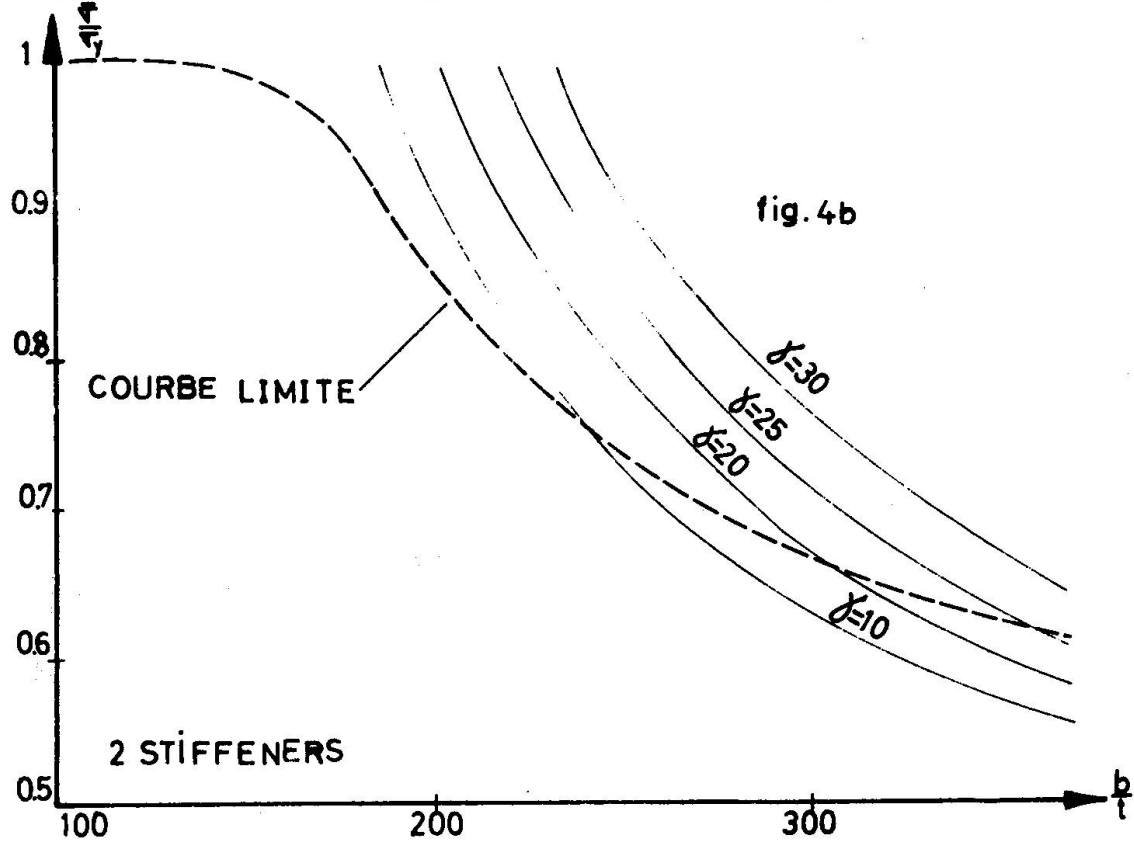
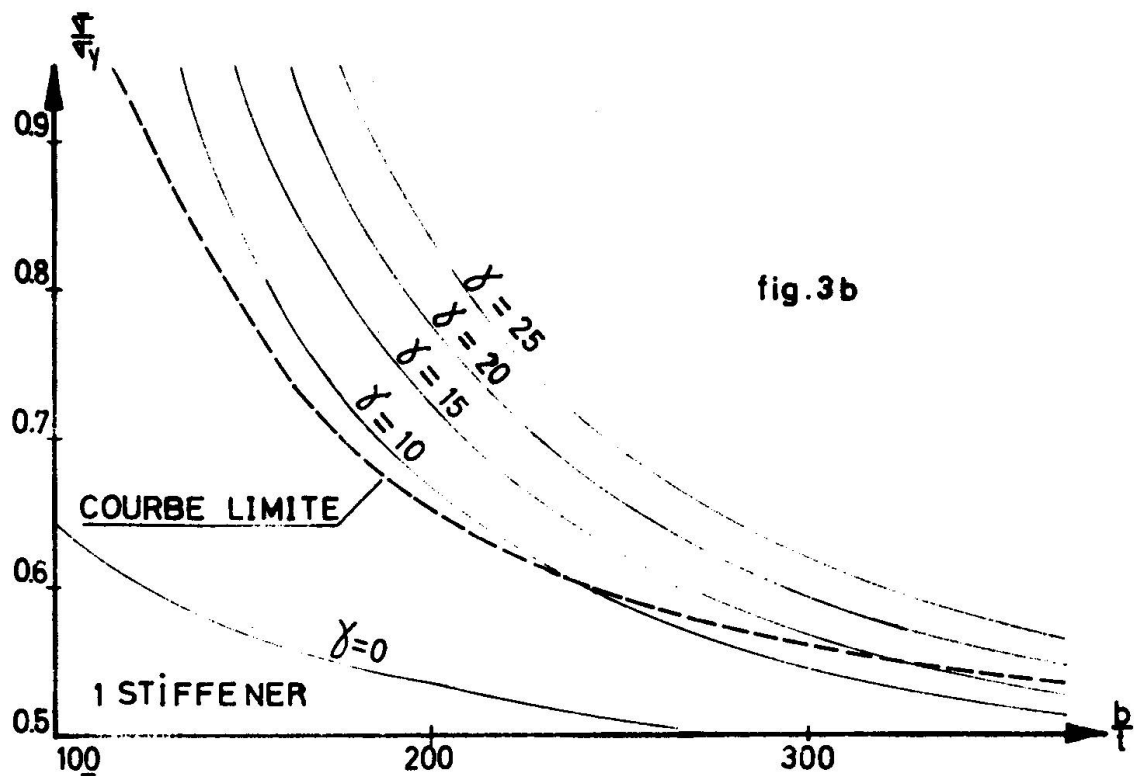






2 STIFFENERS

fig. 4a



$$\frac{\bar{\sigma}}{\sigma_y} = 0.59, \text{ whence } \bar{\sigma} = 1416 \text{ Kg/cm}^2.$$

$$\gamma^* = 11.6. \text{ whence } m = 1.65.$$

The moment of inertia of the stiffener must at least be  $I_r = 109 \text{ cm}^4$ .

### Second problem.

Given a square plate whose dimensions  $a = b$ ,  $t$  are known, stiffened by one (two) stiffener(s) of given relative rigidity, it is asked to determine his ultimate strength.

The solution is immediate by figures 3b and 4b, established for a yield point  $\sigma_y = 2400 \text{ Kg/cm}^2$ . These figures give the value of  $\bar{\sigma}/\sigma_y$  as a function of the  $y$  thickness  $b/t$  of the plate.

The various curves correspond to definite values of  $\gamma$ .

Example:  $a = b = 400 \text{ cm}$  ;  $t = 1 \text{ cm}$  ;  $I_r = 549.5 \text{ cm}^4$ .

First, the relative rigidity

$$\gamma = \frac{10.92 \times 549.5}{400 \times 1} = 15$$

is calculated. Then, from figures 3b or 4 b, one reads :

a) for one stiffener :  $\frac{\bar{\sigma}}{\sigma_y} = 0.515$

b) for two stiffeners :  $\frac{\bar{\sigma}}{\sigma_y} = 0.530$

(\*)

$\delta$  being the ratio  $\frac{\text{area of the stiffener's cross section}}{\text{area of the cross section of the plate}} = \frac{A_r}{bD}$  ,

one has:

one stiffener:  $\alpha \leq \sqrt{8(1+2\delta)} - 1 : \gamma^* = \frac{\alpha^2}{2} [16(1+2\delta) - 2] - \frac{\alpha^4}{2} + \frac{1+2\delta}{2}$

$\alpha \geq \sqrt{8(1+2\delta)} - 1 : \gamma^* = \frac{1}{2} [8(1+2\delta) - 1]^2 + \frac{1+2\delta}{2}$

two stiffeners :

$\alpha \leq \sqrt{18(1+3\delta)} - 1 : \gamma^* = \frac{\alpha^2}{3} [36(1+3\delta) - 2] - \frac{\alpha^4}{3} + \frac{1+3\delta}{3}$

$\alpha \geq \sqrt{18(1+3\delta)} - 1 : \gamma^* = \frac{1}{3} [18(1+3\delta) - 1]^2 + \frac{1+3\delta}{3}$  .

## 6. EFFECT OF AN INITIAL DEFORMATION.

SKALOUD and NOVOTNY have studied in [9] the effect of an initial deformation of a stiffened plate on its ultimate strength for the case of one median stiffener. They have established for this case and for various values of the relative rigidity  $\gamma$  of the stiffener charts giving  $\bar{\sigma}/\sigma_y$  (for  $\sigma_y = 2400 \text{ Kg/cm}^2$ ) as function of the relative thickness  $b/t$  of the plate.<sup>y</sup> The curves are labelled in terms of  $f_0/t$ , where  $f_0$  is the initial deflection in the middle of the panel and  $t$  the plate thickness. The shape of the initial deformation is

$$w_0 = f_0 \sin \frac{\pi x}{a} \sin \frac{\pi y}{b}.$$

and the boundary conditions are the same as previously.

The collapse criterion is the same as that discussed in section 4.

The loss in ultimate strength is especially marked for small values of the thickness  $b/t$  and becomes negligible for a certain value of  $b/t$  which is the smallest for stiffeners with the largest values of the relative rigidity.

Figures 5 and 6 reproduce the charts of SKALOUD and NOVOTNY for the values  $\gamma = 10$  and  $20$  of the relative rigidity, and for  $f_0/t = 0, 1, 2$ . The curve corresponding to  $f_0/t = 2$  has been obtained from the curves  $f_0/t = 0$  and  $f_0/t = 1$  by assuming the  $\bar{\sigma}/\sigma_y$  varies linearly with  $f_0/t$  for  $b/t$  fixed, which is approximately correct.

In test N° 1 of professor DUBAS, (see his fig. 11, p. 14), one has an initial deflection  $f_0 = 4.8 \text{ mm}$  for a thickness  $t = 3.3 \text{ mm}$ . The corresponding ratio  $f_0/t = 1.46$ . As it concerns a laboratory test where the specimens are fabricated with especial care, it is logical to admit that, in an actual bridge, the ratio  $f_0/t$  may reach 2.

Above theoretical results are limited to the case of a single stiffener. Pending new researches, we have supposed that they can be extended to a plate with two longitudinal stiffeners under following assumptions:

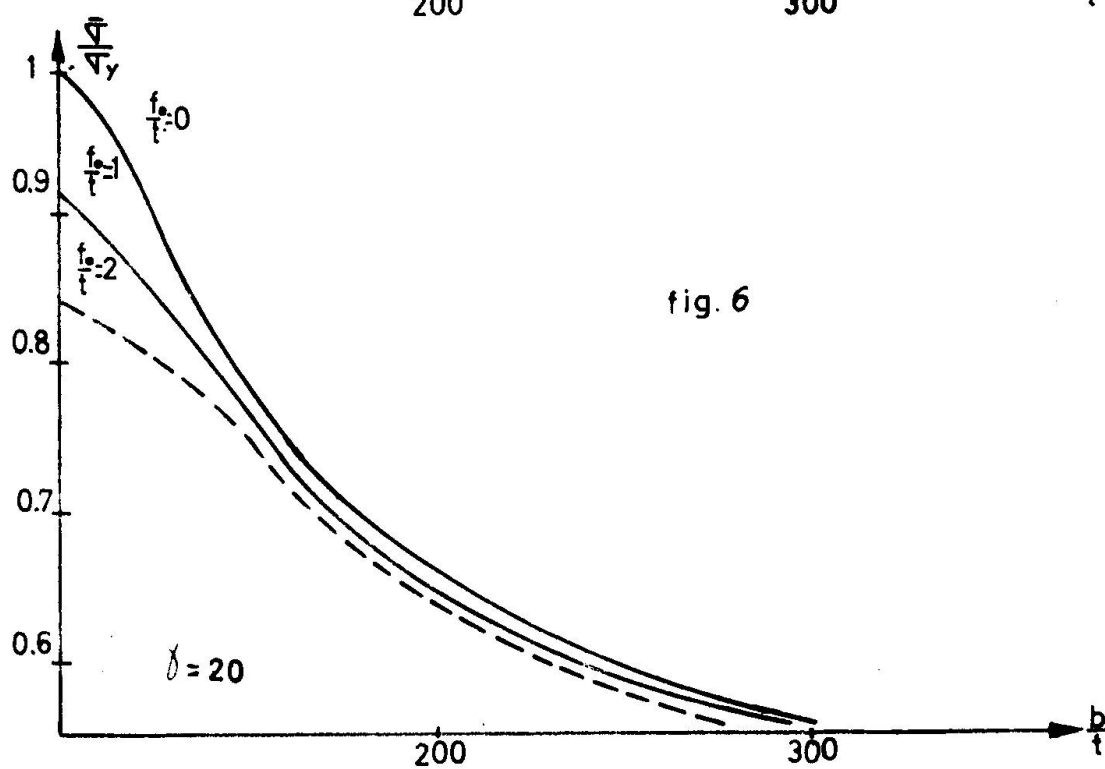
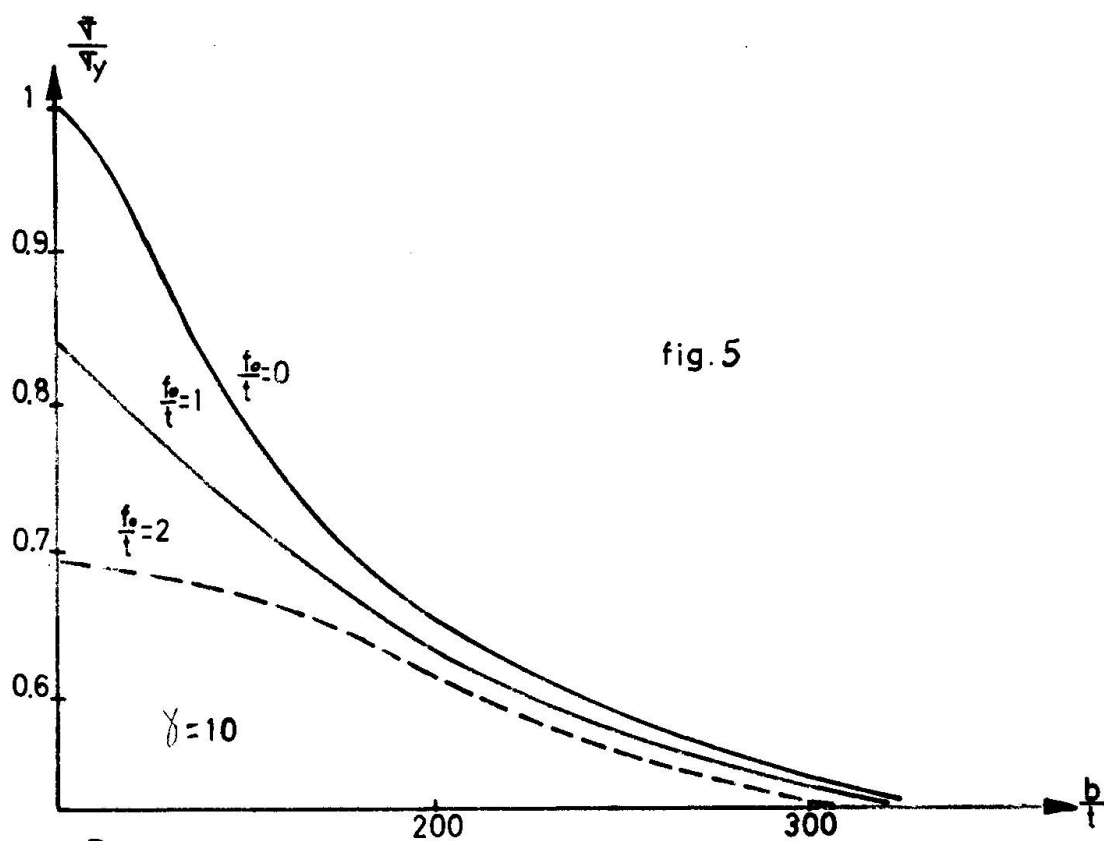
- The two plates have same critical buckling stress according to the linear theory ;
- The ratios of the actual relative rigidity of the stiffeners to the relative optimum rigidity  $\gamma^*$  of the linear theory are identical.

Under these conditions, we assume that the relative reductions of collapse strength are identical for the two plates :

$$\left[ \frac{(\bar{\sigma})_{f_0/t=n}^2 \text{ stiff.}}{(\bar{\sigma})_{f_0/t=0}^2 \text{ stiff.}} \right] \frac{(\gamma_2 \text{ stiff.})}{\gamma_2^* \text{ stiff.}} = m \quad = \quad \left[ \frac{(\bar{\sigma})_{f_0/t=n}^1 \text{ stiff.}}{(\bar{\sigma})_{f_0/t=0}^1 \text{ stiff.}} \right] \frac{(\gamma_1 \text{ stiff.})}{\gamma_1^* \text{ stiff.}} = m \quad (5)$$

$$\sigma_{cr}^2 \text{ stiff} = K \quad \sigma_{cr}^1 \text{ stiff.} = K$$

This generalization is illustrated by example 2 hereafter.



We shall now try to simulate by numerical examples the conditions existing at collapse in the case of the bridge over the Danube (cf. Section 2) namely an actual stress amounting to the critical stress given by linear buckling theory, because of an error on the actual dead weight distribution and of some additional temperature stresses.

Due to lack of theoretical data, we are obliged however, to consider a square panel in mild steel ( $\sigma_y = 2400 \text{ Kg/cm}^2$ ) stiffened by one or two stiffeners only.

Example N° 1 : box girder bridge with the compressed flange defined by following data :

$\alpha = \frac{a}{b} = 1$  ,  $\gamma = 10$  ;  $\frac{b}{t} = 126$  ; Steel AE24 ( $\sigma_y = 2400 \text{ Kg/cm}^2$ )  
one median longitudinal stiffener.

As the adopted  $\gamma$  is larger than  $\gamma^* = 7$ , the linear buckling theory gives for the buckling coefficient  $k = 4 \times 2^2 = 16$  and the critical stress is

$$\sigma_{cr} = 1920 \text{ Kg/cm}^2.$$

If we follow the Austrian Specifications for erection conditions, we should adopt for design stress the lowest of the two ratios (cf. sec. 2) :

$$\frac{\sigma_{cr}}{1.25} = 1536 \text{ Kg/cm}^2$$

$$\frac{\sigma_y}{1.25} = \frac{2400}{1.25} = 1920 \text{ Kg/cm}^2,$$

that means  $1536 \text{ Kg/cm}^2$ .

However, due to above effects, the actual stress has amounted effectively to

$$\sigma_e = \sigma_{cr} = 1920 \text{ Kg/cm}^2.$$

According to the non linear theory of SKALOUD and NOVOTNY, we find, according to figures 5 and 6 :

For  $\gamma = 10$  and  $\frac{f_o}{t} = 0$  :  $\frac{\bar{\sigma}}{\sigma_y} = 0.895$ , whence  $\bar{\sigma} = 2148 \text{ Kg/cm}^2$

$\frac{f_o}{t} = 1$  :  $\frac{\bar{\sigma}}{\sigma_y} = 0.785$ , whence  $\bar{\sigma} = 1884 \text{ Kg/cm}^2$

$\frac{f_o}{t} = 2$  :  $\frac{\bar{\sigma}}{\sigma_y} = 0.682$ , whence  $\bar{\sigma} = 1637 \text{ Kg/cm}^2$

For  $\gamma = 20$  and  $\frac{f_o}{t} = 0$  :  $\frac{\bar{\sigma}}{\sigma_y} = 0.895$  whence  $\bar{\sigma} = 2150 \text{ Kg/cm}^2$

$\frac{f_o}{t} = 1$  :  $\frac{\bar{\sigma}}{\sigma_y} = 0.846$  whence  $\bar{\sigma} = 2030 \text{ Kg/cm}^2$

$\frac{f_o}{t} = 2$  :  $\frac{\bar{\sigma}}{\sigma_y} = 0.805$  whence  $\bar{\sigma} = 1932 \text{ Kg/cm}^2$

We may now calculate the safety given by the effective stress  $\sigma_e = 1920 \text{ Kg/cm}^2$ . The results are given in following table

Values of the effective safety factor for erection conditions  $s = \frac{\bar{\sigma}}{\sigma_e}$

$\gamma/\gamma^*$ $f_o/t$	1,43	2,86
0	1.118	1.118
1	0.981	1.057
2	0.853	1.006

We see that the effective stress may exceed the mean collapse stress according to SKALLOUD - NOVOTNY as soon as the initial imperfection of the plate is of the order of the thickness. If it is recalled in addition that the stiffeners of the Danube bridge gave a ratio  $\gamma/\gamma^*$  approximately equal to one only (cf. sec.2), above table demonstrates that the considered box girder bridge will collapse during erection for values of the relative imperfection  $f_o/t \sim 1$ .

Example N° 2 : We apply now the generalization to a plate with two stiffeners proposed in this section and represented by formula (5). We assume once more that the effective stress is equal to the critical stress, e.g.  $1920 \text{ Kg/cm}^2$ .

The plate homologous to that of example 1 has the following characteristics :

$$\gamma_{2 \text{ stiff}} = \gamma_{2 \text{ stiff}}^* \times \frac{\gamma_{1 \text{ stiff}}}{\gamma_{1 \text{ stiff}}^*} = 11.33 \times \frac{10}{7} = 16.2$$

$\gamma_{2 \text{ stiff}}$  being larger than  $\gamma_{2 \text{ stiff}}^*$ , the two stiffeners remain straight according to linear theory and  $k = 4 \times 3^2 = 36$ .

$$\frac{b}{t} = \sqrt{\frac{36 \times 1,900,000}{1920}} = 189$$

From figure 4b, one has

$$\left[ \left( \frac{\bar{\sigma}}{\sigma_y} \right)_{f_o/t=0}^{1 \text{ stiff}} \right]_{\gamma=16,2, \frac{b}{t}=189} = 0.9 \text{ (limit curve)}$$

whence

$$(\bar{\sigma})_{f_o/t}^{2 \text{ stiff}} = 21.60 \text{ Kg/cm}^2$$

and therefore, according to formula (5)

$$\text{for } \frac{f_o}{t} = 1 : (\bar{\sigma})_{f_o/t=1}^{2 \text{ stiff}} = 21.60 \times \frac{1884}{2148} = 1893 \text{ Kg/cm}^2$$



$$\frac{f_o}{t} = 2 : (\bar{\sigma})_{f_o/t=2}^2 \text{ stiff} = 2160 \times \frac{1637}{2148} = 1643 \text{ Kg/mm}^2.$$

The safeties during erection are therefore respectively :

$\gamma/\gamma^*$ $f_o/t$	
	1,43
0	1.125
1	0.986
2	0.855

and the same conclusions as for example 1 ensue.

### 7. EFFECTIVE WIDTH FORMULAE.

It is well known that the irregular stress distribution across the width  $b$  of the plate (fig. 1) with mean value  $\bar{\sigma}$  and maximum value  $\sigma_{\max}$  may be replaced by a uniform distribution of the maximum stress  $\sigma_{\max}$  on a fictitious width called effective width. For equal resultants,  $\sigma_{\max}$  we need

$$\sigma_{\max} b_e = \bar{\sigma} b$$

whence

$$\frac{b_e}{b} = \frac{\bar{\sigma}}{\sigma_{\max}} = \phi \quad (6)$$

If the stiffeners remain rigid up to collapse, we admit that the maximum stress  $\sigma_{\max}$  is attained also in the plate at each junction with the stiffeners, so that the effective width formula may be applied to the subpanels.

Let us call :

$\sigma_{cr}$  : the critical stress of buckling of a sub-panel ;

$\sigma_{\max}$  : the maximum membrane stress at the edges of a subpanel, taken equal to  $\sigma_y$  at collapse according to SKALOUD's criterion adopted in section 4;

$\beta$  : the ratio of the width  $b$  of a subpanel by the half wave length of longitudinal buckling.

Among the formulae proposed for the effective width for the considered case (simply supported edges and free relative movement of these edges) we shall retain the following

$$\phi = 0.44 + 0.56 \frac{\sigma_{cr}}{\sigma_{\max}} \quad (\text{PAPCOVITCH}) \quad (7)$$

$$\phi = \sqrt[3]{\frac{\sigma_{cr}}{\sigma_{\max}}} \quad (\text{MARGUERRE}) \quad (8)$$

$$\phi = \sqrt{\frac{\sigma_{cr}}{\sigma_{max}}} \quad (\text{von KARMAN}) \quad (9)$$

$$\phi = \frac{1 + \beta^4}{3 + \beta^4} + \frac{2}{3 + \beta^4} \left( \frac{\sigma_{cr}}{\sigma_{max}} \right) \quad (\text{SECHLER}) \quad (10)$$

$$\phi = \sqrt{\frac{\sigma_{cr}}{\sigma_{max}}} (1 - 0.22 \sqrt{\frac{\sigma_{cr}}{\sigma_{max}}}) \quad (\text{WINTER}) \quad (11)$$

$\frac{\sigma_{cr}}{\sigma_{max}}$  WOLMIR [12] indicates however that formula (8) applies only for  $\frac{\sigma_{cr}}{\sigma_{max}} > 0.2$ . He mentions also that formula (9) of von KARMAN is especially applicable in the case of stiffeners whose relative rigidity is much less than  $\gamma_p^*$ . The same is true for formula (11) of WINTER, which derives from von KARMAN's formula.

The table which follows gives the values of  $\phi = \frac{be}{b}$  for various plates, calculated with formulae (7) to (11), and compares them with the values obtained by the theory of SKALOU-NOVOTNY.

The comparison of the results shows that the results of PAPCOVICH, SECHLER and SKALOU agree generally sufficiently well. The MARGUERRE values also are satisfactory in the domain  $\frac{\sigma_{cr}}{\sigma_y} > 0.2$ , whereas the values derived from the KARMAN and WINTER formulae are substantially lower. Using formulae (7) and (10) which are the most satisfactory, we have tested the result obtained experimentally by DUBAS with his test specimen N° 1.

Données						PAPCO- VITCH	(*) MARGUER RE	(*) von KARMAN	SECHLER	(*) WINTER	SKA- LOUD
nombre de raidis- seurs	$\frac{b}{t}$	$\frac{b'}{t}$	$\alpha'$	$\frac{\sigma_{cr}}{\text{Kg/cm}^2}$	$\frac{\sigma_{cr}}{\sigma_y}$						
1	200	100	2	759	0.316	0.617	0.680	(0.563)	$\beta=1$ 0.658	(0.493)	0.65
1	270	135	2	417	0.174	0.537	(0.558)	(0.417)	$\beta=1$ 0.587	(0.378)	0.58
1	360	180	2	240	0.100	0.496	(0.464)	(0.316)	$\beta=1$ 0.550	(0.294)	0.54
1	450	225	2	150	0.062	0.475	(0.396)	(0.249)	$\beta=1$ 0.531	(0.235)	0.53
2	210	70	3	1550	0.646	0.802	0.865	0.804	$\beta=1$ 0.823	(0.662)	0.82
2	300	100	3	759	0.316	0.617	0.680	(0.563)	$\beta=1$ 0.658	(0.493)	0.66
2	375	125	3	486	0.202	0.553	0.598	(0.450)	$\beta=1$ 0.601	(0.409)	0.60
2	450	150	3	337	0.140	0.518	(0.520)	(0.374)	$\beta=1$ 0.570	(0.344)	0.57

Values of  $\phi = \frac{be}{b}$  or  $\frac{be'}{b'}$  for a stiffened plate ( $\alpha = 1$ ) whose stiffeners remain rigid up to collapse, for  $\sigma_{max} = \sigma_y = 2400 \text{ Kg/cm}^2$ .  
(\*) see the remarks made after formula (11))

### 8. APPLICATION TO DUBAS TEST N° 1

For the actual dimensions of the model DUBAS, the parameters have following values :

thinness of the plate :  $\frac{b}{t} = 242$  ;  
 side ratio of the panel :  $\alpha = 1.125$   
 relative rigidity :  $\gamma = 17.7$   
 relative area :  $\delta = 0.041$

From these characteristics, DUBAS draws from his buckling chart (Fig.4) pertaining to a uniformly compressed plate with three longitudinal stiffeners the value of the buckling coefficient

$$k = 50.7.$$

As the "optimum" relative rigidity  $\gamma^*$ , in the sense of the linear theory, is about 20, the stiffeners will be deformed by the plate and this fact has, indeed, been observed experimentally by DUBAS.

The critical stress calculated by linear buckling theory is

$$\sigma_{cr}^{lin} = 50.7 \cdot \frac{1,900,000}{\left(\frac{b}{t}\right)^2} = 1640 \text{ Kg/cm}^2.$$

From the measurements made for  $P = 1.75 \text{ t}$ , a load for which the whole cross section is effective, we calculate the value of coefficient

$$K = \frac{\sigma}{P} = \frac{335}{1750} = 192.10^{-3} \text{ cm}^{-2}.$$

As the experimental collapse observed by DUBAS does not coincide with SKALOUDE's collapse criterion adopted in present paper (sec. 4), we must assume that collapse occurs when the yield point  $\sigma_y = 3000 \text{ Kg/cm}^2$  is reached at the edges of the stiffened plate, or, equivalently, when  $\epsilon$  reaches  $\frac{3000}{2,100,000} = 1.43 \text{ ‰}$ . From the  $(P, \epsilon)$  diagram given by DUBAS (his fig. 8), we see that corresponding load is  $P = 7.4 \text{ t}$  and constitutes our collapse load. The corresponding mean compressive stress calculated by NAVIER formula

$$\sigma_{exp}^{(1)} = 192.10^{-3} \times 7400 = 1420 \text{ Kg/cm}^2$$

is the experimental collapse stress.

This stress is less than the critical buckling stress of the linear theory in the ratio

$$\frac{\sigma_{exp}^{(1)}}{\sigma_{cr}^{lin}} = \frac{1420}{1640} = \frac{1}{1.15}.$$

If now we abandon SKALOUDE's collapse criterion and revert to the experimental collapse load  $P = 7.95 \text{ t}$ . observed by DUBAS, we have to adopt as collapse stress  $\sigma_{exp}^{(2)} = 1525 \text{ Kg/cm}^2$ .

It is seen that this collapse stress of the whole structure is lower than the critical stress of the stiffened plate given by linear theory, which justifies the statement made at the beginning of the introduction of this paper.

In his report, professor DUBAS has applied the effective width formula to estimate the magnification factor  $m = \gamma^*/\gamma^*$  of the stiffeners. By applying effective width formulae (7) and (10) <sup>P</sup>to the full plate of DUBAS considered as unstiffened, we obtain successively :

$$\beta = \alpha = 1.125 ; \quad \sigma_{cr} = \frac{7,593,400}{(242)^2} = 130 \text{ Kg/cm}^2 ; \quad \sigma_{max} = \sigma_y = 3000 \text{ Kg/cm}^2$$

$$\frac{\sigma_{cr}}{\sigma_y} = 0.0434.$$

a) PAPCOVITCH formula (7) gives  $\frac{b_e}{b} = 0.465$  whence  $\bar{\sigma} = 1395 \text{ Kg/cm}^2$ .

b) SECHLER formula (10) gives  $\frac{b_e}{b} = 0.475$  whence  $\bar{\sigma} = 1425 \text{ Kg/cm}^2$ .

(2) We see that a rather good agreement exists between the experimental value  $\bar{\sigma}_{exp} = 1525 \text{ Kg/cm}^2$  and the two theoretical estimates.

However, in principle, the use of an effective width formula for the entire plate is not permissible when this plate is stiffened, because the stiffeners increase the stability of the plate, even if they do not remain straight. One of the main aims of future research is precisely to establish the effect of this kind of stiffeners on the mean collapse stress.

The rather good agreement obtained hereabove between DUBAS test and effective width formulae (7) and (10) only means that the stiffeners of DUBAS first test have a very low efficiency in the collapse stage. The unstiffened plate has a very low buckling stress (130 Kg/cm<sup>2</sup>), but above calculations show that it has a very large postbuckling strength, which is nearly the same as that of the stiffened plate.

## 9. RECOMMENDATIONS FOR FUTURE RESEARCH.

Research on stiffened box girders has to be pushed forward theoretically as well as experimentally.

In the field of theoretical research, we need first calculations of the same type as those developed by SKALoud and NOVOTNY, but for a larger number of stiffeners.

A second phase would consist to investigate the effect of new parameters, such as geometrical imperfections, welding residual stresses, dissymetry of the stiffeners with respect to the mean plane of the stiffened plate, effect of the relative area  $\delta$  of the stiffeners and of their eventual torsional rigidity (in the case of closed section stiffeners).

From all these non linear calculations, practical design charts should be built, which would take account realistically of the conflicting effects of imperfections and postcritical resistance.

In parallel with above theoretical studies, an important series of tests should be undertaken to control the theoretical results. In particular, we need some fatigue tests to investigate the effect of the repeated "breathing" of the compressed flange due to its imperfections. In waiting for the conclusions of such researches, the safety factors against buckling should be immediately increased for box girders, so as to avoid new accidents.

REFERENCES.

- [1] MASSONNET, Ch.: Essais de voilement sur poutres à âme raidie.  
Mémoires A.I.P.C., Vol. 14, pp. 125 - 186, Zürich 1954.
- [2] MASSONNET, Ch.: Stability considerations in the design of plate girders  
Proceedings of the American Institute of Civil Engineers,  
Journal of Structural Division, Vol. 86, Janvier 1960,  
pp. 71 - 97.
- [3] OWEN, D.R.J., ROCKEY, K.C., SKALLOUD, M.: Ultimate load behaviour of  
longitudinally reinforced webplates subjected to pure  
bending. Mém. AIPC, vol. 18, pp. 113-148, Zürich 1970.
- [4] CICIN, P. : Betrachtungen über die Bruchursachen der neuen Wiener  
Donaubrücke - Tiefbau, Vol. 12, pp. 948 - 950, 1970.
- [5] SATTTLER, K. : Betrachtungen über die Bruchursachen der neuen Wiener  
Donaubrücke - Tiefbau, Vol. 12, pp. 665-674, 1970.
- [6] DUBAS, P. : Essai sur le comportement postcritique de poutres en  
caisson raidies. Publication préliminaire. Colloque  
AIPC, Londres, 25 et 26 mars 1971.
- [7] SKALLOUD, M. et NOVOTNY, R.: Überkritisches Verhalten einer gleichförmig  
gedrückten, in der mitte mit einer Längsrippe versteiften  
Platte. Acta Technica CSAV n° 3, 1964.
- [8] SKALLOUD, M. et NOVOTNY, R.: Überkritisches Verhalten einer gleichförmig  
gedrückten, in der dritteln mit zwei Längsrippen versteif-  
ten Platte. Acta Technica CSAV n° 6, 1964.
- [9] SKALLOUD, M. et NOVOTNY, R.: Überkritisches Verhalten einer anfänglich  
gekrümmten gleichförmig gedrückten, in der mitte mit einer  
Längsrippe versteiften Platte. Acta Technica CSAV n° 2  
1965.
- [10] SKALLOUD, M.: Grundlegende Differentialgleichungen der Stabilität  
orthotroper Platten mit Eigenspannungen. Acta Technica  
CSAV n° 4, 1965.
- [11] SKALLOUD, M.: Le critère de l'état limite des plaques et des systèmes  
de plaques. Contribution au Colloque sur le comportement  
postcritique des plaques utilisées en Construction Métal-  
lique, Liège, 12 et 13 novembre 1962.
- [12] WOLMIR, A.S. : Biegsame Platten und Schalen. V.E.B. Verlag für Bauwesen,  
Berlin, 1962.

Leere Seite  
Blank page  
Page vide

### III

#### Ultimate Strength of Plates When Subjected to In-Plane Patch Loading

Résistance à la ruine des âmes soumises à des charges transversales locales

Tragfähigkeit von Stehblechfeldern bei örtlicher Randstreckenlast

**K.C. ROCKEY**

M.Sc., Ph.D., C.Eng., F.I.C.E.  
Professor of Civil  
and Structural Engineering

**M.A. EL-GAALY**

M.S.E., D.Sc., M.ASCE.  
Research Fellow  
Department of Civil  
and Structural Engineering

University College, Cardiff, England

#### 1. INTRODUCTION

Frequently web plates are subjected to local in-plane compressive patch loading, such as that shown in figure 1. If the depth to thickness ratio of the web is sufficiently high then it will buckle before it fails. Such web buckling is not synonymous with failure but simply represents a transition from one load carrying mechanism to another load carrying mechanism and the present study has been conducted to obtain relationships between the ultimate load capacity of a panel and its buckling load.

The test program involved a study of how the ultimate load varied with the loading parameter  $\beta$  ( $= c/b$ ), the panel aspect ratio  $\alpha$  ( $= b/d$ ) and the slenderness ratio ( $d/t$ ). It will be shown that a linear relationship exists between the ratio of the ultimate load to the buckling load of a panel and its slenderness ratio  $\frac{d}{t}$  and the loading parameter,  $\beta$ .

#### 2. ELASTIC BUCKLING LOADS

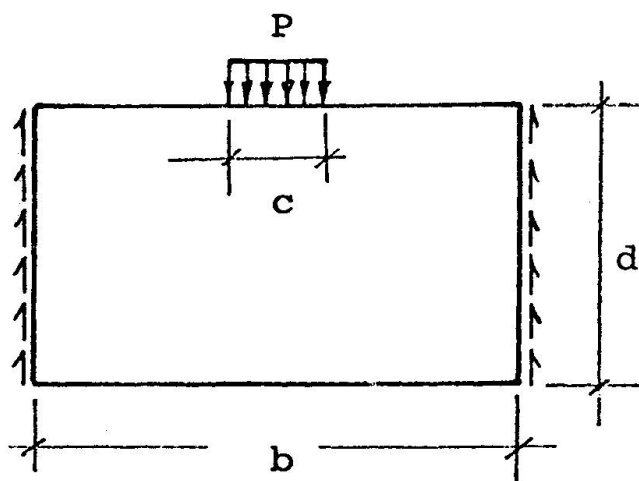


Fig. 1

Theoretical critical load values have been determined for the buckling of plates when subjected to uniform edge load and also for the more difficult case of a panel subjected to partial edge loading (1 - 10). Rockey and Bagchi (10) used the Finite Element Method to determine the buckling load of a rectangular panel when subjected to a patch load on one longitudinal edge and supported by shear forces on the two transverse edges as shown in figure 1. Results were also obtained for the cases where an in-plane moment or an in-plane



shear stress acts in addition to the stress field set up by the patch loading.

The compressive patch load ( $P_{cr}$ ) which will cause buckling of a rectangular plate is given by equation (1).

$$\frac{P_{cr}}{bt} = K \frac{\pi^2 D}{d^2 t} \quad (1)$$

Figure 2, gives the relationship between the non-dimensional buckling coefficient  $K$ , the loading parameter  $\beta$  ( $= c/b$ ) and the aspect ratio  $\alpha$  ( $= b/d$ ).

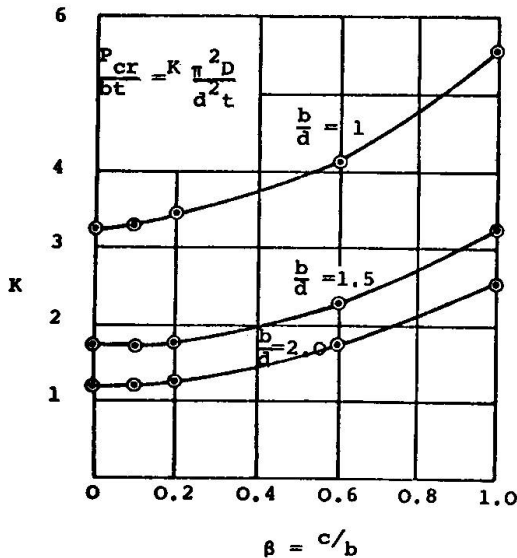


Fig. 2. Variation of the buckling coefficient  $K$  with the loading parameter  $\beta$  and the panel aspect ratio  $b/d$ .

The presence of either an additional shear or moment will reduce the applied edge load necessary to buckle the panel. Figure 3 presents the interaction curves which have been obtained for the following two cases,

- a simply supported square plate subject to a combination of uniform edge-loading and in-plane moment
- a simply supported square plate subject to a combination of discrete edge loading ( $\beta = 0.2$ ) and in-plane moment

Figure 4 gives the corresponding interaction curves for the combination of a transverse edge loading and an additional uniform shear load.

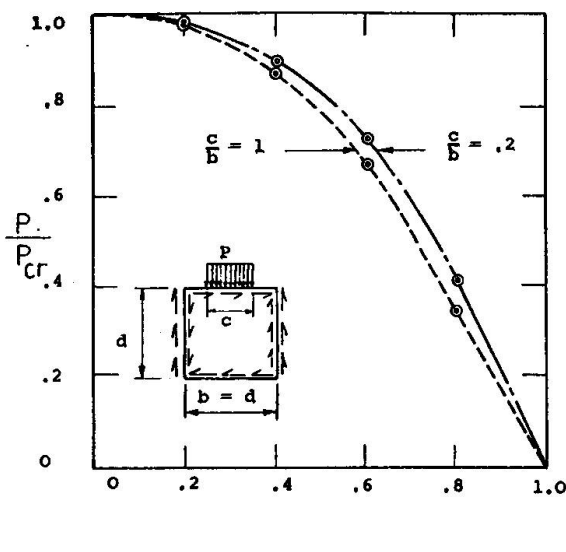


Fig. 3. Influence of a co-existent shear upon the magnitude of the critical patch load.

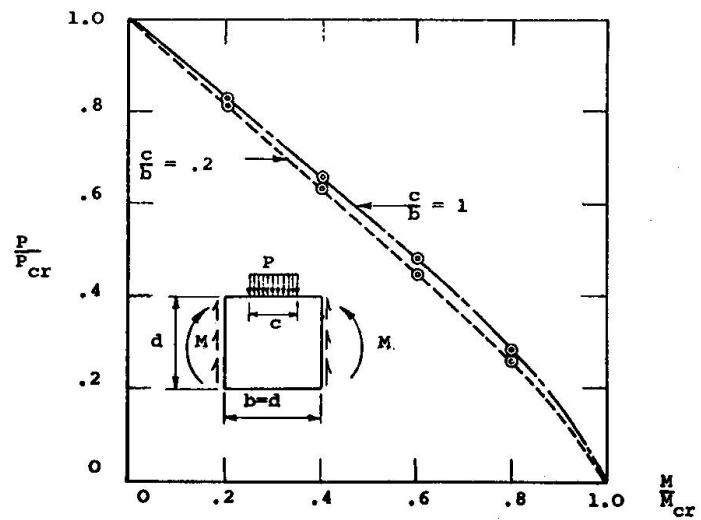


Fig. 4. Influence of a co-existent bending moment upon the magnitude of the critical patch load  $P$ .

### 3. TEST PROGRAM

The tests were conducted to determine the ultimate load strength characteristics of the webs of a sheet steel flooring system. Figure 5 shows the cross section of the unit (one bay) which was tested.

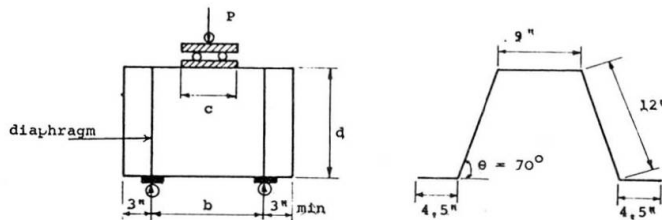


Fig. 5. Details of Test Specimen.

and was distributed over a distance  $c$ , as shown in figure 6. An electric load cell was placed between the ram and the test specimen as can be noted in the figure.

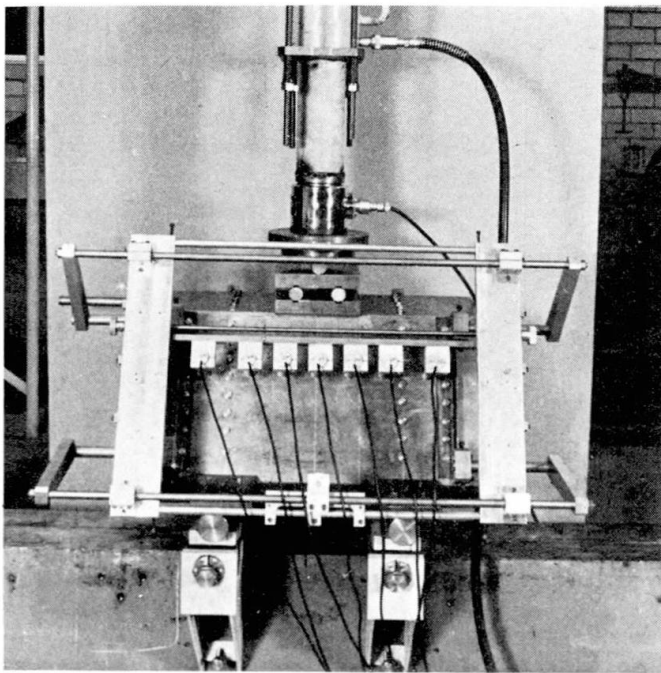


Fig. 6.

The test specimen was supported on roller supports which could be adjusted to ensure that the load was applied to both webs. At each support a very strong diaphragm was fitted and straps were fitted across the base of the specimen thus ensuring that no splaying of the webs would occur.

The specimens were tested in a self straining frame and the load was applied by means of a push type hydraulic ram through a central roller

The lateral deflection of the web was recorded using the special deflection recording apparatus shown in figure 6. With the aid of this frame, the seven linear displacement transducers could be adjusted to any position. These transducers were connected to a data logger which printed out directly the values of the deflections in units of 0.001 inch. In addition, dial gauges, calibrated in units of 0.001 inch were used to record the lateral deflections at specific positions.

Loads were applied to the test specimens in small increments in the elastic range, and in smaller increments after yielding had begun. In the inelastic range, all plastic flow was allowed to take place at each load increment before

any lateral deflection readings were taken.

To determine the material properties three test coupons were tested from each plate to determine the yield stresses and other material properties. All of the test coupons behaved in a manner typical of that expected for mild structural steel and the results showed that the yield stress did not vary markedly from one gauge of material to another.

## 4. EXPERIMENTAL RESULTS

TABLE 1.

Test No.	d inch	b inch	c inch	t inch	$\alpha = \frac{b}{d}$	$\beta = \frac{c}{b}$	$\frac{d}{t}$	$P_u$ tons	$P_{cr}$ tons	$\frac{P_u}{P_{cr}}$
1.1	12	12	2.4	.037	1	.2	325	.37	.17	2.17
1.2	12	12	2.4	.048	1	.2	250	.54	.38	1.43
1.3	12	12	2.4	.06	1	.2	200	.84	.74	1.13
1.4	12	12	2.4	.075	1	.2	160	1.30	1.43	.91
1.5	12	12	2.4	.102	1	.2	118	2.56	3.58	.72
1.6	12	12	2.4	.128	1	.2	94	4.20	7.08	.59
2.1	12	12	6	.037	1	.5	325	.58	.19	3.06
2.2	12	12	6	.048	1	.5	250	.85	.43	1.98
2.3	12	12	6	.06	1	.5	200	1.23	.83	1.48
2.4	12	12	6	.075	1	.5	160	2.04	1.61	1.27
2.5	12	12	6	.102	1	.5	118	3.95	4.04	.98
2.6	12	12	6	.128	1	.5	94	6.08	7.96	.76
3.1	12	12	1.2	.06	1	.1	200	.71	.70	1.01
3.2	12	12	2.4	.06	1	.2	200	.84	.74	1.13
3.3	12	12	3.6	.06	1	.3	200	.97	.76	1.27
3.4	12	12	4.8	.06	1	.4	200	1.1	.80	1.38
3.5	12	12	6	.06	1	.5	200	1.23	.83	1.48
4.1	12	18	3.6	.037	1.5	.2	325	.41	.13	3.15
4.2	12	18	3.6	.048	1.5	.2	250	.54	.29	1.90
4.3	12	18	3.6	.06	1.5	.2	200	.86	.57	1.51
4.4	12	18	3.6	.102	1.5	.2	118	2.5	2.77	.90
4.5	12	18	3.6	.128	1.5	.2	94	4.10	5.49	.75

The details of the test program are summarized in Table 1. In all the tests, the section was subjected to a patch load together with the reactive shear forces.

Figure 7 shows how the lateral deflection across the central section of the panel varied throughout the test. It will be noted that the deformations are located in the upper half of the panel adjacent to the patch load.

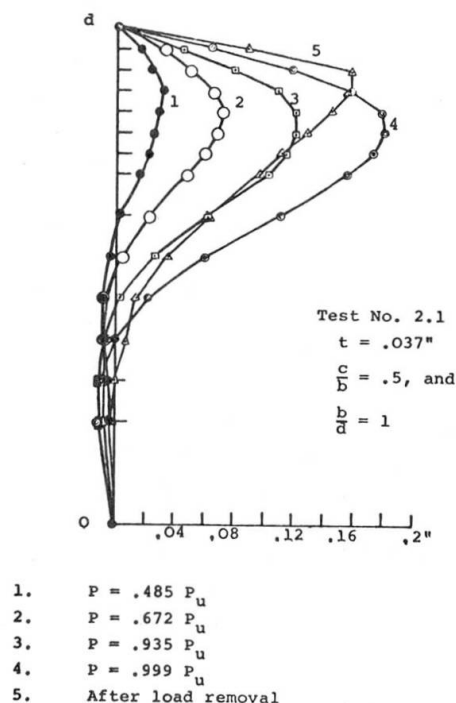


Fig. 7. Variation of lateral deflection of web at the mid section with increasing values of the patch load  $P$ .

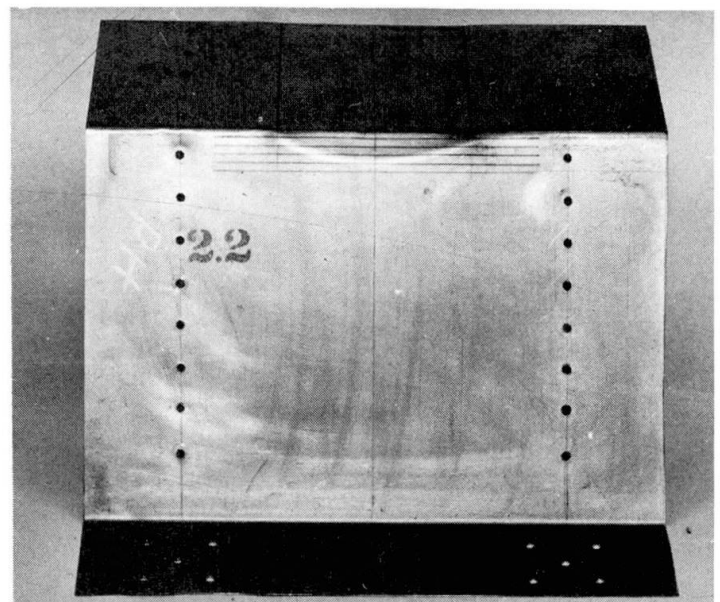
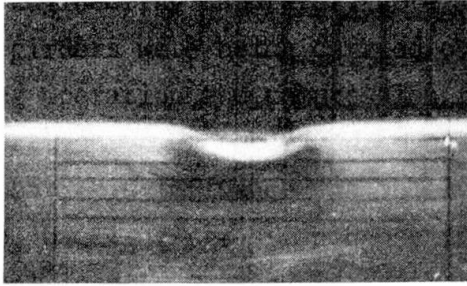
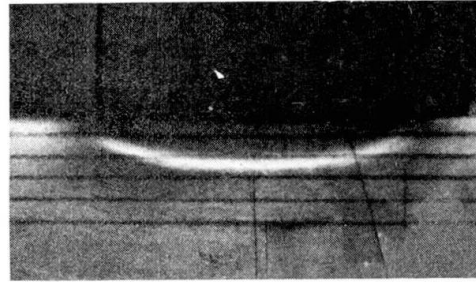


Fig. 8. Failure of a Test Panel showing yield curve.

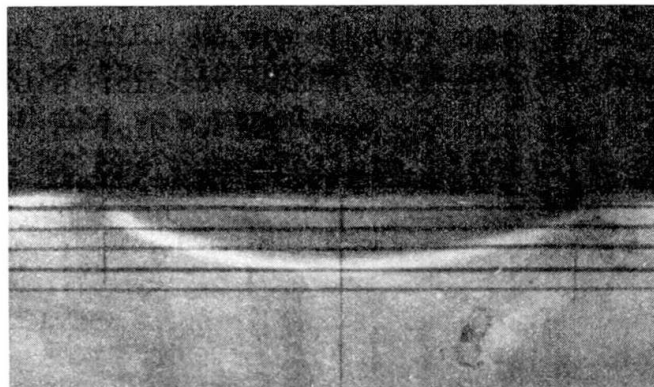
A most significant result is the failure mechanism, in all of the tests failure occurred by the formation of a local yield curve, as shown in figure 8. This yield curve corresponds closely to a segment of a circle, and has a width equal to that of the patch load. It was also noted that the depth of the curve is proportional to the width of the load as can be seen in figure 9. The grid lines in figure 9 are of equal spacing and the variation in the depth of the curve with the  $c/b$  ratio is clearly seen. It was also observed that the shape of the yield curve did not vary with  $d/t$  values.



$c/b = 0.1$  ( $c = 1.2"$ )



$c/b = 0.3$  ( $c = 3.6"$ )



$c/b = 0.5$  ( $c = 6.0"$ )

Fig. 9. Yield Curve Shape and Location on Test Panel ( $b = d$ )

It can be seen, from table 1, that the ratio  $P_u/P_{cr}$  decreases with decreasing values of the  $d/t$  ratio and increases with increasing values of the  $c/b$  ratio. Figure 10 shows how for the specific case of a panel having a depth to thickness ratio of 200:1, the ratio  $P_u/P_{cr}$  varies with the width of the patch load. In figure 11 the  $P_u/P_{cr}$  values for the specific cases of  $c/b = 0.2$  and  $0.5$  and  $\alpha = 1.0$ , are plotted against  $d/t$  values. From figures 10 and 11 the relationship between  $P_u/P_{cr}$ ,  $c/b$  and  $d/t$  given in equation 2 has been obtained.

$$\frac{P_u}{P_{cr}} = \left( 4.5 + 6.4 \left( \frac{c}{b} \right) \right) \frac{d}{t} \times 10^{-3} \quad (2)$$

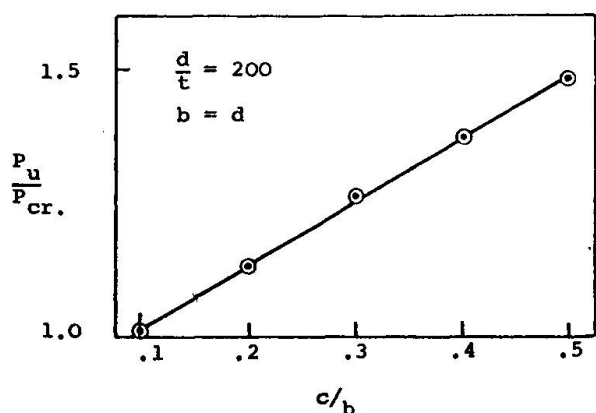


Fig. 10. Variation of the load ratio  $P_u/P_{cr}$  with the load parameter ( $\beta$ ).

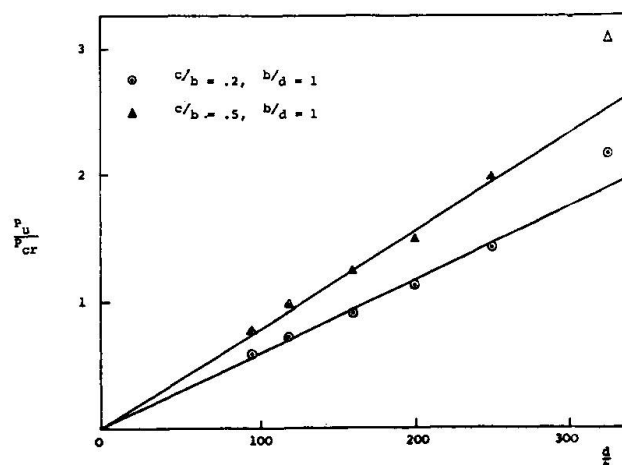


Fig. 11. Variation of the load ratio  $P_u/P_{cr}$  with the slenderness ratio ( $d/t$ ).

Substituting the value of  $c/b = 1.0$  and  $d/t = 288$  into equation 2, it reduces to  $P_u/P_{cr} = 3.14$  which compares closely to the relationship  $P_u/P_{cr} = 3.0$  which Bossert and Ostapenko (11) derived from their tests on panels having a  $d/t$  ratio of 288.

The ratios  $P_u/P_{cr}$  were found to be smaller for the smaller aspect ratio when  $\beta$  is kept constant and equal to 0.2, see table 1. This result contradicts with a conclusion by Bossert and Ostapenko (11) that the post buckling strength varies inversely with the square root of the aspect ratio  $\alpha$ , when  $\beta = 1$  and  $d/t = 288$ . The authors feel that more tests are needed to study the effect of varying  $\alpha$ , and also to examine the influence of flange stiffness upon the ultimate load characteristics. Currently the authors are examining the effect of the presence of an additional shear or moment, see figures 3 and 4, upon the ultimate load characteristics.

## 5. CONCLUSIONS

The test results have shown that there is a considerable amount of post buckling strength for panels having high slenderness ratios. This post buckling strength also increases with the increase in the loading parameter  $\beta$  ( $= \frac{c}{b}$ ). It has been shown that a linear relationship exists between the ratio of the ultimate load ( $P_u$ ) to the buckling load ( $P_{cr}$ ) and the  $c/b$  and  $d/t$  ratios. Failure of all test panels was defined by the formation of a localised yield curve under the load. The width of this curve was found to be equal to that of the load and its depth proportional to its width.

## ACKNOWLEDGEMENT

This study is based on research work conducted for the British Steel Corporation to whom the authors wish to make grateful acknowledgement.

NOTATION

b	length of panel
c	width of patch load
d	depth of panel
D	flexural rigidity of the plate $(= \frac{Et^3}{12(1-\mu^2)})$
d/t	slenderness ratio of panel
E	Young's modulus
K	non-dimensional buckling coefficient
P	applied load
P <sub>cr</sub>	theoretical buckling load
P <sub>u</sub>	ultimate load
t	thickness of plate
$\alpha$	panel aspect ratio, $\frac{b}{d}$
$\beta$	loading factor, $\frac{c}{b}$
$\mu$	Poisson's ratio

REFERENCES

1. Zommerfield, A.Z., J. Math. Phys. 54 (1906).
2. Timoshenko, S.P., J. Math. Phys. 58, 357 (1910).
3. Girkmann, K., IABSE Final Report (1936).
4. Zetlin, L. Proc. ASCE 81, paper 795 (September, 1955).
5. Wilkesmann, F.W., Stahlbau (October, 1960).
6. White, R.M., and Cottingham, W., J.E.M.Div.Proc. ASCE October (1962).
7. Kloppel, K. and Wagemann, C.H., Stahlbau (July, 1964).
8. Warkenthin, W., Stahlbau (January, 1965).
9. Yoshiki, M., Ando, N., Yamamoto, Y. and Kawai, T., The Society of Naval Architects of Japan, Vol. 12, 1966.
10. Rockey, K.C., and Bagchi, D.K., Int.J.Mech.Sci. Pergamon Press, 1970, Vol. 12, pp. 61 - 76.
11. Bossert, T.W. and Ostapenko, A., Fritz Eng. Lab. Report No. 319.1 (June, 1967).

Leere Seite  
Blank page  
Page vide



### III

#### Additional Study on Static Strength of Hybrid Plate Girders in Bending

Contribution à l'étude de la résistance statique des poutres hybrides fléchies

Zur statischen Tragfähigkeit hybrider Blechträger unter Biegung

YUKIO MAEDA

Dr.-Eng.

Professor of Civil Engineering  
Osaka University, Osaka, Japan

A part of study on ultimate static strength of hybrid plate girders in bending, which is being carried out at Osaka University, is presented in this paper.

#### 1. Static Bending Tests

The concept of "hybrid construction" has been introduced to meet the functional, economic, and safety requirements of a structure. To examine hybrid feature at a plate girder in terms of its static flexural behavior and ultimate strength, four large-scale welded hybrid plate girders with longitudinal stiffeners were tested statically up to their failure under two concentrated loads. Web slenderness ratio of a test panel, which is arranged at the middle part of girder and subjected to a uniform bending moment, was intended for the value of 150, 200, 250 and 300.

A section at the test panel consists of such three steel materials as SM58 for a compression flange, SS41 for a web and HT80 for a tension flange. SM50 steel is used for stiffeners. SS41, SM50 and SM58 steels are specified at the Japanese Industrial Standards, and respectively an ordinary carbon steel, a high-strength structural steel and a high-yield strength quenched and tempered steel. HT80 steel is a high-yield strength quenched and tempered alloy steel, not yet specified at the Japanese Industrial Standards. The average values of upper yield stresses  $\sigma_{yu}$ , lower yield stress  $\sigma_{yl}$ , tensile strength  $\sigma_t$  and elongation  $\epsilon$  of these steels were shown by coupon tensile tests as follows:

Steel	$\sigma_{yu}$ (kg/mm <sup>2</sup> )	$\sigma_{yl}$ (kg/mm <sup>2</sup> )	$\sigma_t$ (kg/mm <sup>2</sup> )	$\epsilon$ (%)
HT80	84.64	84.28	88.40	12.3
SM58	54.80	53.64	62.02	19.6
SM50	38.06	36.81	51.52	25.4
SS41	31.44	30.06	42.94	36.5

Sectional areas of the upper and lower flanges of the test girders, are designed so that the both flange materials may reach their yielding stress at the almost same time at the extreme fibers of flanges.

Actual dimensions of the test girders and the yielding stresses of steels for calculations are summarized in Table 1.

#### 2. Discussions of Test Results

(1) Collapse loads  $P_{ex}$ , ultimate bending moments  $M_u$ , modes of failure of test panels and locations of failure are shown in Table 2.

A contribution of web post-buckling strength to ultimate bending strength of the test panel, a beneficial effect of longitudinal stiffeners on the web



post-buckling strength and a mode of final failure of the girders being controlled by the rigidity of compression flange and longitudinal stiffeners, have been observed in hybrid girders as well as in non-hybrid girders.

The failure of BL-3 and BL-4 girders is shown in Figs. 1 and 2.

(2) First of all, the web showed a larger lateral deflection after the web yielding at its compression edge for BL-1, -2, and -3 girders and before the web yielding for BL-4 girder, and then the yielding of web penetrated toward the neutral axis of section. Thereafter, the yielding in compression flange developed and extended over its entire thickness, and then its lateral buckling with a torsional buckling in BL-1, -2, and -3 girders and with a vertical buckling in BL-4 girder, was observed. In non-hybrid girders, when a compression flange yielded, a web had not yielded, but in the hybrid girders, the web had already yielded before the flange yielding.

Hence, it follows that the compression flange area alone may resist against a buckling of the flange without a contribution of effective strip of the web, although in non-hybrid girders a compression flange area plus an effective strip of web along the flange can resist flange buckling. At a girder with high hybridness, it will be optimum to select a material for web which buckles at its yielding stress.

Such a behavior can be seen clearly at a typical flexural strain distributions in the test panel of BL-2 and -3 girders as shown in Figs. 3 and 4.

(3) In non-hybrid girders, a loss of web section was observed for a girder with web slenderness ratio larger than 250, but at the present tests the girder with web slenderness ratio of about 300 showed a slight loss of the web section.

(4) Larger initial web deflections were observed for the less rigidities of anchoring frames consisting of flanges and stiffeners. This tendency was recognized more remarkably than in non-hybrid girders. It does not seem that the initial web deflections which were measured to be 0.11 t, 0.36 t, 0.89 t and 1.08 t respectively for BL-1, -2, -3, and -4 girders, influenced greatly on the ultimate strength. The final web deflections were measured to be about 1.0 t - 2.0 t.

(5) Since restraining of the web against a buckling of the compression flange may not be expected after the web yielding, a width-thickness ratio of the compression flange has to be made smaller, to be provided with an equivalent rigidity which is secured by contribution of the effective strip of web section in non-hybrid girders.

(6) The use of a very high strength steel HT80 for the tension flange is beneficial for the compression side of a section, because the neutral axis of the section moves upward, due to the tension flange area about 40% smaller than in non-hybrid girders.

(7) The observed ultimate bending moment  $M_u$  is non-dimensionalized by dividing by the theoretical full-plastic moment  $M_p^{th}$ , as shown in Table 3 and Fig. 5, and  $M_u$  divided by the theoretical flange yielding moment  $M_{yf}^{th}$  is given in Table 3 and Fig. 6. The theoretical moments were calculated following the models of stress and strain in Fig. 7.

The tests of non-hybrid girders consisting of SM58 - SM50 - SM58 showed that the flange yielding moment could be secured up to about  $\beta = h/t_w = 400$ .

At the present hybrid girders of SM58 - SS41 - HT80, however, the possible web slenderness ratio to secure the flange yielding moment has been lowered down to about 300.

Fatigue tests of longitudinally stiffened hybrid plate girders will be soon carried out at Osaka University.

Table 1 Dimensions of Test Girders and Yielding Stresses of Steels

GIRDER	COP. FLANGE ( $2b \times t_c$ mm)	TEN. FLANGE ( $2b \times t_t$ mm)	WEB ( $h \times t_w$ mm)	$t_s \times b_s$ (mm)	$\beta = \frac{h}{t_w}$	$b/t_c$	$\alpha = \frac{a}{b}$	$\gamma/\gamma^*$	$\rho = \frac{A_w}{A_{fc}}$	$\sigma_{yfc}$ ( $\text{kg/mm}^2$ )	$\sigma_{yft}$ ( $\text{kg/mm}^2$ )	$\sigma_{yw}$ ( $\text{kg/mm}^2$ )
BL-1	$200 \times 12.9$	$200 \times 8.0$	$675 \times 4.8$	$8 \times 65$	141	7.75	1.0	5.34	1.26	53.6	84.3	30.1
BL-2	$200 \times 12.9$	$200 \times 8.0$	$900 \times 4.8$	$8 \times 70$	188	7.75	1.0	5.67	1.67	53.6	84.3	30.1
BL-3	$200 \times 12.9$	$200 \times 8.0$	$1125 \times 4.8$	$8 \times 75$	234	7.75	1.0	6.06	2.00	53.6	84.3	30.1
BL-4	$200 \times 12.9$	$200 \times 8.0$	$1350 \times 4.8$	$8 \times 80$	281	7.75	1.0	6.50	2.50	53.6	84.3	30.1

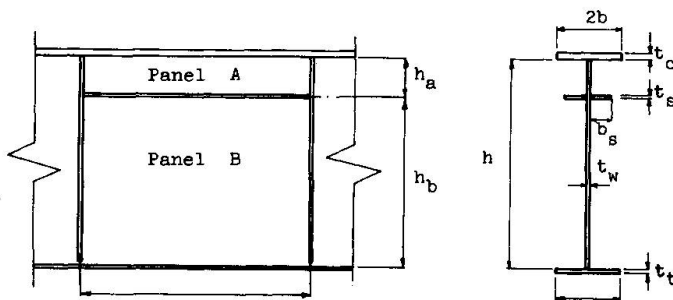


Table 2 Test Results of Failure of Test Girders

GIRDER	$P_{gx}$ (t)	$M_u$ (t-m)	MODE OF FAILURE	LOCATION OF FAILURE
BL-4	147	257	VERTICAL BUCKLING LATERAL BUCKLING	
BL-3	110	220	VERTICAL BUCKLING LATERAL BUCKLING	
BL-2	85	170	OUTSIDE OF TESTPANEL (VERTICAL BUCKLING) LATERAL BUCKLING	
BL-1	62.5	125	OUTSIDE OF TESTPANEL (TORSIONAL BUCKLING) LATERAL BUCKLING	

Table 3 Ultimate Bending Moments

GIRDER	$\beta$	$M_u$ (tm)	$M_{yf}^{th}$ (tm)	$M_p^{th}$ (tm)	$M_u / M_{yf}^{th}$	$M_u / M_p^{th}$
BL-1	141	125	111	113	1.126	1.106
BL-2	188	170	156	160	1.090	1.063
BL-3	234	220	205	210	1.073	1.048
BL-4	281	257	259	265	0.992	0.970

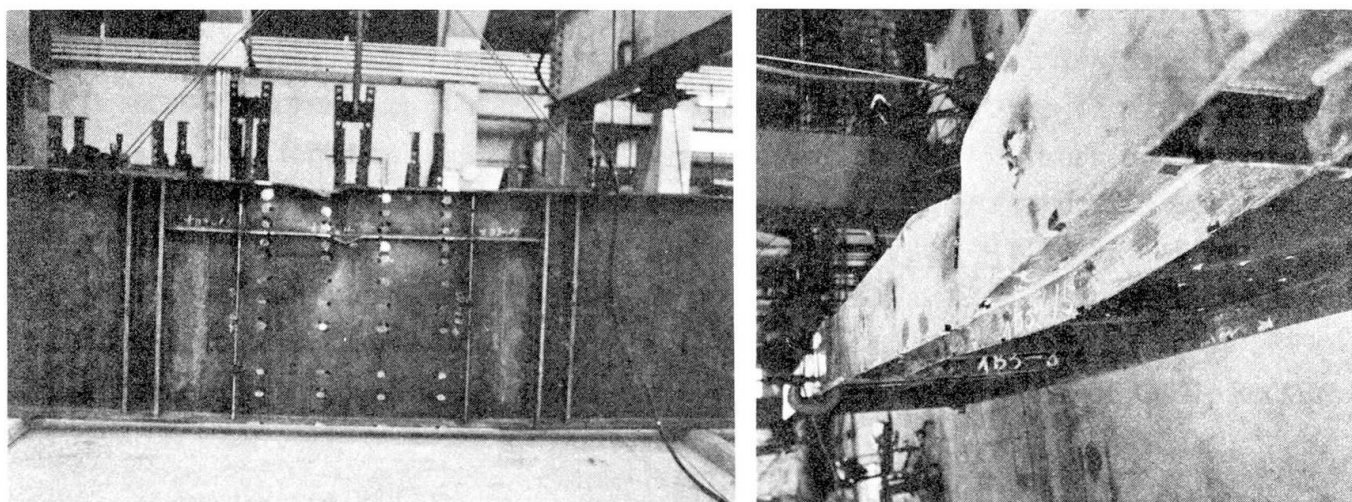


Fig. 1. Failure of Test Girder BL-3

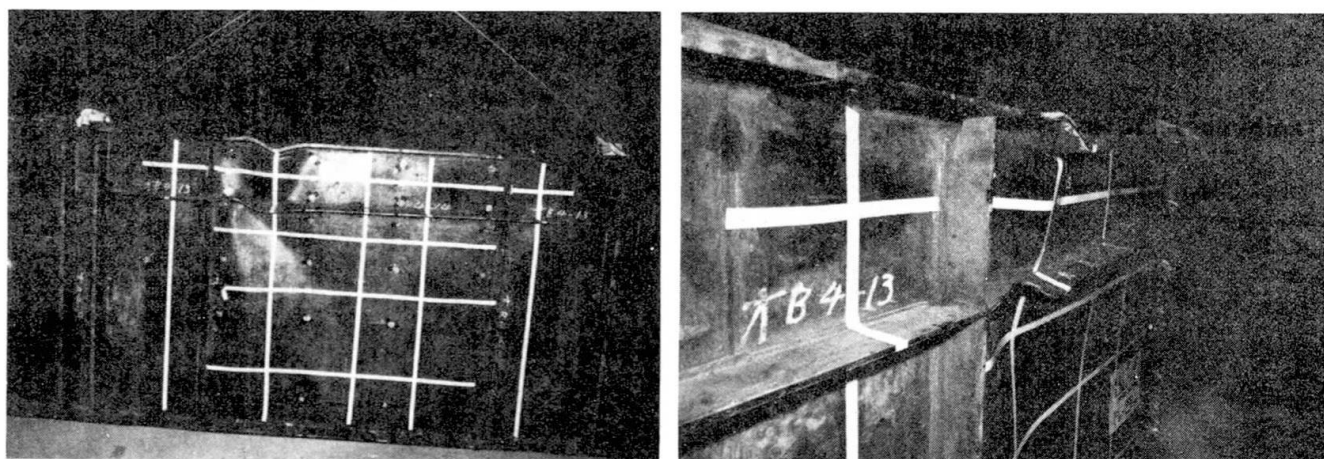


Fig. 2. Failure of Test Girder BL-4

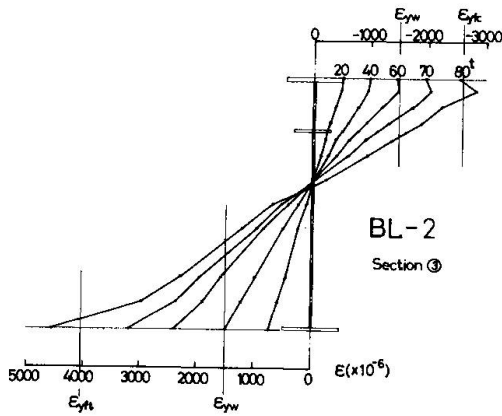


Fig. 3. Strain Distribution in Test Panel of BL-2 Girder

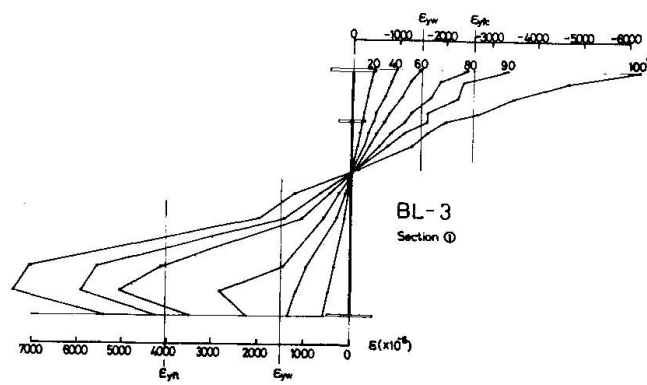


Fig. 4. Strain Distribution in Test Panel of BL-3 Girder

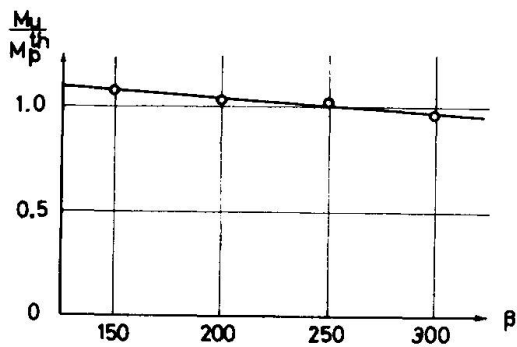


Fig. 5.  $M_u / M_p^{th}$  versus  $\beta = h/t_w$

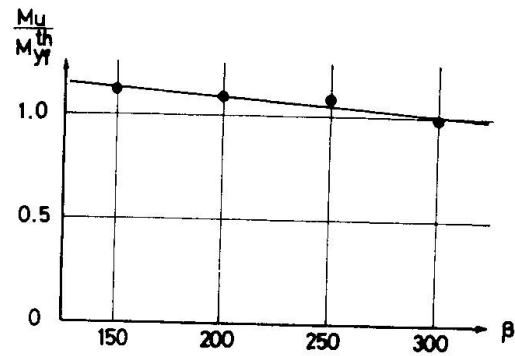


Fig. 6.  $M_u / M_{yf}^{th}$  versus  $\beta = h/t_w$

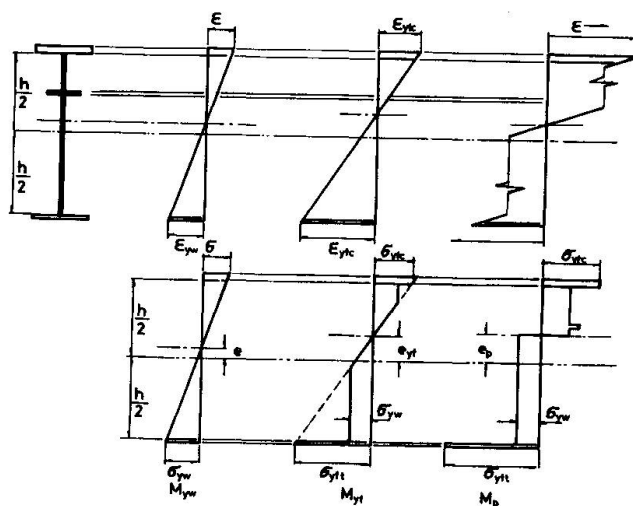


Fig. 7. Models of Development of Stress and Strain

Leere Seite  
Blank page  
Page vide

### III

Prepared Discussion in regard to the Report Presented by Professor P. Dubas:  
"Essais sur le comportement postcritique de poutres en caisson raidies"

Discussion préparée du rapport du Prof. P. Dubas:  
"Essais sur le comportement postcritique de poutres en caisson raidies"

Vorbereitete Diskussion zum von Prof. P. Dubas vorgelegten Bericht:  
"Essais sur le comportement postcritique de poutres en caisson raidies"

MIROSLAV ŠKALOUD

Doc., CSc., Ing.

Senior Research Fellow

at the Czechoslovak Academy of Sciences

Institute of Theoretical and

Applied Mechanics in Prague, Czechoslovakia

The author would like to support the very interesting and valuable conclusions quoted a) in Professor Dubas's report "Essais sur le comportement post-critique de poutres en caisson raidie" and the prepared discussion by Professor Massonnet and R. Maquoi, entitled "The Conventional Design of Box Girders Is Unsafe .....": both regarding the post-buckled behaviour of longitudinally stiffened compression plates of box girders.

Professor Massonnet has already mentioned some of our theoretical conclusions in his prepared discussion. Other theoretical and experimental evidence obtained by our team in Prague has the same trend; therefore, it does not need quoting here.

The author would only like to mention three general conclusions which sum up our main results and observations in the aforesaid field (/1/, /2/, /3/, /4/, /5/):

1) Longitudinal stiffeners designed by the linear theory of web buckling (s.c. concept of  $\varphi^*$ ) do not provide sufficient support for the web in the whole post-buckled range of its behaviour. The limit of efficacy of such stiffeners is considerably reduced, so that the stiffeners practically do not operate in a significant part of the post-critical domain of the web in question. The ultimate strength of the plate (and, consequently, the load-carrying capacity of the whole girder) is then



substantially reduced.

2) It was noted that for the longitudinal stiffeners to remain rigid and fully effective up to the collapse of the girder, it was necessary that they should have a flexural rigidity equal to a multiple of the linear theoretical rigidity  $\mathcal{J}^*$  ( $\mathcal{J}_0 = k \mathcal{J}^*$ ).

For such rigid stiffeners, the load-carrying capacity attains the highest possible value. Then the thinnest possible (i.e. optimum) web is obtained.

3) An analysis of our results also indicates that the afore-said concept is only a limiting case of a more general philosophy.

The relationship between ultimate load and stiffener rigidity is shown in Fig.1. The reader will note there that for small values of  $\mathcal{J}$  the ultimate strength grows fast, but then the rate slows down so that, for values near to  $\mathcal{J}_0$ , the increase in the load-carrying capacity is only slight.

Therefore, by considerably reducing the stiffener rigidity with respect to  $\mathcal{J}_0$ , a very small reduction in ultimate load is obtained. In other words, if the stiffener dimensions are significantly diminished, only a slight increase in web thickness is needed. Considering that the number of available thin sheets of different thicknesses is limited, the slight reduction in load-carrying capacity does not frequently lead to any practical increase in web thickness.

From this it follows that the concept of rigid stiffeners, furnishing an optimum web, need not necessarily lead to the most economic alternative, if the designer has not in mind merely the web (or compression plate element) alone, but desires to optimize

the whole system of web (or plate element) + stiffeners; or, in other words, desires to optimize the whole girder.

To conclude the author wishes to state that he shares the view, quoted in the two afore-mentioned contributions, that the current design concept based on the  $\mathcal{J}^*$  - value ought to be abandoned. Further research in regard to the post-buckled behaviour of compression plates fitted with longitudinal stiffeners should be conducted as soon as possible, in order that the afore-said efficiency factor  $k$  could be determined for various kinds of stiffening. A new design procedure, taking account of the post-critical performance of compressed stiffened elements of

box girders, can then be established; and further accidents, like those of Vienna, Milford Haven and Melbourne, will thereby be avoided.

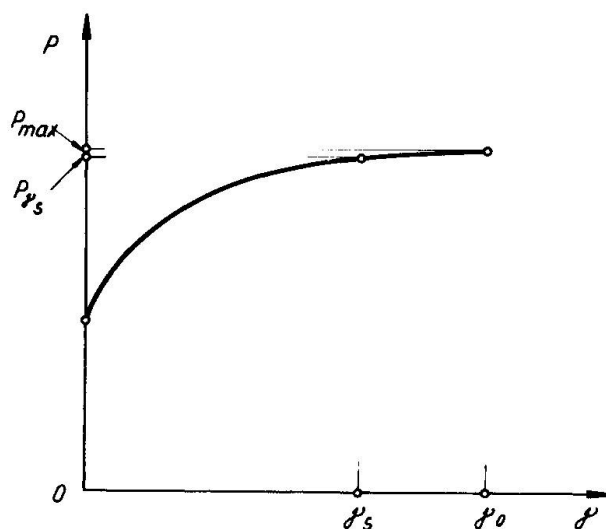


Fig. 1.

#### References:

- /1/ Škaloud, M., Novotný, R.: Überkritisches Verhalten einer gleichförmig gedrückten, in der Mitte mit einer Längsrippe versteiften Platte.  
Acta technica ČSAV, n° 3, 1964.
- /2/ Škaloud, M., Novotný, R.: Überkritisches Verhalten einer gleichförmig gedrückten, in den Dritteln mit zwei Längsrippen versteiften Platte.  
Acta technica ČSAV, n° 6, 1964.



- /3/ Škaloud, M., Novotný, R.: Überkritisches Verhalten einer anfänglich gekrümmten, gleichförmig gedrückten, in der Mitte mit einer Längsrippe versteiften Platte.  
Acta technica, n° 2, 1965.
- /4/ Škaloud, M.: Überkritisches Verhalten gedrückter mit nachgiebigen Rippen versteifter Platten (Experimentelle Untersuchung).  
Acta technica ČSAV, n° 5, 1963.
- /5/ Škaloud, M.: Post-buckled behaviour of stiffened webs, Book. Rozpravy ČSAV. Publishing House "Academia", 1970.

### III

#### **Prepared Discussion in regard to the Post-Buckled Behaviour and Incremental Collapse of Webs Subjected to Concentrated Loads**

Discussion préparée du thème:

"The Post-Buckled Behaviour and Incremental Collapse of Webs Subjected to Concentrated Loads"

Vorbereitete Diskussion zum Thema:

"The Post-Buckled Behaviour and Incremental Collapse of Webs Subjected to Concentrated Loads"

**MIROSLAV ŠKALOUD**

Doc., CSc., Ing.

Senior Research Fellow

at the Czechoslovak Academy of Sciences

Institute of Theoretical and

Applied Mechanics in Prague, Czechoslovakia

**PAVEL NOVÁK**

Doc., CSc., Ing.

Research Fellow at the Structural Institute  
in Prague, Czechoslovakia

#### **Introductory Remarks**

The investigation /1/, /2/ into the post-buckled behaviour of webs in shear having been completed, a new research project regarding the ultimate load behaviour of plate girders was started in Prague. This deals with the effect of flange stiffness upon the ultimate load performance of thin webs subjected to a) static and b) variable repeated concentrated loads, which are applied to the flange of the girder at the mid-distance of the vertical stiffeners of the web. This problem is frequently encountered in the design of crane girders, certain types of bridge girders and similar structures, and also in the case of girders without vertical stiffeners (see the very interesting contribution by Bergfelt /3/). The objective of our new research is to study not only the static failure mechanism of such girders, but also the deflection stability of the web under variable repeated, cyclic loading, and the incremental collapse of the web and the whole girder.

#### **Test Girders and Apparatus**

The aforesaid research project consists, in the first stage, of testing 8 steel panels shown in Fig. 1 and 7 large-scale steel test girders. Further test series will follow. Some of the panels and girders are subjected to static loads, the others to cyclic pattern loading.

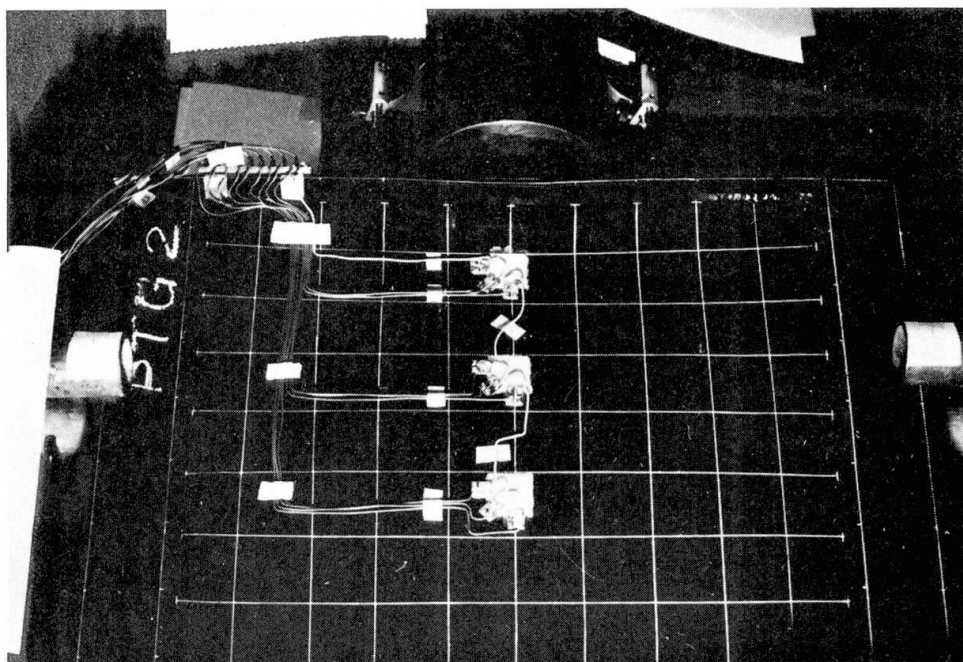


Fig. 1.

The research on steel girders is accompanied by a photoelasticity investigation conducted by the first of the authors and J. Kratěna on reduced-scale epoxy-resin models.

The buckled pattern of the web is measured by means of a stereophotogrammetric method which has been established by one of the authors /4/. One of the advantages of this method consists in making it possible to measure not only the web deflection perpendicular to the web, but also the other two components of the spatial displacement vector of any point of the web and flanges. Thus it is possible, for instance, to evaluate the distortion, in terms of load, of the projection of the mesh that was marked on the web, and which serves as a basis for the determination of the contour maps of the buckled surfaces of the web. The distortion of the projected mesh is not negligible, as can be seen in an enlarged scale in Fig. 2, this being particularly the case in the vicinity of the applied load. The contour plots of the buckled surface of the

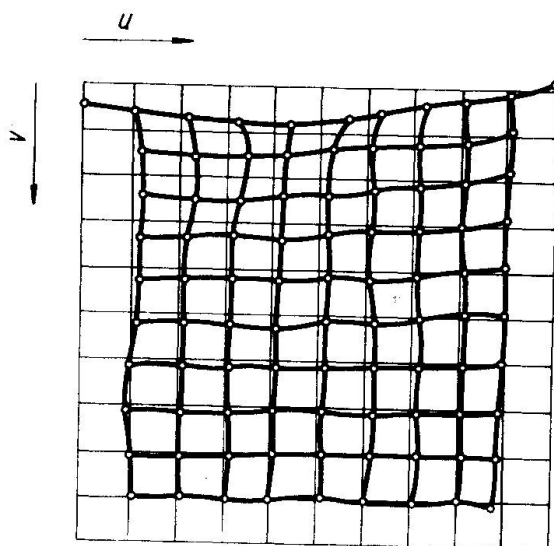


Fig. 2.

web are then related to the distorted mesh and to the deformed boundary framework of the web panel.

The contour map of the post-failure plastic residue in a web panel, subjected to a concentrated load at the mid-distance of the vertical stiffeners, and in the deflected flange are shown in Fig. 3.

The stereophotogrammetric method is also successfully used to measure the web buckled pattern and the flange deflection in the cyclic loading tests. An oscilloscope "Disa" and additional apparatus (Fig. 4) enable the writers to measure the deformation at any time moment of a loading cycle - for instance, at the moment when the deflection amplitude is reached.

The stress state in the web and flanges is measured by numerous electric resistance strain gauges. In the case of cyclic loading, some of the strain gauges and dynamic deflection pick-ups are linked to an automatic recorder "Ultralette", which records

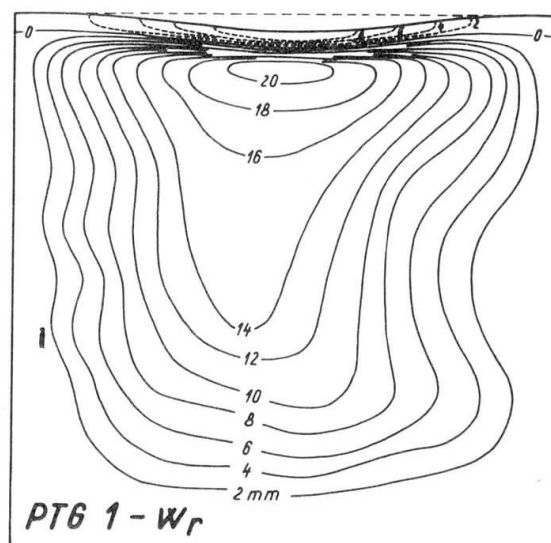


Fig. 3.

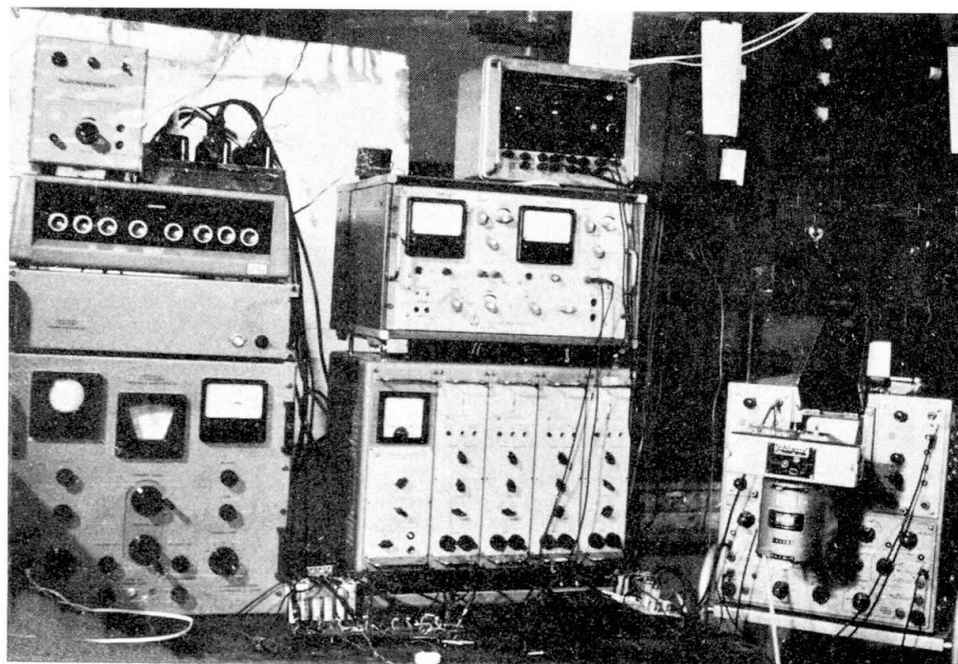


Fig. 4.

the corresponding signals on recording paper (see Fig. 5, showing an increase in web deflection during cyclic loading).

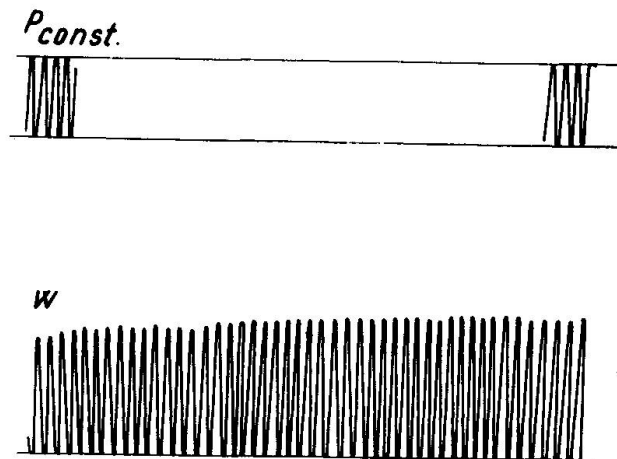


Fig. 5.

### Test Results

An analysis of the static test results indicates that thin webs subjected to concentrated loads manifest a considerable post-critical reserve of strength, which ought to be taken into account in the design of steel plate girders.

The load-carrying capacity of such webs is significantly affected by the flexural rigidity of flanges. While for web panels attached to flexible flanges, whose  $I_f/a^3t = 3.49$  ( $I_f/a^3t$  denoting the same flange stiffness parameter as was used in /1/, /2/), the ratio ultimate load  $P_{ult}$ /critical load  $P_{cr} = 1.73$ : in the case of webs attached to heavier flanges,  $I_f/a^3t = 63.5$ , the same ratio amounted, on an average, to 2.445.

In the tests on plate girders subjected to variable repeated loading, the question of stability of post-critical web deflection is of importance.

When the girder operates in the plastic range, an increase in web deflection during a certain number of loading cycles is noted (Fig. 5). The problem is then to determine the maximum load for which these deflection increments cease after a limited number of cycles of load application, and the structure then responds to the load in a purely elastic manner. The corresponding load, which is referred to as the "stabilizing load", is the highest force the girder can sustain. Any further increment in load brings about a breakdown of the girder through incremental collapse.

Fig. 5 relates to a load which was practically equal to the "shake-down load" of the test girder. A slight further increment in load caused instability of web deflection and, shortly afterwards, a collapse of the girder.

A complete report on the above mentioned research project will appear shortly after the completion of the tests.

#### References:

- /1/ Rockey, K.C., Škaloud, M.: The ultimate load behaviour of plate girders loaded in shear. Contribution presented at the IABSE Colloquium "Design of Plate and Box Girders for Ultimate Strength", London, March, 1971.
- /2/ Škaloud, M.: Ultimate load and failure mechanism of thin webs in shear, dtto.
- /3/ Bergfelt, A.: Studies and tests on slender plate girders without stiffeners. dtto.
- /4/ Novák, P.: Méthode photostéréométrique dynamique des modèles. Colloque International de RILEM, Bucaresti, 9.-11.sept. 1969.

### III

English Translation of part of the text of pages 13, 14 and 15 of the book:  
**Beulwerte ausgesteifter Rechteckplatten, Vol. II by K. Klöppel and  
 K.H. Möller, Editor W. Ernst und Sohn, Berlin, 1968**  
 (Reproduced with the Permission of Professor K. Klöppel)

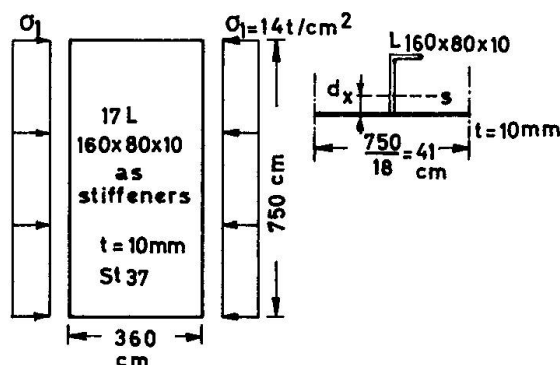
Traduction anglaise d'une part du texte des pages 13, 14 et 15 du livre:  
 Beulwerte ausgesteifter Rechteckplatten, Vol. II par K. Klöppel et  
 K.H. Möller, Editeur W. Ernst und Sohn, Berlin 1968  
 (reproduit avec l'autorisation du Prof. K. Klöppel)

Englische Übersetzung eines Teils des Textes der Seiten 13, 14 und 15 des  
 Buches:  
 Beulwerte ausgesteifter Rechteckplatten, Bd. II von K. Klöppel und  
 K.H. Möller, Verlag W. Ernst und Sohn, Berlin 1968  
 (Mit Genehmigung von Prof. K. Klöppel)

#### Page 13.

In the use of tables for uniformly distributed stiffening, it is necessary exert caution about two questions :  
 First, about the calculations of the effective moment of inertia, secondly, about the safety required against buckling.  
 The Standard DIN 4114 Ri 18.13. accepts, for eccentric stiffeners, to relate the moment of inertia to the upper edge of the plate. The basis of this rule is an assumption about the effective width of a corresponding strip of the buckled plate. But when the stiffeners are regularly spaced, the effective width cannot be larger than the distance between two stiffeners.  
 If the moment of inertia of such a plate strip is calculated, then values significantly smaller than according to DIN 4114 are usually obtained. For closely spaced stiffeners, it is therefore always recommended to calculate the moment of inertia both according to the Standard and also for a plate strip composed of a stiffener and a web strip having as width the distance between two stiffeners, the example figure 11 should serve an illustration. According to DIN 4114, the moment of inertia with respect to the upper edge of the web is

$$J_{DIN} = J_L + F_L (a - e_x)^2 = 611 + 23,2 \times (16 - 5,63)^2 = 3115 \text{ cm}^4$$





With the largest value for the effective width, namely the distance between two stiffeners, the distance of the centroid to the upper edge of the web is found to be, according to fig. 11 :

$$d_x = \frac{F_L \left(a + \frac{t}{2} - e_x\right)}{F_L + F_{web}} = \frac{23,2 (16 + 0,5 - 5,63)}{23,2 + 41} = 3,92$$

which yields

$$J = J_2 = F_L \left(a + \frac{t}{2} - e_x - d_x\right)^2 + F_{web} d^2 = 2360 \text{ cm}^4$$

It is seen therefore that  $J_{DIN}$  does not apply for the calculation of the buckling stress.

#### Page 14.

As already mentioned in the Introduction, one has to distinguish between the linear buckling, connected with idealized structural and geometrical assumptions, with the buckling load as limit load, which is the basis for the specification DIN 4114 and for the present book, and a second postcritical non linear buckling, described by non linear differential equations to which is associated a limit load which is called ultimate load. This load is regularly higher than the buckling load, because additional membrane stresses come into play. On this theoretically more complicated way, the influences of unavoidable initial deflections may also, for example, be taken in consideration. The ultimate load above the buckling load can be determined either by the entry into the plastic range or by inacceptably large deformations.

#### Page 15.

It is necessary to come back to the question whether by plate buckling a second equilibrium state establishes itself or not. Let us imagine the plate to be studied by linear buckling theory in the buckled state. In addition to the membrane stresses existing already before buckling, we have now flexural stresses, that may be considered to be produced by the fictitious transverse load

$$q = \sigma_x t \frac{\sigma_w^2}{\sigma_x^2} + \sigma_y t \frac{\sigma_w^2}{\sigma_y^2} + \tau t \frac{\sigma_w^2}{\sigma_x \sigma_y}$$

where  $\sigma_x$ ,  $\sigma_y$  and  $\tau$  are the edge stresses of the plate. If the buckling shape is not known, one shall imagine that the plate is subjected to a uniform transverse load. A large limit load is then to await, when these fictitious transverse loads are supported in all directions nearly on the same way, in other words when we have an extended plate action. If, on the contrary, these imagined transverse loads are supported only in the direction of the greatest compressive stresses, then we can as a good approximation to reality imagine the plate to be cut in strips by cuts parallel to the largest compressive stresses. The individual beamlike strip wall then behave like a buckled stult.

It is recommended now, for plates which support the fictitious transverse loads nearly uniquely in the direction of the large compressive stresses, to require larger safeties than  $\varphi_b = 1,25$  or  $\varphi_b = 1,35$ .

According to the opinion of the authors, which is supported by sections 17.5 and 17.6 of the DIN 4114, safeties are to be required which in the limit case coincide with those for the compressed bar. Numerical comparisons have led to following formule - which cannot be demonstrated, which should give the required safety

$$\varphi_R^k = \frac{\varphi_k + 100 \bar{\alpha}^2 \varphi_B}{1 + 100 \bar{\alpha}^{-2}}$$

The side ratio  $\bar{\alpha}$  is obtained through the differential equation of the orthotropic plate, under the assumption of a definite torsional rigidity, by a coordinate transformation.  $\bar{\alpha}$  is the side ratio of an unstiffened comparison plate with the same buckling shape as the stiffened plate :

$$\bar{\alpha} = \alpha \sqrt[4]{\frac{1 + \frac{\varphi_0}{\varphi_2}}{1 + \frac{\varphi_0}{\varphi_2}}}$$

An unstiffened plate with the side ratio  $\alpha$  behave therefore similarly as an unstiffened plate with the side ratio  $\bar{\alpha}$ .

For the above example, (fig.11),  $\varphi_L = 615$  and

$$\bar{\alpha} = 0,48 \sqrt[4]{\frac{1}{616}} = 0,096$$

According to Table 7 of DIN 4114, we have for loading case 1

$$\varphi_k = 2,18$$

and one obtains

$$\varphi_R^k = \frac{\varphi_k + 100 \bar{\alpha}^2 \varphi_B}{1 + 100 \bar{\alpha}^{-2}} = 1,69$$

This safety against buckling at least should be required, in this example, in the opinion of the Authors.

In the choice of the stiffener section, it must be in addition taken care that stiffeners do not buckle before reaching the plate buckling load.

Leere Seite  
Blank page  
Page vide

### III

#### **Excerpts of a Letter of Professor F. Leonhardt to Professor Ch. Massonnet (Reproduced with the Permission of Professor F. Leonhardt)**

Extraits d'une lettre du Prof. F. Leonhardt au Prof. Ch. Massonnet  
(reproduits avec la permission du Prof. F. Leonhardt)

Auszüge aus einem Brief von Prof. F. Leonhardt an Prof. Ch. Massonnet  
(abgedruckt mit Bewilligung von Prof. F. Leonhardt)

For the stiffened bottom plate or the bottom flange of a box-girder under negative moments, with compression in the bottom flange, there is almost no post buckling carrying capacity, as the example of the Danube-Bridge demonstrated. After buckling of the bottom flange, the box can usually carry only more or less as a hinge in the elevation of the stronger orthotropic top plate. This situation makes it necessary to calculate the bottom flange more or less like a compressed column with a buckling length equal to the distance of the transverse stiffeners, if the stiffeners have sufficient rigidity. With soft stiffeners the buckling length becomes even larger. Also in this case, we assume a certain excentricity of the compressive force to take care of unavoidable deviations from the straight line of the axes of the cross-section of a flange (plate plus longitudinal stiffeners). For the longitudinal stiffeners we usually take profiles with a top flange.

The deviations of the actual profiles from the straight lines, which we assume in our calculations, must be laid down on the working drawings and specifications as allowable tolerances and immediately after the erection of portions of the box girder, the actual deviations must be checked and must be kept within these limits.

For the bottom flanges we must also keep in mind, that the principal compressive stresses in the plate are not parallel to the longitudinal axis of the box-girder, but inclined and the angle of inclination depends upon the shear force and the torsion. This can have some influence on the spacing of longitudinal stiffeners and on the buckling safety of the bottom plate itself.

Dimensioning the bottom flange in this way does usually result in only a very small amount of additional steel quantity, because the increased stiffness of the longitudinal stiffeners allows to use a thinner plate. Only the additional rigidity of the transverse stiffeners may increase the weight.

But also here the difference is so small, that it should not count economically.

I am sending to you a drawing of a cross-section of Moseltal-Brücke Winnigen, which we have designed along these lines about 2 years ago and which is under construction just now. It has spans up to 240 m and is erected by the free-cantilevering method, giving rather high compressive force to the bottom slab.

Leere Seite  
Blank page  
Page vide

### III

#### DISCUSSION LIBRE / FREIE DISKUSSION / FREE DISCUSSION

Topic: **Box Girders, Hybrid Girders, Fatigue Problems, Special Problems, Concentrated Loads, Plates with Holes**

Poutres en caisson, poutres hybrides, problèmes de fatigue, problèmes spéciaux, charges concentrées, plaques avec trous

Kastenträger, Hybridträger, Ermüdungsprobleme, Sonderprobleme, konzentrierte Lasten, Platten mit Löchern

Chairman: **K.C. ROCKEY**  
M.Sc., Ph.D., C.Eng., F.I.C.E.  
Professor of Civil  
and Structural Engineering  
University College, Cardiff, England

PROF. K.C. ROCKEY      Chairman's introductory remarks.

During this third and last working session, we shall be discussing the very important subject of the behaviour of box girders together with the special problems involved in the design of webs containing cut outs, the design of hybrid girders, the buckling and ultimate load behaviour of webs subjected to edge patch loading and the fatigue behaviour of plate girders.

These are all problems of considerable importance and since we will have much to discuss, we must of necessity endeavour to keep our comments to a minimum.

-----

Each author was given the opportunity of briefly introducing his report and the following discussion ensued.

-----

PROF. FUKUMOTO.

I would like to add a few comments with respect to the paper by Professor NISHINO and OKUMURA. I refer you to Page 19 where there is a brief description of the plate girder research and the first part is on the shear strength

of welded built up girders and this report has already been presented in the final report of the 8th Congress of I.A.B.S.E. and Professors ROCKEY, BASLER and OSTAPENKO have already referred to this paper in the discussion of experimental results yesterday, so I am not going to present the first part of their report.

The second report is on the moment carrying capacity of large size rolled I beams with the depth of 900 mm and 300 mm in the flange width. They have three different kinds of beams. The first of their tests was carried out on "as rolled" I shapes and the second one on "annealed" I shapes and the third on cambered I shapes; the cambering is due to the stretching of the compression flange during the rolling process. The main aim of their study was to measure the major residual stresses in all 3 shapes and all three involve a different fabrication process. They noticed that the maximum magnitude on the residual stresses reaches 60 % and in some 90 % of the yield strength and they are distributed over the wider portion of the cross section. Due to presence of these large compression residual stresses in the web plate, there are a number of specimens in which the conditions in the web plates become critical for buckling. During the bending test of full size rolled beams, it was observed that the test beams behaved as if they were made of materials of different strength, which was due to the penetration of premature yielding at portions where larger magnitude of residual stress occurs. The fact indicates that a larger reduction of rigidity occurs even at relatively small loading conditions; however, the width to thickness ratios of component plates of rolled beams were so small that stability was not lost by the reduction of rigidity due to the premature yielding and as a consequence the moment carrying capacity exceeded full plastic moment. It was noticed that a beam with buckled web plates, prior to the application of external load, stabilized with the increase of bending moment.

PROF. MASSONNET.

Professor FUKUMOTO, I want to know whether you have special provisions in Japan for the design of box girders, a subject that we shall treat later on in this morning's session, because I was quite interested to see what you said about railway bridges, road bridges and ships.

PROF. FUKUMOTO.

I think that some parts of the Japanese specifications are like those of the German specifications. We do not have special specifications for box girders. We can deal with the design of the compression flange of the box girder as a stiffened plate. Since we do have a specification for the design of a stiffened plate girder, they apply also to stiffened plates under uniform compression. But we do not have special codes for the box girders.

PROF. MASSONNET.

Is this specification to which you refer one derived for ship structures or for compressed stiffened plates ?

PROF. FUKUMOTO.

Yes, we use the specification developed for ship design. They have been studying this problem. If there is time later this morning I will discuss the behaviour of compressed stiffened plates.

PROF. MASSONNET.

Yes, good, because in my opinion the behaviour of box girders depends very much, almost uniquely, about the behaviour of the compressed plate.

PROF. ROCKEY.

If I understood you correctly, Professor FUKUMOTO, you said that, if the web is initially deformed then you find that on loading the bending stresses tend to straighten the webs out. That is what SKALoud and myself also experienced. Nowhere in the Conference today have we really mentioned the influence of residual stresses; there is for example, the paper by OWEN who measured the residual stresses in plate girders and it is clear that the presence of these stresses would be to reduce the buckling stress of the web. This is a consideration which none of us have brought into our previous discussions. This, for example, will mean that in the shear models the critical stress distribution which acts in the "triangular areas" will be reduced because of the presence of residual stresses. Have you any comments on this factor ?



PROF. FUKUMOTO.

Actually, for the large rolled section girder, there was an extremely high residual compressive stress in the web and, when the bending moment is applied in the tension area, you eliminate these high compression stresses and this stabilizes the web - that is one of the findings in their paper. In some cases, especially in bending, the initial compressive stresses in the web can result in a higher ultimate load.

PROF. OSTAPENKO.

It seems to me that buckling of the web will be promoted by the compression zone and restrained by the tension zone, so the findings do not appear to be quite logical.

PROF. FUKUMOTO.

Due to the presence of compressive residual stresses of large magnitude in web, the web plates are critical for buckling.

PROF. OSTAPENKO.

Also, residual stresses are usually considered in buckling computation indirectly by taking the material to be linear up to about 50 to 80 % of the yield stress and then introducing some kind of a transition curve up the yield analogous to a column buckling curve.

PROF. FUKUMOTO.

There are very high compressive stresses at the beginning and during the rolling of girders. We have already experienced the buckling of the web plate due to high compressive residual stresses.

PROF. OSTAPENKO.

Well, the web is never perfectly flat anyway.

PROF. FUKUMOTO.

And also, along the connection between the flange and web there are high tensile residual stresses and I am not sure which part of the web from the top of the flange does possess high compressive stresses. This high tensile residual stress along the flange-web weld line gives favourable results to the web buckling.

PROF. OSTAPENKO.

This may also be the function of the depth of the girder in inches since the width of the tensile residual stress is only about 2" which is usually a small portion of the total depth and the remainder is under compression.

PROF. FUKUMOTO.

Professor NISHINO computed the linear buckling of the plate with initial stresses and also they found good agreement of their computation values with the test results.

PROF. OSTAPENKO.

But that was for uniformly distributed strain.

PROF. FUKUMOTO.

No, for bending of the web.

PROF. DUBAS.

Do you have curves for buckling of the webs of rolled shapes ?

PROF. FUKUMOTO.

Yes. These are the curves for rolled shapes. As a result of rolling of the large size girders, we sometimes obtain a buckled web after the rolling process.

---

OWEN R. Welding Residual Stresses in plate girders. Civil Engineering  
TRANSACTIONS, Institute of Australian Engineers, Oct. 1969, p.157-161.

PROF. BEEDLE.

Are you referring to the inspection of the shape after it is rolled and the web is waving ?

PROF. FUKUMOTO.

Yes, for the large size panels of side 900 mm, one has a big problem in preventing the web buckling during the rolling process.

PROF. BEEDLE.

What depth to thickness ratio would you have ?

PROF. FUKUMOTO.

The limiting thickness ratio is 60 or 65 because of the initial buckling of the web due to the rolling processes.

PROF. BEEDLE.

How are these cooled ?

PROF. FUKUMOTO.

It is during normal cooling on the cooling bed that they start to wave in their web.

PROF. BEEDLE.

But these are rejected, are they not ?

PROF. FUKUMOTO.

Yes, they are rejected.

PROF. BEEDLE.

So this is a development that you observed on the cooling bed ?

PROF. FUKUMOTO.

Yes.

PROF. BEEDLE.

Well, that shows a very high cooling rate I would guess and I would just like to make an observation. The very first evidence of residual stresses at Fritz Engineering Laboratory were in the 1930's when tests of box girders for crane girders were being carried out. These girders were welded and after the welding operation the compression flange plates, which they knew initially were straight, were observed to have waves in them, and this was the first time that this influence was observed and, of course, it leads to a lowering of the 'buckling stress' because the plate is already buckled before any external load is applied.

PROF. ROCKEY.

Thank you Professor BEEDLE. We are all very aware of the very valuable and interesting work which Professor LAMBERT TALL and his co-researchers have carried out at Lehigh. The work by OWEN (see foot note page 5) to which I referred was conducted on a deep plate girder web where he shows that these residual stresses can be significant. Our next paper is by Mr. HÖGLUND. I found the paper by Mr. HÖGLUND very interesting since this is clearly a topic which is becoming increasingly important in building construction. I would like to ask Mr. HÖGLUND if he foresees any difficulties in applying his method to the case where you have holes spaced regularly along a beam. I would suspect that one would not presumably attempt to use this method in the analysis of that type of problem.

MR. HÖGLUND.

Well, I have not studied the problem of a plate with many holes, only the case where the distance between the holes is so large that one hole will have a very small influence on the web behaviour around other holes. Restrictions about the distance between the holes are given in my paper and I think the model could be extended to the case of many holes too, but this will need further research work.

PROF. MASSONNET.

I want to raise a very highly academic question. You may know about the paper by MANSFIELD, a distinguished researcher of the Royal Aircraft Establishment, about neutral holes in plane stress. Suppose you take the fuselage of an aeroplane and you want to find the optimum window. I think this study arose from the accident of the Comet N° 2 - I think - that crashed after an explosion due to fatigue of the fuselage. MANSFIELD has solved the problem of the design of reinforced holes of such a shape that the sheet does not realise there is a hole in it, there is no stress concentration at all. You have the optimum size of the hole on one side and the optimum reinforcement around the hole on the other side. Now I would like to ask the same question for buckling. We could ask - it is highly academic of course - how to reinforce the opening so that the buckling stress of the web with a hole is just the same as that of a web without a hole.

MR. HÖGLUND.

My investigation is confined to the case of holes in unstiffened thin web.

PROF. ROCKEY.

Professor CHEUNG, Dr. ANDERSON and myself have provided this information in a recent paper and this work is currently being extended.

PROF. OSTAPENKO.

Mr. HÖGLUND, have you compared your results with BOWER's and REDWOOD's studies ? Some of their work has been published in A.S.C.E. Journals.

MR. HÖGLUND.

Yes, I have seen this work.

PROF. OSTAPENKO.

BOWER used the Theory of Elasticity with the limitations that the hole be at the mid-depth and its diameter should not exceed, I think, 60 % of the depth. I notice that you go up to 90 %. But how do your results compare with his ?

MR. HÖGLUND.

His tests were on girders with webs much thicker than those employed in my girders.

PROF. OSTAPENKO.

Yes, yes, I understand.

PROF. HÖGLUND.

Therefore we used BOWER's tests to see whether my theory for thin webs was applicable for girders with thick webs. My theories are ultimate load theories.

PROF. OSTAPENKO.

He made elastic studies and also considered plastification, i.e. ultimate capacity. Thus his results should apply to your case also for low depth-to-thickness ratios. He also established curves for designing holes and reinforcements.

DR. FLINT.

Who has done that work ?

PROF. OSTAPENKO.

Jack BOWER. He is at U.S. Steel.

PROF. BEEDLE.

Alex, would the unpublished work that KUSUDA did with Bruno (THÜRLIMANN) have any application to this problem ?

PROF. OSTAPENKO.

That was a formulation of a Vierendeel truss deformation mechanism for rectangular holes. They studied the reinforcement requirements needed to develop the plastic moment capacity of the original section.

PROF. BERGFELT.

You asked for investigations on webs with closely spaced holes (cf. page 7 ). A special case, castellated beams, has been investigated also in a thesis by Dr. R. TEPFERS, CTH, Göteborg. If you wish, I will ask him to send a copy to you and anyone else who is interested.

PROF. ROCKEY.

Thank you very much.

PROF. OSTAPENKO.

I would draw your attention to the fact that Professor REDWOOD at McGill University is also doing research on webs having closely spaced holes.

PROF. ROCKEY.

The next paper is the paper on box girders study by Professor DUBAS; perhaps Professor MASSONNET you could summarise this work in English.

PROF. MASSONNET.

Well, Professor DUBAS in his written report has considered the case of a box girder with longitudinal stiffeners having the theoretical optimum rigidity  $\gamma^*$ . That means stiffeners for which you can guess whether the stiffener will be bent or remain straight at the critical stress given by the linear theory. But, of course, all these stiffeners bend in the post critical range. Professor DUBAS, in his first test, used this type of stiffener and he has shown that there was a large pocket in the stress distribution. You have seen that the stresses at the edges of the box girder were at yield and the stresses in the middle were very much lower. Now, the second test specimen which has the reference N° 1 in his report, has the same proportions as the other one, except that the stiffeners have been increased to four times the theoretical  $\gamma^*$  rigidity. Then he has obtained a completely different picture with a stress distribution at failure only having a small general pocket. The increase of strength which is achieved is about 85 %. Now, the additional cost of steel is almost nothing because fabrication costs are the same in both cases. Professor DUBAS strongly recommends to use a 'm' factor of about 5 for multiplying

PROF. MASSONNET (continued)

the theoretical value of the optimum rigidity ( $\gamma^*$ ). He has also tried to apply some of the formulae presented by Professor COOPER by considering one of the stiffeners as a bar subjected to column buckling and he reports that he obtained bad agreement in this case. He proposes to use the linear buckling theory but to increase the flexural stiffness of the stiffeners five times.

PROF. OSTAPENKO.

Did I understand correctly that Professor DUBAS includes 20 times the plate thickness to act with the stiffener ?

PROF. DUBAS.

Yes.

PROF. OSTAPENKO.

And also did you consider that the load was applied to an unsymmetrical stiffener section ?

PROF. DUBAS.

The beam is subjected to pure bending, so that the stress distribution is constant.

PROF. MASSONNET.

Professor OSTAPENKO means by his question; is the compression acting at the centroid ? Is that right ?

PROF. OSTAPENKO.

Actually, it is not applied to the centroid of the plate-stiffener combination - it is applied through the plate and therefore the stiffener would tend to bend away from the plate and thus weaken the whole panel.

PROF. DUBAS.

In the tested panel, the shear stresses between stiffener and plate are



PROF. DUBAS (continued).

theoretically zero, so that the total compression is acting in the centroid of the stiffened plate.

PROF. OSTAPENKO.

However, at the later stages of loading the effective width of the plate is reduced and the assembly behaves as a beam-column.

PROF. DUBAS.

Oh no, not in this case.

DR. FLINT.

I am in agreement with Professor DUBAS. Professor MASSONNET, the question of effective width is important, I am interested in this comparison with the strut. As the plate between the stiffeners deforms, the effective stiffness decreases until in fact it eventually vanishes altogether, when you reach yield at the junction. So that you should allow for a variable effective width as the strut buckles and of course this interaction goes on to complete failure. Have you tried doing this ?

PROF. DUBAS.

No. I compared the two test results and, for this relative behaviour, the value of the effective plate width is not very important.

PROF. COOPER.

Professor DUBAS says that the agreement with the column formula was poor. Does that mean that the column formula predicted a higher strength?

PROF. DUBAS.

Yes, this question is discussed at length in my report.

PROF. BEEDLE.

Professor DUBAS, I wonder if the difference there could not be the difference simply of post buckling strength that you observed in the web of a girder as compared with the behaviour of the flange acting as a column.

PROF. MASSONNET.

I want to say that if you look at the American specification A.I.S.I. developed by Professor George WINTER, you see that for the light gauge steel construction there is a large reserve in post buckling strength, even in box girders.

PROF. BEEDLE.

I would not say there is not any but I would simply state without making any studies at all, guess that the post buckling strength would be greater in the case of the longitudinal stiffener in the web than it would be in the cross flange of a box girder, so that I would expect that the influence of the residual stresses and so on, to be greater in this context than in the longitudinal stiffened web.

PROF. MASSONNET.

The only point that I want to make is that considering the stiffened compressed flange as an assembly of independent struts would be going backwards and to be unnecessarily safe.

DR. FLINT.

I do not think that you are necessarily going backwards in considering the assembly of the struts providing you consider those struts to have an increased Euler load which allows for the plate behaviour. You could use a fictitious strut, by using orthotropic plate calculation together with the effective width formula.

PROF. MASSONNET.

That is just the point I want to discuss in my paper.

PROF. ROCKEY.

Thank you Professor DUBAS for your contribution, we will come back to discuss this. Professor MASSONNET, after he presents his own contribution to the prepared discussion, is going to very kindly communicate to the body here, the views of Professor LEONHARDT and Professor KLÖPPEL, which have been expressed both to Professor MASSONNET and myself in private communication.

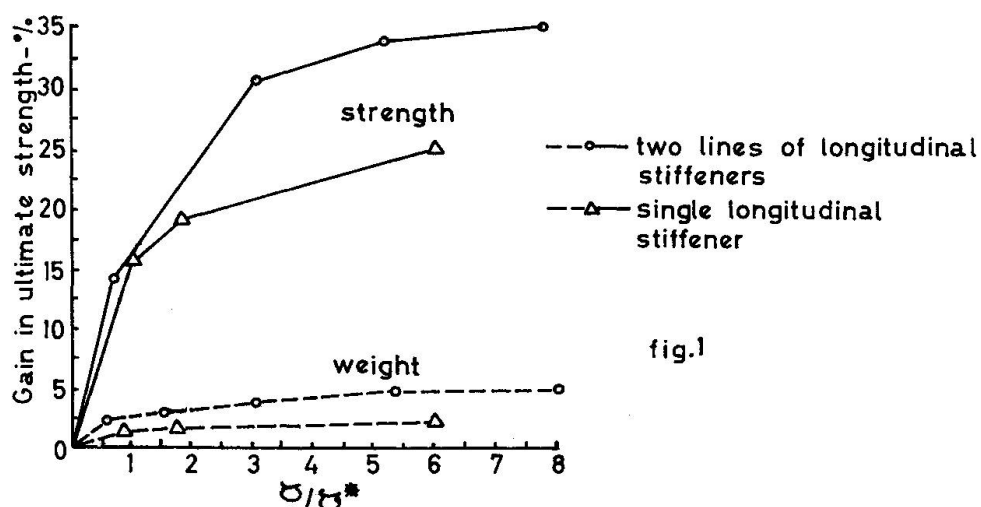
PROF. MASSONNET.

I wish to emphasise one of the main points contained in the paper by Mr. MAQUOI and myself.

You know what are strictly rigid stiffeners (defined by their theoretical relative rigidity  $\gamma^* = \frac{EI_s}{ID}$ .) They are the smallest stiffeners which the linear buckling theory predicts to remain straight under the critical stress when the plate is perfectly flat. This theory does not say anything about the behaviour of such stiffeners in the post buckling range, because, according to the linear theory, no such range does exist. Anyway, as practical plates are never flat, all experiments have shown that  $\gamma^*$  stiffeners invariably bend since the beginning of the loading.

I insist therefore very strongly on the point that, even for plate girders, the safety against collapse offered by such stiffeners is insufficient because the experiments show that the elastic collapse stress of my model girders so stiffened was only about 95 per cent of the yield stress of the material. We attach therefore a basic importance to the recommendation given in (1,2)\*: for longitudinal stiffeners, take  $\gamma = m\gamma^*$  with  $m = 6$  to  $8$ , and you will obtain an increase in ultimate strength of 20 to 25 %, with an increase in weight less than 5 % and an increase in price still smaller. This result has been nicely confirmed and precised by a paper of OWEN, ROCKEY and SKALLOUD (3).

The diagram Fig. 1, taken from this paper, shows that the benefit derived by adopting for the two longitudinal stiffeners,  $m = 7$  instead of 1, is about 20 %.



\* The numbers between brackets refer to the references placed at the end of the paper submitted for the Prepared Discussion.

PROF. MASSONNET (continued)

We are presently trying to develop a non linear theory for the ultimate strength of box girders. In our mind, the same factor of safety should be applied against this collapse strength as against yield for members subjected to tension or bending, namely 1.5 in the regular case and 1.33 for erection conditions.

Now that several accidents have taken place, we hear that we should calculate the stiffeners as compressed struts. We at Liège are against this viewpoint because it is oversafe to do so; you would waste much steel.

An ultimate strength theory of stiffened box girders must, we feel, take account of the following facts:

- 1) the initial deflection  $f_0$  of the stiffened panel ;
- 2) the eccentric position of the stiffeners. I have discussed the effect of this eccentricity in a paper published in the 1959 Volume of the "Publications of IABSE", entitled - Plaques et Coques à raidisseurs dissymétriques.

My paper was based on a study made in Germany by Professor A. PFLÜGER.

- 3) the stiffeners are much too numerous to be considered individually. Doing so would be wasting computer time. Like in the so-called GUYON-MASSONNET method for calculating slab and multiple beam bridges, we have to spread out the rigidities of the stiffeners continuously, but still taking account of their eccentric position. We have been able, these last two weeks, to generalise PFLÜGER's theory by adding to the classical expression of the strains  $\epsilon_x = \partial u / \partial x$ ,  $\epsilon_y = \partial v / \partial y$ , etc.. the non linear second order terms  $1/2 (\partial w / \partial x)^2$  etc.. which are given by finite theory of elasticity and which have been introduced in theory of plates by Th. von KARMAN.

This generalised theory yields two coupled fourth order non linear partial differential equations: an equilibrium equation governing the transverse displacement  $w$  and a compatibility equation governing the AIRY stress function  $\phi$  for the membrane stress state in our membrane plate.

Regarding the boundary conditions concerning  $w$ , we may assume simple support along the four edges ( $w = \text{curvature} = 0$ ).

The boundary conditions concerning the AIRY stress function are more complicated: First, we may assume  $N_{xy} = 0$  along the four edges (Fig. 2).

PROF. MASSONNET (continued).

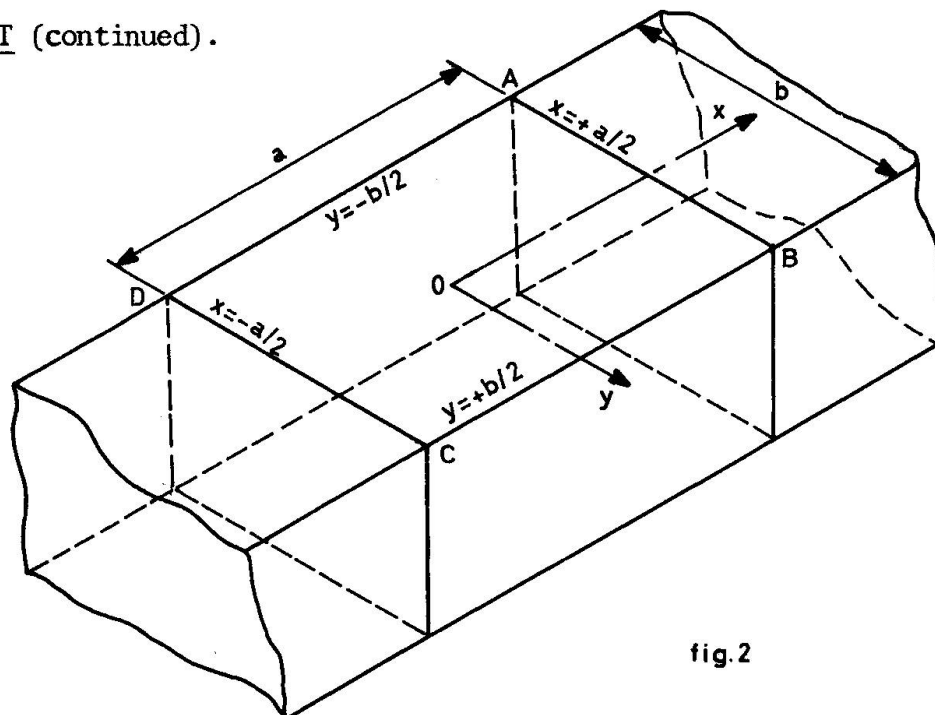


fig. 2

Along the unloaded edges  $y = -b/2$  and  $y = +b/2$ ,  $N_y$  must be zero, because the webs of the box girder are very flexible normally to their plane.

Along the loaded edges,  $x = -a/2$  and  $x = +a/2$ , we must express the condition that these edges are actually nodal lines, which remain straight by symmetry, even in the post critical domain. We then express mathematically the condition that the variation in distance between  $x = -a/2$  and  $x = +a/2$  is the same for all corresponding points, and therefore does not depend on  $y$ .

With the coordinate axes placed as indicated by fig. 2, we may for simplicity assume an initial deflection of the shape

$$w_0 = f_0 \cos \frac{\pi x}{a} \cos \frac{\pi y}{b}.$$

If we take for supplementary deflection the first buckling mode

$$w = f \cos \frac{\pi x}{a} \cos \frac{\pi y}{b},$$

we may integrate the compatibility equation rigorously in closed form, but it is impossible to integrate the equilibrium equation rigorously because above expression of  $w$  is too simple.

We then resort to the BUBNOV-GALERKIN technique, which gives the value of the amplitude  $f$  minimising the error throughout the rectangular field of integration ABCD.

We adopt the same collapse criterion as VOLMIR and SKALOD, namely that collapse occurs when the mean membrane stress along the unloaded edges  $y = -b/2$  and  $y = +b/2$  reaches the yield stress.

PROF. MASSONNET (continued)

After lengthy calculations, we obtain an expression for the mean collapse stress  $\bar{\sigma}_c$  and, in our opinion, box girder bridges should be designed so as to present under the (collapse) factored loads SP, with S equal to 1.5 or 1.33, an actual mean stress  $\sigma_a < \bar{\sigma}_c$ .

PROF. ROCKEY.

I thank our speakers who have presented very interesting and revealing comments with respect to the behaviour of the compressed flanges. I wonder if anyone wishes to raise any specific questions ?

DR. SKALLOUD.

I would like to sum up in just three sentences the prepared discussion which I have prepared. The theoretical research is based on the non linear deflection and the experimental research which we have conducted at the Institute of Applied Mechanics at Prague has demonstrated that the currently held  $\gamma^*$  concept does not ensure that the stiffeners will remain effective in the post buckling range. I agree with Professor DUBAS and Professor MASSONNET that this concept should be abandoned as soon as possible in order that accidents like those mentioned by Professor MASSONNET should be avoided and I would like to take this opportunity to recommend to the Organising Committee that further research in this area, both theoretical and experimental should be included in the recommendations presented in the final report.

PROF. ROCKEY.

Thank you Dr. SKALLOUD. Professor COOPER.

PROF. COOPER.

I am convinced, and I think perhaps others are also convinced, that a column analysis of the stiffener acting with a part of the web can be applied to this problem. Professor MASSONNET has pointed out that part of the problem of applying this type of analysis is to determine the effective width of the web plate to be used with the stiffeners. Another problem is: what are the end conditions of the column ? Anyway, it is clear that this stiffener-column problem can be solved, and I am a little bit puzzled as to why it has not been done successfully to date.

DR. FLINT.

There is another aspect to the column problem. If you apply the two modes of failure to the column, one case is that of reaching yield in the outstand which might be with the column buckling away from the outstand and the other is of course the collapse of the plate associated with the column. If however you buckle in the opposite direction, you have to consider what would be the exact conditions and you have to consider the composite column with a decreasing flange with a failure condition which is not the onset to yield - at the junction between the plate and the stiffener but is something less than that perhaps - something much less because you see you have got a rather complex problem. I think that a practical approach, using an equivalent Euler load to start with, to take into account the two dimensional nature of the system, would I think, be the way to deal with the problem in the first instance.

PROF. CLARK.

I think that in many practical cases the effective length would probably be the full length of the panel. It would only be for relatively long panels that you would have a shorter effective length.

PROF. MASSONNET.

Professor DUBAS has already demonstrated that it was not so.

PROF. DUBAS.

It is perhaps the effective length. Oui, mais la longueur de flambement d'une poutre dans un milieu élastique, ce n'est pas la longueur réelle.

PROF. BEEDLE.

You are saying that the points of lateral strength did not correspond to the points of inflection but instead you had a longer effective length of the panel.

PROF. DUBAS.

Yes, yes. In a pony truss, the effective length is not the sine length, because you have the reaction of the medium.

PROF. BEEDLE.

Flexibility of the supports ?

PROF. MASSONNET.

The second figure by Professor DUBAS has shown that the wave lengths in the longitudinal direction as well as that in the transverse direction are very short when the compressed plate is effectively stiffened. Five waves being formed in the longitudinal direction and 4 in the transverse direction, i.e. the development of small longitudinal buckles, like those I have shown in the photograph of the damaged sections of the Vienna Bridge.

PROF. COOPER.

Did you not have transverse stiffeners ?

PROF. DUBAS.

Only one transverse stiffener.

DR. FLINT.

But this is what I mean by an effective Euler load, that you take into account that wave length which will come out on the orthotropic plate theory.

PROF. GACHON.

Le problème est encore plus compliqué, parce que le raidisseur a un comportement élastique mais non linéaire.

PROF. ROCKEY.

I wonder if Professor MASSONNET could very briefly communicate to us the views of Professor LEONHARDT and Professor KLÖPPEL.

PROF. MASSONNET.

Well you know, Professor LEONHARDT, although unable to attend the Colloquium, readily agreed to explain in broad terms the procedure of his consulting office in checking buckling stability. He sent me a letter on February 22nd. I shall read you the second part of the letter rather slowly.

(see corresponding text on pages 429).



PROF. ROCKEY.

Does anyone wish to comment on this letter from Professor LEONHARDT ?

PROF. MASSONNET.

This is an expression of the point of view of a practical man engaged in bridge design.

DR. SKALOUD.

Does Professor LEONHARDT make any recommendations for determining stiffer proportions ?

PROF. MASSONNET.

He told me that he tried to verify them as struts. On this point I do not agree with him, but I believe it to be a safe procedure.

PROF. COOPER.

It seems to me that the transverse diaphragms for the box girder should be proportioned such that they could be considered rigid in their support of the longitudinal stiffeners and that the other intermediate transverse stiffeners between diaphragms would be there to get orthotropic action.

PROF. MASSONNET.

I think that the opinion of Professor KLÖPPEL will perhaps clarify a little more the situation. It is not my own contribution but it just presents the views of Professor KLÖPPEL.

Professor KLÖPPEL sent a letter to Professor ROCKEY on March 2nd and said that he could not come and he said -- it is in German, I shall try to translate in English. "Maybe I can draw your attention on the problem of the design of "box girders, which because of these accidents is now very much up to date," and he refers us to pages 13, 14 and 15 of the second volume of his book "Beulwerte ausgesteifter Rechteckplatten" written by himself and Mr. MÖLLER. I received this notice only last Tuesday and I hurried to make a rather poor translation from German into English. On page 13 he says: (see corresponding text on pages 425 to 427).

DR. FLINT.

Can I ask a question. Is  $\mu_k$  against a theoretical critical collapse or is it against a reduced collapse calculation ?

PROF. MASSONNET.

The German Specification DIN 4114 for short struts is based on the JAEGER theory which concerns an elastic -- completely plastic strut, with an initial eccentricity  $e = \frac{i}{20} + \frac{1}{500}$ . The safety factor is  $\mu_k = 1.5$  against collapse; then, for long struts you adopt the Euler theory and you take a safety factor  $\mu_k$  of 2.5.

PROF. ROCKEY.

I am sure we are all very grateful to Professor MASSONNET for the time he has taken to translate it for those of us who are poor linguists and also for presenting these two communications so well.

Leere Seite  
Blank page  
Page vide

### III

## RAPPORT DE SYNTHÈSE / ZUSAMMENFASSENDE BERICHT / SUMMARY REPORT

### 0. INTRODUCTION.

The various items examined at the Colloquium have been arranged in the following order :

- Sec. 1. Transversely stiffened plate girders :
  - 1.1. Ultimate shear strength
  - 1.2. Ultimate bending strength
  - 1.3. Ultimate strength under combined bending and shear.
- Sec. 2. Longitudinally stiffened plate girders.
- Sec. 3. Girders without intermediate stiffeners
- Sec. 4. Hybrid girders
- Sec. 5. Fatigue problems
- Sec. 6. Box girders
- Sec. 7. Special problems :
  - 7.1. Finite element approach
  - 7.2. Web crippling under transverse loads
  - 7.3. Plate girders with web holes
  - 7.4. Girders with curved webs
  - 7.5. Curved girders.

Numbers within brackets refer to the list of Colloquium reports placed at the end of present report. This list has been arranged in the alphabetic order of participating countries. Numbers within parentheses correspond to other research papers given in references.

## 1. TRANSVERSELY STIFFENED PLATE GIRDERS.

The first model for representing the behaviour of a plate girder with flexible flanges at ultimate load was developed by BASLER and THURLIMANN in 1960. Since that time, it has been incorporated into the American AISC (1) and AASHTO (2) Specifications. Several other countries are on the verge of incorporating this design concept in their Specifications. This pioneering work is represented to this Colloquium by the summary report of BASLER [15]. The initial BASLER-THURLIMANN model will therefore be considered as the basis for the discussions of the Colloquium and is not discussed per se in this Summary. It assumes that the shear strength is composed of the buckling strength of the web plus the postbuckling strength of the web represented by the formation of a tension field band. The limiting condition is given by yielding of the web within the band. One of the aims of the Colloquium is to improve and extend this concept.

### 1.1. TRANSVERSELY STIFFENED PLATE GIRDERS-ULTIMATE SHEAR STRENGTH.

New test data have been provided by ROCKEY and SKALLOUD [5], KOMATSU [10] SKALLOUD [17], CLARK and SHARP [21], OSTAPENKO and CHERN [23] and STEINHARDT and SCHRÖTER [27].

Several authors have proposed new ultimate strength mechanisms involving incomplete diagonal tension fields which are more refined than the original scheme proposed by BASLER [15].

FUJII [8a] gives a short summary of the theory he presented in 1968 at the New-York Congress of IABSE. This theory, which assumes that the web is fixed along the flanges and simply supported at the stiffeners, incorporates the effect of the strength of the flanges by a plastic beam mechanism under a uniformly distributed load. FUJII also provides [31] a numerical comparison of the ultimate load given by the various theories with available experimental results.

The theory presented by ROCKEY and SKALLOUD [5] assumes that, for normal construction, the edges of the web are simply supported. However, in the case of tubular flanges, the use of a fixed support condition would be assumed. The theory is based upon the development of a beam type mechanism in the flanges and thereby allows for the influence of the flange rigidity upon the collapse load.

The theory proposed by KOMATSU [10] assumes the same web boundary conditions as FUJII. It allows for the influence of flange rigidity by allowing the formation of a plastic beam mechanism under bi-linear varying transverse loading.

OSTAPENKO and CHERN [23] include the effect of the flanges through the use of a frame (panel) mechanism. As in models proposed by FUJII and KOMATSU, the web is assumed to have fixed - simply supported boundary conditions.

It is remarkable that, in spite of considerable divergence in basic assumptions, all these approaches give acceptably good correlation with test results, on symmetrical girders. However, the method proposed by OSTAPENKO and CHERN [23] also applies to unsymmetrical girders, that is, girders having flanges of unequal area.

CLARK and SHARP [21] develop a mathematical model which superimposes three different stress fields. Their analysis does not take into account the effect of the formation of plastic hinges in the flanges, but does attempt to show the effect of elastic deformation of the flanges on web behaviour. CLARK and SHARP, in addition, provide detailed design guides for girders made of aluminium alloy.

STEINHARDT and SCHROTER [27] give a description of how the web stress distribution is influenced by the elastic deformation of the flanges. They suggest [37] an analytical approach based on this concept.

In connection with the above problem, attention must be drawn to the constructive remarks of OSIPOV [19] concerning the effect of the degree of unfairness in fabrication upon the ultimate strength of plate girders subjected to shear.

## 1.2. TRANSVERSELY STIFFENED PLATE GIRDERS-ULTIMATE BENDING STRENGTH.

New test data on the behaviour of plate girders subjected to bending have been presented by FUKUMOTO [8b]. He has paid particular attention to the variation of the effective width of the compressed part of the web under increasing load. In addition, the new tests executed by MAEDA [9] give further information on the same problem.

In his contribution [8a], FUJII gives a formula for the ultimate bending strength of unstiffened panels based on yielding of the compression flange. FUKUMOTO [8b] studies the effective width of the web plate in the postbuckling range. He shows that the ultimate moment can be determined by using lateral torsional buckling theory if the effect of residual stresses is included (3).

A study was carried out by NISHINO and OKUMURA [8c] on large size rolled I beams with a depth of 900 mm, in order to study the magnitude and distribution of residual stresses inherent in the beams and their effect on the moment carrying capacity of the beams.

## 1.3. TRANSVERSELY STIFFENED PLATE GIRDERS-ULTIMATE STRENGTH IN BENDING AND SHEAR.

New test data have been presented by GACHON [4].

New theories have been proposed ([6], [8], [23]) and evaluated by comparison with the available test data.

In his contribution [8a], FUJII proposes criteria for constructing a polygonal interaction curve combining the effects of bending and shear. Using this curve, FUJII obtained good agreement with the experimental data obtained at Lehigh University and reported by BASLER (4). From first principles, one merit of FUJII's approach over BASLER's theory is that the first side AB of the polygonal curve is slightly sloping toward the shear axis, instead of being horizontal as in BASLER's approach. However, the available experimental results are too few to decide conclusively between the two approaches and clearly further tests are needed.

The only theoretical models which allow combining the effects of shear and bending in a continuous manner are those proposed by ROCKEY [6] and OSTAPENKO and CHERN [23]. Both models incorporate the basic features of their respective shear models but modify them to include the effect of bending on the web buckling stress, on the plastic capacity of the flanges and of the ultimate strength criterion.

## 2. LONGITUDINALLY STIFFENED PLATE GIRDERS.

In connection with longitudinally stiffened plate girders, predominant interest at the colloquium was on the bending strength although other types of loading were also considered.

In his experimental study, MAEDA [9] demonstrates the beneficial effects which can be obtained on the bending strength by employing longitudinal stiffeners and tubular compression flanges. Due to the high torsional rigidity of such a flange, it fails by lateral buckling instead of by lateral torsional buckling.

COOPER [22] demonstrates that BASLER-THURLIMANN's theory can be applied to higher values of web slenderness ratio than originally proposed. He mentions that one test girder with a slenderness ratio of 751 behaved in accordance with the theory. COOPER shows that longitudinal stiffeners can contribute to bending strength by (22) controlling lateral web deflections in the compressed portion of the web, thereby eliminating the need for the reduction in the ultimate moment. (see further reference to this point in Sec. 5 devoted to fatigue). According to COOPER, if the longitudinal stiffeners are not proportioned to remain straight up to ultimate load, then their influence should be ignored.

OSTAPENKO and CHERN [23] determine the ultimate bending strength defined by buckling of the compression flange column. They use the same approach as COOPER (5) with respect to longitudinal stiffeners. In the case of a one-sided stiffener, beam-column analysis is recommended.

The same design method is advocated by BASLER (4), who remarks that this concept will in general require larger longitudinal stiffeners than those required by the linear plate buckling theory. It is however not correct, remarks BASLER, to take advantage of the stress redistribution occurring after the critical stress has been surpassed, and simultaneously to design the panel framing members according to the linear theory. As the loading capacity of a plate girder does not bear a fixed ratio to the critical loading of a web panel, it is also not correct, according to BASLER, to base this increased requirement about the stiffeners on plate buckling calculations only. Either stiffeners must fulfill their function up to the collapse of the girder, or they should not be introduced into the calculations.

This approach should be compared with that proposed by MASSONNET (6) and endorsed by OWEN, ROCKEY and SKALOUD (7), namely to adopt for the relative rigidity  $\gamma = EI_s/bD$  of the stiffener a definite multiple  $m$  of the theoretical optimum rigidity  $\gamma^*$ :

$$\gamma = m\gamma^* \quad (1)$$

OWEN, ROCKEY and SKALOUD (7) have shown that, for longitudinal stiffeners rigid up to collapse, that is with  $m = 6$  to  $8$  in equation (1), the ultimate bending moment of a girder reinforced by longitudinal stiffeners becomes equal to the plastic moment of a section composed of the part of the cross section subjected to tension plus the compressed flange, the longitudinal stiffeners and adjacent portions of the web determined by an effective width formula.

In the case of flexible longitudinal stiffeners, the problem of determining the ultimate strength becomes exceedingly difficult and has not been sufficiently studied.

The shear strength of a longitudinally stiffened plate girder is determined by FUJII [34], ROCKEY [6], KOMATSU [10], and OSTAPENKO and CHERN [23] by adding the shear strengths of the individual subpanels as determined using their respective theories developed for transversely stiffened girders. This approach was originally proposed by COOPER [6], but he did not consider the contributions made by the flanges and longitudinal stiffeners.

ROCKEY [6] proposes to obtain the ultimate strength of longitudinally stiffened girder subjected to a combination of bending and shear by using the same criterion as for transversely stiffened girders. OSTAPENKO and CHERN [23] require compatibility of deformations between subpanels. Both papers ([6],[23]) define a continuous interaction relationship between bending and shear. OSTAPENKO and CHERN's theoretical and experimental results indicate that addition of a longitudinal stiffener may increase the strength of a girder much more substantially under combined loads than under pure shear or bending.

Much more work is needed to define the role and the strength of the longitudinal stiffeners, especially if they start deflecting before the ultimate capacity of the girder panel is reached.

### 3. GIRDERS WITHOUT INTERMEDIATE STIFFENERS.

The Swedish Provisional Rules give rules for the design of plate girders without intermediate stiffeners. They are valid for welded plate girders in roof construction subjected to static loads. The rules include a set of fabrication tolerances. BERGFELT (10) presented in 1968 at the New-York IABSE Congress a paper reporting on tests on this type of girders and he has further dealt with these studies in part of his report to the Colloquium [12].

New tests on this type of girder are presented at the Colloquium by HÖGLUND [13]. HÖGLUND also proposes a lattice truss analogy for determining the ultimate strength.

### 4. HYBRID GIRDERS.

Much progress has been made recently in this field in the United States (11). Design rules are proposed in the 1969 AISC Specification on Steel Buildings (1) as well as in the AASHO Specifications (2). AISC rules apply only to webs with  $b/t < 70$ .

Much of the earlier work, which dealt with webs having low  $b/t$  ratios, may be found in papers by CARSKADDAN (12) and TOPRAC (13). Further tests on webs having  $b/t$  ratios up to 300 and with longitudinal stiffeners are presented at the Colloquium by MAEDA [9], [32].

Analytic approaches for high web slenderness ratios are proposed by BASLER (4), by FUJII [8a] and by OSTAPENKO and CHERN [23].



## 5. FATIGUE PROBLEMS.

New significant fatigue tests are presented by MAEDA [9], who classifies the various types of fatigue cracks observed. This author shows that the use of strong longitudinal stiffeners and of a tubular type of compression flange reduces greatly the "breathing" of the web and achieves an improved behaviour of the girder.

Fatigue seems to be of special concern in the case of hybrid girders, because the ductility of the web steel has been reduced by plastic deformations. Additional fatigue tests on hybrid girders would be therefore particularly welcome.

## 6. BOX GIRDERS.

Only one report is devoted to this theme, that of DUBAS [16]. The failures involving large steel box girder bridges which have occurred recently emphasize the need for more research in this nearly completely neglected field.

The striking result of DUBAS's first test is that a compressed flange reinforced by stiffeners which only have the theoretical rigidity  $\gamma^*$  necessary to ensure that they remain straight when the panel buckles exhibits a very variable and unsatisfactory stress distribution. The consequence of this is that the mean collapse stress  $\bar{\sigma}$  is less than the critical stress  $\sigma_{cr}$  given by the linear buckling theory for an ideally perfect flange. In DUBAS's second test [33], which uses the same size plate as in the first one but with stiffeners having rigidity five times that of those used on the first test, the resulting stress distribution is nearly uniform, with small waves between the stiffeners. As a result, the strength of the compressed flange was increased by 85 per cent.

DUBAS considers that longitudinal stiffeners should be designed so as to remain straight up to collapse and recommends to use stiffeners with relative rigidities  $\gamma = 5 \gamma^*$ .

This report draws attention to the fact that the low safety factors used at present with the classical design approach based on linear buckling theory, while they may be satisfactory for plate girders, are certainly too low for the compressed flanges of box girders and should be increased.

The contribution to the Prepared Discussion presented by MASSONNET and MAQUOI [29] emphasizes these points.

These authors show that the low mean collapse stress obtained by DUBAS can be demonstrated theoretically, which may explain the recent collapse of the longitudinally stiffened box girders of the Vienna bridge (14). They recommend therefore to increase for box girders the safety factor against buckling. (See in this connection [38] and [39]).

Much additional research is needed in this field, to develop a theory which would be able to predict the strength of compressed stiffened plates, not only reinforced by stiffeners remaining straight up to collapse, but also by "flexible stiffeners", because it has not been proved that the use of the latter type of stiffening does not correspond to the most economical solution.

## 7. SPECIAL PROBLEMS.

### 7.1. FINITE ELEMENT APPROACH.

GACHON [4] gives an approximate analytical method using the finite element technique, for thin anisotropic stiffened plates with initial deformations. This analysis takes into account the large displacements of the plate as well as of the stiffeners. The computer program is used, at the present time, as an experimental tool; in the future it is expected to be extended to the plastic range.

### 7.2. WEB CRIPPLING UNDER CONCENTRATED LOADS.

In Part II of his report [12], BERGFELT investigates the influence of flange stiffness on the crippling load. He also states that, for girders with slenderness ratios in excess of 150, the crippling load does not depend as much on the web depth as predicted by the elastic theory. SKALOUD and NOVAK [36], examining the ultimate behaviour of transversely stiffened girders subjected to a transverse load applied between the stiffeners, also demonstrate that the load carrying capacity of the web is affected by the rigidity of the flanges. ROCKEY and EL-GAALY [30] show that a linear relationship exists between the ultimate carrying capacity of girders subjected to a concentrated load and their buckling load.

### 7.3. WEBS WITH HOLES.

HÖGLUND [14] presents a paper dealing with the ultimate behaviour of long unstiffened plate girders of the type discussed in Section 2 when the web contains holes of various shapes. The diagonal tension field of the latticed truss model proposed by HÖGLUND is shown to provide failure loads in close agreement with experimental values. It would be of interest to see this approach extended to girders containing more closely spaced openings.

### 7.4. GIRDERS WITH CURVED WEBS.

Girders with curved webs are discussed in report [18] by ILYASEVITCH and KLUJEV. Except for the studies on curved panels conducted by the aircraft industry, only limited research has been conducted on girders with curved webs.

ILYASEVITCH and his collaborator have used the MARGUERRE non-linear equations and, using a computer, have succeeded in producing design charts. In addition to their theoretical study, they have conducted a limited experimental program, which indicates that their theory overestimates slightly the collapse capacity of the girders. It is of interest to note that if, generally, the curvature produces an increase in buckling load, there is an accompanying decrease in the postbuckling reserve strength.\*

### 7.5. CURVED GIRDERS.

DABROWSKI and WACHOWIAK [11] consider the behaviour of a panel of a thin web which is curved longitudinally to a constant radius. The authors consider their linear analysis as a first step towards a more comprehensive investigation of the problem. As a consequence, the present study, while providing some interesting features, is not sufficiently well advanced to result in the development of suitable design rules.

**Remark:**

**Some contributions mentioned herein are not included in the present Report.**

LIST OF REPORTS PRESENTED AT  
THE COLLOQUIUM.

-----

- |      |  |   |
|------|--|---|
| [2]  | G. BURGERMEISTER<br>and H. STEUP                         | Zum Einfluss verzinkungsabhängigen Vorbeulen auf die Tragfähigkeit von Vollwandträgern.   |
| [3]  | H. GACHON  | Analyse du comportement des plaques minces raidies dans le domaine des grands déplacements.   |
| [4]  | H. GACHON  | Essais sur une poutre à âme mince et à membrures symétriques.   |
| [5]  | K.C. ROCKEY and<br>M. SKALoud                            | The Ultimate Load Behaviour of Plate Girders Loaded in Shear.   |
| [6]  | K.C. ROCKEY  | The Ultimate Load Behaviour of Stiffened Plate Girders Loaded in Shear and Bending.   |
| [7]  | G. CERADINI  | Postbuckling Analysis of Stiffened Elastic Plastic Plate Girders by Finite Element Methods.   |
| [8]  | T. FUJII,<br>Y. FUKUMOTO<br>F. NISHINO and<br>T. OKUMURA | <div style="display: flex; align-items: center;"> <div style="margin-right: 10px;"> a<br/>b<br/>c<br/>d </div> <div> Research Works on Ultimate Strength of Plate Girders and Japanese Provisions on Plate Girder Design. </div> </div> |
| [9]  | Y. MAEDA   | Ultimate Static Strength and Fatigue Behaviour of Longitudinally Stiffened Plate Girders in Bending.  |
| [10] | S. KOMATSU   | Ultimate Strength of Stiffened Plate Girders Subjected to Shear.  |
| [11] | R. DABROWSKI   | Stresses in Thin Cylindrical Webs of Curved Plate Girders.  |
| [12] | A. BERGFELT  | Studies and Tests on Slender Plate Girders without Stiffeners.  |
| [13] | T. HÖGLUND   | Simply supported Long Thin Plate I - Girders without Web Stiffeners subjected to Distributed Transverse Load.   |
| [14] | T. HÖGLUND   | Strength of Thin Plate Girders with Circular or Rectangular Web Holes without Web Stiffeners.   |
| [15] | K. BASLER  | Vollwandträger : Berechnung im überkritischen Bereich.  |

- [16] P. DUBAS                      Essais sur le Comportement Post-Critique de Poutres en Caisson Raidies.
- [17] M. SKALLOUD                  Ultimate Load and Failure Mechanism of Webs of Large Width-to-Thickness Ratios, Subjected to Shear and Attached to Flanges of Various Flexural Rigidities.
- [18] S. ILYASEVITCH and B.N. KLUJEV      Stabilität der elastischen Zylinderbauplatte bei Querbiegung eines dünnwandigen Stahlträgers mit doppelter X - förmiger Wand.
- [19] S.V. OSIPOV                   Effect of Initial Distorsions on the Carrying Capacity of Welded I - Girders.
- [20] P.S. CARSKADDAN              Research on Hybrid Plate Girders.
- [21] J.W. CLARK and M.L. SHARP              Limit Design of Aluminium Shear Webs.
- [22] P.B. COOPER                   The Ultimate Bending Moment for Plate Girders.
- [23] A. OSTAPENKO and C. CHERN              Strength of Longitudinally Stiffened Plate Girders Under Combined Loads.
- [26] B.T. YEN and J.S. HUANG              Some Considerations on the Stiffener Requirements of Plate Girders.
- [27] O. STEINHARDT and W. SCHRÖTER              Das überkritische Verhalten von Aluminium - Vollwandträgern mit Quersteifen.
- [28] K. KLÖPPEL and W. BILSTEIN              Das Torsionverhalten von Stäben mit dünnwandigen, offenen Profilen bei Berücksichtigung grosser Verformungen und Eigenspannungen.
- [29] C. MASSONNET and R. MAQUOI              Discussion of the Report by Professor P. DUBAS : Essais sur le Comportement Post-Critique de Poutres en Caisson Raidies.
- [30] K.C. ROCKEY and M.A. EL-GAALY              A Note on the Ultimate Strength of Plates when Subjected to Discrete (Patch) Loading.
- [31] T. FUJII                        Comparison between the Theoretical Shear Strength of Plate Girders and the Experimental Results.
- [32] Y. MAEDA                        Additional Study on Static Strength of Hybrid Plate Girders in Bending.
- [33] P. DUBAS                        Complément au Rapport N° 16: Essais sur le Comportement Post-Critique de Poutres en Caisson Raidies
- [34] M. SKALLOUD                   Prepared discussion in regard to the Ultimate Load Behaviour of Webs in Shear.

- [35] M. SKALLOUD      Prepared Discussion of the Report presented by Professor P. DUBAS: "Essais sur le comportement post-critique de poutres en caisson raidies".
- [36] M. SKALLOUD      Prepared Discussion regarding the Post-buckled Behaviour and Incremental Collapse of Webs subjected to Concentrated Loads.
- [37] O. STEINHARDT and W. SCHROTER      Addition to the Report : Postcritical Behaviour of Aluminium Plate Girders with Transverse Stiffeners.
- [38] K. KLÖPPEL      English translation of excerpts of pages 13, 14 and 15 of the book by K. KLÖPPEL and K.H. MÖLLER: Beulwerte ausgesteifter Rechteckplatten, Vol. II, W. ERNST Ed., 1968.
- [39] F. LEONHARDT      Excerpts of a letter of Professor F. LEONHARDT to Professor C. MASSONNET reproduced with the permission of Prof. LEONHARDT.

REFERENCES.  
-----

- (1) American Institute of Steel Construction: Specification for the Design, Fabrication and Erection of Structural Steel for Buildings (adopted February 12, 1969). IISC, ed., 101, Park Avenue, New-York.
- (2) American Association of State Highway Officials, Interim Specifications for Highway Bridges, 1971, AASHO, Washington, 1971.
- (3) FUKUMOTO, Y.:
- (4) BASLER, K.: Vollwandträger - Berechnung im überkritischen Bereich.  
ed.: Schweizer Stahlbau - Vereinigung, 8034 Zürich, 111pp.  
1968.
- (5) COOPER, P.B.: Bending and Shear Strength of Longitudinally Stiffened Plate Girders - Fritz Engineering Laboratory Report N°3046; Lehigh University, Sept. 1965.
- (6) MASSONNET, C.: Essais de Voilement sur Poutres à âme raidie.  
IABSE Publications, Vol. 14, pp.125 - 186, 1954.
- (7) OWEN, D.R.J., ROCKEY, K.C., SKALLOUD, M.: Ultimate Load Behaviour of Longitudinally Reinforced Webplates Subjected to Pure Bending. IABSE Publications, Vol.18, pp.113-148, 1970.
- (8) KLÖPPEL, K. und SCHEER, J.: Beulwerte Ausgesteifter Rechteckplatten, Band I, Ed. W. ERNST und Sohn, Berlin, 1960.
- (9) KLÖPPEL, K. und MÖLLER, K.H.: Beulwerte ausgesteifter Rechteckplatten, Band II, Ed. W. ERNST und Sohn, Berlin 1968.
- (10) BERGFELT, A. and HÖVIK, J.: Thin-walled deep Plates Girders under Static Load. 8th Congress of IABSE, Final Report, pp. 465 - 478, 1969.
- (11) Design of Hybrid Steel Beams - Report of the Subcommittee 1 on Hybrid Beams and Girders. - Joint ASCE - AASHO Committee on Flexural Members Journ. Struct. Div., Proc. ASCE, Vol. 94, N° ST6, June 1968.
- (12) CARSKADDAN, P.S.: Shear Buckling of Unstiffened Hybrid Beams.  
Journ. Struct. Div., Proc. ASCE, Vol. 94, N°ST8, August 1968 .
- (13) TOPRAC, A.A., and ENGLER, R.A.: Plate Girders with High Strength Steel Flanges and Carbon Steel Webs - Proc. AISC, pp.83-94, 1961.  
  
TOPRAC, A.A.: Fatigue Strength of Full Size Hybrid Girders. A Progress Report. Proceedings AISC, 1963.

- (14) CICIN, P.: Betrachtungen über die Bruchursachen der neuen Wiener Donaubrücke. Tiefbau, Vol. 12 , pp. 665-674, 1970.

SATTLER, K.: Nochmals: Betrachtungen über ..... Donaubrücke.  
Tiefbau, Vol. 12, pp. 948-950, 1970.

ROIK, K.,: Nochmals: Betrachtungen über .... Donaubrücke  
Tiefbau, Vol. 12, p. 1152, 1970